5-2013

FUNCTIONAL MORPHOLOGY AND PERFORMANCE OF ECOLOGICAL SYSTEMS WITH EXTREME PRESSURES: WATERFALL CLIMBING AND PREDATOR-PREY INTERACTION IN AMPHIDROMOUS GOBIOID FISHES

Takashi Maie
Clemson University, maie045@gmail.com

FUNCTIONAL MORPHOLOGY AND PERFORMANCE OF ECOLOGICAL SYSTEMS WITH EXTREME PRESSURES: WATERFALL CLIMBING AND PREDATOR-PREY INTERACTION IN AMPHIDROMOUS GOBIOID FISHES

A Dissertation
Presented to
the Graduate School of
Clemson University

In Partial Fulfillment
of the Requirements for the Degree
Doctor of Philosophy
Biological Sciences

---

by
Takashi Maie
May 2013

Accepted by:
Dr. Richard W. Blob, Committee Chair
Dr. Heiko L. Schoenfuss
Dr. Margaret B. Ptacek
Dr. Michael J. Childress
Dr. Timothy E. Higham

ABSTRACT

Understanding the functional capacity and performance of organisms provides a strong foundation for recognizing the forces that are responsible for their form, and how they might adapt to variable or changing environmental conditions. Amphidromous stream goby fishes live in a habitat subject to two potentially extreme selective pressures: (1) predation on juvenile fish returning to freshwater from the ocean, and (2) the demand to climb waterfalls to reach adult breeding habitats. Recognizing these selection pressures, I present studies evaluating (1) the mechanisms underlying the functional capacity for adhesive performance, and (2) the risk that predation imposes on amphidromous gobies. Specifically, these evaluations are based on measurements of the musculoskeletal biomechanics underlying adhesive performance in climbing and non-climbing species of gobies, and measurements of feeding kinematics and performance by piscivorous gobioid predators attacking juvenile gobies. Through the biomechanical and functional studies I present, we reach better understandings of how the functional demands of an extreme habitat are met across a range of related species.

ACKNOWLEDGMENTS

The writing of a dissertation can be a lonely and isolating experience, as many PhD candidates would say. However, journey of writing it was not the result of some lonesome act. Constant interactions and discussions with my colleagues, students, friends and family have given me strength to reach this point. Therefore, I dedicate my dissertation to all who helped me get to where, who, and what I am now. First of all, I am grateful for my graduate advisor and mentor, Dr. Rick Blob, for his endless support and encouragement in every possible direction of life in graduate school. His sincere, creative, and enthusiastic attitude toward natural science and biology taught me great appreciation of research in biomechanics and how to survive through the hard times faced over years of conducting research projects.

Dr. Heiko Schoenfuss, who has long-served as a mentor, got me into the world of anatomy and inspired me in scientific and philosophical education. He taught me great appreciation of field research in Hawai'i, and the importance of stream studies on the island.

Dr. Rick Blob, Dr. Heiko Schoenfuss, Dr. Margaret Ptacek, Dr. Michael Childress and Dr. Tim Higham all provided me with energetic, logical and moral support for the preparation of my dissertation. These five impacted greatly my scientific and educational maturation.

I would also like to thank Dr. Robert Nishimoto, Darrell Kuamo'o, Wade Ishikawa, Glenn Higashi, Skippy Hau, Lance Nishiura, Tim Shindo, Troy Shimoda, Troy Sakihara, Alysha Cabral, and Kenneth Saito at the Division of Aquatic Resources (DAR),

Jonatha Giddens (University of Hawai'i, Hilo and now Manoa), and the late Dr. Mike Fitzsimons (Louisiana State University) for not only field assistance and logistical support during long years of fieldwork in Hawai'i, but also ever-lasting friendship and endless encouragement. For fieldwork in Dominica, I am thankful to Dr. Saara DeWalt, Dr. Kalan Ickes, and Dr. John Hains of Clemson University; Nancy Osler and the staff of Clemson's Archbold Tropical Research and Education Institute at Springfield Plantation; and E. Hypolite and J. Andre of Dominica Division of Forestry and Wildlife for coordinating research permission. During fieldwork I conducted in Japan, I am thankful to Dr. Yuko Ikebe and Dr. Nagahiro Nakazato of the International Society of Mangrove Ecosystems for helping me coordinate trips to Ryukyu Islands and a remote waterfall in the deep mountain of Wakayama Prefecture on the island of Honshu.

Fish were captured, experiments were conducted, and data were collected and analyzed thanks to support from Dr. Matthew Julius and Dr. Gordon Schrank (St. Cloud State University), my fellow graduate and undergraduate students, Kristine Moody and Sandy Kawano (Clemson graduate students); Steffanie Meyer, Holly Burchfield, Caitlin McPherson, Josh Cullen, David Boerma, and Patrick McGarity (Clemson undergrad students); Roberto Cediel (St. Cloud State University graduate student); and Jerry Leonard, Kelsey Lesteberg, Andrew Meister (St. Cloud State University undergraduate students). I would also like to extend my thanks to Blob and Ptacek lab mates and the Clemson teaching/research community, especially around the Department of Biological Sciences, including Dr. Nora Espinoza, Dr. Gabe Rivera, Dr. Angie Rivera, Jenn Seda, Casey Gosnell, Dr. Andrew Clark, Emily Kane, Jeff Olberding, Kathleen Foster, Dr.

Tamara McNutt-Scott, Dr. Glen Scott, Dr. John Parrish, and Dr. Mike Butcher, and Dr. Alfred ‘Hap’ Wheeler.

I was also deeply touched by personal support and encouragement that accounted as much as any academic support or research/field assistance. I am greatly indebted to my wife, Erika K. Maie Mork, for her patience, understanding and loving support. In addition, she gracefully caught the very first fish of my 2011 field season! I would like to thank my father, Kazuo Maie, and my mother, Yuko Maie, who raised me with unconditional support and who always believe in me. Exposure to nature, wildlife, and science earlier life nourished my passion and interest in natural science today. I would never imagined that I would still be “playing” with a little goby fish as I did when I was a three-year-old boy.

Finally, this study was made possible thanks to numerous grants and funding resources. Hawaiian fieldwork was supported by grants to from Raney Award from American Society of Ichthyologists and Herpetologists, Clemson University Graduate School (Professional Enrichment Grants), Alexander P. & Lydia Anderson Graduate Fellowship, R.C. Edward Fellowship, grants to H.L. Schoenfuss (NSF IOS-0817911 and St. Cloud State University Faculty Improvement grant), and grants to R.W. Blob (NSF IOS-0817794 and Clemson University Research Investment Fund Award). All collection and animal use procedures were reviewed and approved by the Clemson University Animal Research Committee (Animal Use Protocols 40061 and 2011-057).

TABLE OF CONTENTS

LIST OF TABLES

List of Tables (Continued)

Table Page

LIST OF FIGURES

List of Figures (Continued)

Figure Page

List of Figures (Continued)

Figure Page

“When we try to pick out anything by itself, we find it hitched to everything else in the universe.”

— John Muir

CHAPTER ONE

INTRODUCTION

The environment in which animals live exposes them to numerous physical forces that can impose a wide range of functional demands (Denny, 1993; Vogel, 1994; Wainwright and Reilly, 1994; Herrel et al., 2006), but the morphological and physiological traits of species often help to meet those demands by improving the performance of specific functions (e.g., feeding or locomotion). As a result, animal morphology and physiology often correlate well with aspects of ecology (Alexander, 1967, 1983; Arnold, 1983; Wainwright and Reilly, 1994). For example, morphological characteristics in fishes often correlate with trophic ecology (Barel, 1983; de Visser and Barel, 1996; Wainwright, 1988; Wainwright and Richard, 1995; Wainwright, 1996; Bouton et al., 1998, 1999, 2002; Osenberg et al., 2004) and spatial distribution (Hugueny and Pouilly, 1999; Bellwood and Wainwright, 2001; Fulton et al., 2001; Wainwright et al., 2002; Bhat, 2005; Ohlberger et al., 2006). In addition, the significance of functional demands often varies greatly with the body size of animals (Carrier, 1996; McMahon, 1975; Schmidt-Nielsen, 1984; Maie et al., 2007). For example, through the course of growth the forces to which animals are exposed may change, potentially requiring compensatory allometric changes in the size or performance of support or propulsive structures if functional capacities are to be maintained as juveniles mature into adults (McGuire, 2003; McHenry and Lauder, 2006). Without such changes, the ability of adults to perform some tasks may be impaired, unless initial performance levels were sufficiently high to absorb size-related declines (Carrier, 1996; Blob et al., 2007).

Biomechanical studies permit development of hypotheses regarding how, in animals, morphology and patterns of performance are interrelated, and can yield insights into ecological consequences of particular morphological structures (e.g., Wainwright, 1987, 1988; Wainwright et al., 1991; Westneat, 1994; Greaves, 1995; Koolstra and van Eijden, 1997; Peck et al., 2000; Herrel et al., 2002; Westneat 2003; Carroll et al., 2004; Huber and Motta, 2004; Van Wassenbergh et al., 2005; Grubich et al., 2008; Habegger et al., 2011). In my research, I have examined the functional performance of an unusual group of teleostean fishes, the amphidromous gobioids, focusing on two primary functional systems that relate directly to survivorship and, therefore, fitness: migratory locomotion and feeding. I have selected the extreme case of this teleostean group, which includes waterfall climbing species, in order to better understand how performance and its ontogenetic change in systems under strong selection pressures contribute to the success of species through their life history.

Gobioid fishes, including the gobies and their sister taxon, the eleotrids, are a tremendously speciose vertebrate group (>2000 species with ~270 genera: Lauder and Liem, 1983; Akihito et al., 2000; Thacker, 2003; Gill & Mooi, 2012) with a worldwide distribution and wide range of ecological niches and life histories (Miller, 1973; Iwata et al., 2001; Kon and Yoshino, 2002; Rüber et al., 2003; Watson and Walker, 2004; Ahnelt and Scattolin, 2005), as well as great anatomical diversity (osteology, myology, splanchnology, lateral line system: Regan, 1911; Takagi, 1950; Gosline, 1955; Akihito, 1971; Miller, 1973; Birdsong, 1975; Springer, 1983; Akihito et al., 1984; Birdsong et al., 1988; Takagi, 1988; Harrison, 1989; Hoese and Gill, 1993; Ahnelt and Göschl, 2004;

Thacker, 2005; Asaoka et al., 2011). Amphidromy is a common life history pattern among gobioid fishes of the Indo-Pacific and Caribbean islands (e.g., Manacop, 1953; Maciolek, 1977; Fukui, 1979; Sakai and Nakamura, 1979; Radtke et al., 1988; Kinzie, 1988; McDowall, 1992; Harrison, 1993; Parenti and Maciolek, 1993; Fitzsimons and Nishimoto, 1995; Bell, 1994; Shen et al., 1998; Berrebi et al., 2005; Yamasaki and Tachihara, 2007; Maeda et al., 2008; McDowall, 2009). In this strategy, larvae that hatch in perennial freshwater streams are swept downstream into the ocean (Keith, 2003; McDowall, 2003, 2004, 2009) where, after several months of growth and development as marine zooplankton, postlarval-juveniles return to freshwater and actively migrate upstream to reach adult habitats for further maturation, establishing territories, and spawning (Radtke et al., 1988; Fitzsimons et al., 1990; Zink et al., 1996; Keith, 2003; McDowall, 2003, 2004, 2010). However, the stream habitats of volcanic islands like the Hawaiian Archipelago (Ford and Kinzie, 1982) produce physical challenges to juveniles making migratory efforts. In the Hawaiian Islands, juvenile gobies (or hinana) entering streams encounter the predatory eleotrid species Eleotris sandwicensis (or ‘o’opu ‘akupa) Vaillant and Sauvage 1875 (Tate, 1997; Schoenfuss and Blob, 2007). Although eleotrids are known to feed on fishes (McKaye et al., 1979; Nordlie, 1981; Kido, 1996; Tate, 1997; Winemiller and Ponwith, 1998; Bacheler et al., 2004; Schoenfuss and Blob, 2007) and to have large jaw closing muscles and high velocity advantage for jaw movements (Maie et al., 2009b), the risk they pose to migrating juvenile gobies is uncertain because their feeding performance, which could potentially impose strong selective pressure on juvenile gobies (Blob et al., 2010), has not been evaluated.

The steep elevational gradient of the Hawaiian Islands, as a product of volcanic origin (Carson and Clague, 1995), poses a second challenge to migrating gobies by punctuating streams with numerous tall waterfalls. On older islands like Kaua'i these falls can be far inland, but on younger islands like Hawai'i they can be very near to the shore. Because of such stream segmentation, species distribution has been suggested to be determined by functional capacities of gobies to overcome rapid stream current and waterfalls (Nishimoto and Kuamo'o, 1997; Cook, 2004; Blob et al., 2006). Three of four Hawaiian goby species, Sicyopterus stimpsoni ('o'opu nopili) Gill 1860, Lentipes concolor ('o'opu alamo'o) Gill 1860, and Awaous guamensis ('o'opu nakea) Valenciennes 1837, along with several species from other steep volcanic islands (e.g., Sicydium punctatum Perugia 1896 from Dominica, West Indies; Sicyopterus japonicus Tanaka 1909 from Japan), are able to climb these falls and penetrate upstream habitats to different degrees (Schoenfuss et al., 2011), though one Hawaiian goby species, Stenogobius hawaiiensis ('o'opu naniha) Watson 1991, and the predator E. sandwicensis do not climb. In addition, waterfall-scaling is carried out not only by migrating juveniles but also adult individuals displaced downstream by, for example, catastrophic discharges (e.g., flash floods after Hurricane Iniki: Fitzsimons and Nishimoto, 1995; Blob et al., 2007). Station-holding and climbing behaviors are common among goby species world-wide, and are aided by an anatomical specialization in which their pelvic fins are fused into an adhesive sucker (Schoenfuss and Blob, 2003; Maie et al., 2007; Budney and Hall, 2010). However, with the exception of a study of size-related scaling of the pelvic sucker in two goby species (Maie et al., 2007), it is unknown how the performance and structure

of the pelvic sucker vary across species and through ontogeny, and how that might contribute to the distributions of species within streams. For example, isometric scaling of the pelvic sucker with respect to body size during ontogeny of S. stimpsoni from Hawai'i and S. punctatum from Dominica, West Indies, suggested that adhesive capacity that relies on suction would decline as these fish grew in size (Maie et al., 2007). However, actual measurements of suction pressure and force are not available to test this hypothesis, nor are anatomical data that might help explain observed differences in adhesive capacity between climbing and non-climbing species.

As mentioned above, amphidromous stream goby fishes live in a habitat subject to two potentially extreme selective pressures: (1) predation on juvenile fish returning to freshwater from the ocean, and (2) the demand to climb waterfalls to reach adult breeding habitats. Recognizing these selection pressures, I present studies, in four chapters, evaluating (1) the mechanisms underlying the functional capacity for adhesive performance, and (2) the risk that predation imposes on amphidromous gobies. Specifically, these evaluations are based on measurements of in vivo adhesive performance and mechanics in climbing and non-climbing species of gobies (Chapter 2), the musculoskeletal biomechanics underlying adhesive performance in these species of gobies (Chapter 3), feeding kinematics and performance by piscivorous gobioid predators attacking juvenile gobies (Chapter 4), and a comparison of the biomechanics and functional capacity of the feeding apparatus between a gobioid predator and a gobiid algal grazer (Chapter 5).

Through the biomechanical and functional studies I present here, I believe that we reach better understanding of how a current mosaic of ichthyofauna in streams of the oceanic Islands is shaped, and in perhaps many tropical and subtropical island systems that have showcased the assemblage and dynamics of organisms common to many oceanic islands.

LITERATURE CITED

Ahnelt H, Göschl J. 2004. The pattern of the lateral line system on the caudal fin of *Perccottus glenii* Dybowski, 1877 (Teleostei: Odontobutidae), with comments on the arrangement of the lateral line system on the caudal fin of Gobioidei. Proceedings of the California Academy of Sciences 55:358-372.

Ahnelt H, Scattolin G. 2005. The pattern of the mechanosensory lateral line on the caudal fin of the two deep-water gobiid fishes *Deltentosteus collonianus* and *Deltentosteus quadrimaculatus* (Teleostei: Gobiidae). Natural History 39:4127-4135.

Akihito, Prince. 1971. On the supratemporals of gobiid fishes. Jpn J Ichthyol. 18:57-64.

Akihito, Prince, Hayashi M, Yoshino T, Shimada K, Yamamoto T, Senou H. 1984. Suborder Gobioidei. In: The Fishes of the Japanese Archipelago, Masuda H, Amaoka K, Araga C, Uyeno T, Yoshino T (Eds). Tokai University Press, Tokyo. Pp.235-258.

Akihito, Prince, Iwata A, Kobayashi T, Ikeo K, Imanishi T, Ono H, Umehara Y, Hamamatsu C, Sugiyama K, Ikeda Y, Sakamoto K, Fumihito A, Ohno S, Gojobori T. 2000. Evolutionary aspects of gobioid fishes based upon a phylogenetic analysis of mitochondrial cytochrome b genes. Gene 259:5-15.

Alexander RMcN. 1967. Functional design in fishes. 1st ed. London, Hutchinson & Co.

Alexander RMcN. 1983. Animal mechanics. 2nd ed. Oxford, Blackwell Scienctific Publications.

Arnold SJ. 1983. Morphology, performance and fitness. American Zoologist 23:347-361.

Asaoka R, Nakae M, Sasaki K. 2011. Description and innervation of the lateral line system in two gobioids, *Odontobutis obscura* and *Pterogobius elapoides* (Teleostei: Perciformes). Ichthyol Res 58:51-61.

Bacheler NM, Neal JW, Noble RL. Diet overlap between native bigmouth sleepers (*Gobiomorus dormitor*) and introduced predatory fishes in a Puerto Rico reservoir. Ecology of Freshwater Fish 13:111-118.

Birdsong RS. 1975. The osteology of *Microgobius signatus* Poey (Pisces: Gobiidae), with comments on other gobioid fishes. Bulletin of Florida State Museum, Biological Sciences 19:135-187.

Birdsong RS, Murdy EO, Pezold FL. 1988. A study of the vertebral column and median fin osteology in gobioid fishes with comments on gobioid relationships. Bulletin of Marine Science 42:174-214.

Blake RW. 2006. Biomechanics of rheotaxis in six teleost genera. Can J Zool 84:1173-1186.

Blob RW, Rai R, Julius JL, Schoenfuss HL. 2006. Functional diversity in extreme environments: effects of locomotor style and substrate texture on the waterfall climbing performance of Hawaiian gobiid fishes. J Zool Lond 268:315-324.

Blob RW, Wright KM, Becker M, Maie T, Iverson TJ, Julius ML, Schoenfuss HL. 2007. Ontogenetic change in novel functions: waterfall climbing in adult Hawaiian gobiid fishes 273:200-209.

Blob RW, Kawano SM, Moody KN, Bridges WC, Maie T, Ptacek MB, Julius ML, Schoenfuss HL. 2010. Morphological selection and the evaluation of potential tradeoffs between escape from predators and the climbing of waterfalls in the Hawaiian stream goby *Sicyopterus stimpsoni*. Integrative and Comparative Biology 50:1185-1199.

Budney LA, Hall BK. 2010. Comparative morphology and osteology of pelvic fin-derived midline suckers in lumptishes, snailfishes and gobies. Journal of Applied Ichthyology 26:167-175.

Carson HL, Clague DA. 1995. Geology and biogeography of the Hawaiian Islands. In: Wagner WL, Funk VA, editors. Hawaiian biogeography: evolution on a hotspot archipelago. Washington, DC: Smithsonian Institution Press. pp 14-29.

Cook RP. 2004. Macrofauna of Laufuti stream, Taú, American Samoa, and the role of physiography in its zonation. Pacific Science 58:7-21.

Cutwa MM, Turingan RG. 2000. Intralocality variation in feeding biomechanics and prey use in *Archosargus probatocephalus* (Teleostei, Sparidae), with implications for the ecomorphology of fishes. Environmental Biology of Fishes 59:191-198.

Emerson SB, Diehl D. 1980. Toe pad morphology and mechanisms of sticking in frogs. Biological Journal of the Linnean Society 13:199-216.

Fitzsimons JM, Schoenfuss HL, and Schoenfuss TC. 1997. Significance of unimpeded flows in limiting the transmission of parasites from exotics to Hawaiian stream fishes. Micronesica 30:117-125.

Fitzsimons JM, McRae MG, Schoenfuss HL, Nishimoto RT. 2003. Gardening behavior in the amphidromous Hawaiian fish *Sicyopterus stimpsoni* (Osteicthyes: Gobiidae). Ichtyol. Explor. Freshwaters 14:185-191.

Ford JI, Kinzie RA III. 1982. Life crawls upstream. Natural History 91:60-67.

Gill AC, Mooi RD. 2012. Thalasseleotrididae, new family of marine gobioid fishes from New Zealand and temperate Australia, with a revised definition of its sister taxon, the Gobiidae (Teleostei: Acanthomorpha). Zootaxa 3266:41-52.

Gosline WA. 1955. The osteology and relationships of certain gobioid fishes, with particular reference to the genera *Kraemeria* and *Microdesmus*. Pacific Science 9:158-170.

Grubich JR, Westneat MW. 2006. Four-bar linkage modelling in teleost pharyngeal jaws: computer simulations of bite kinematics. J Anat 209:79-92.

Harrison IJ. 1989. Specialization of the gobioid palatopterygoquadrate complex and its relevance to gobioid systematics. Natural History 23:325-353.

Hoese DF, Gill AC. 1993. Phylogenetic relationships of eleotridid fishes (Perciformes: Gobioidei). Bulletin of Marine Science 52:415-440.

Iwata A, Hosoya S, Larson HK. 2001. *Paedogobius kimurai*, a new genus and species of goby (Teleostei: Gobioidei: Gobiidae) from the West Pacific. Records of the Australian Museum 53:103-112.

Janzen FJ, Stern HS. 1998. Logistic regression for empirical studies for multivariate selection. Evolution 52:1564-1571.

Keith P. 2003. Biology and ecology of amphidromous Gobiidae of the Indo-Pacific and the Caribeean regions. Journal of Fish Biology 63:831-847.

Kido MH. 1996. Morphological variation in feeding traits of native Hawaiian stream fishes. Pacific Science 50:184-193.

Kier WM, Smith AM. 1990. The morphology and mechanics of octopus suckers. Biological Bulletin 178:126-136.

Kon T, Yoshino T. 2002. Extremely early maturity found in Okinawan gobioid fishes. Ichthyological Research 49:224-228.

Lande R, Arnold SJ. 1983. The measurement of selection on correlated characters. Evolution 37:1210-1226.

Lauder GV, Liem KF. 1983. The evolution and interrelationships of the actinopterygian fishes. Bull Mus Comp Zool 150:95-197.

Lee JC. 1982. Accuacy and precision in anuran morphometrics: artifacts of presevation. Systematic Zoology 31:266-281.

Maie T, Schoenfuss HL, Blob RW. 2007. Ontogenetic scaling of body proportions in watefall-climbing gobiid fishes from Hawai'i and Dominica: implications for locomotor function. Copeia 2007:755-764.

Maie T, Wilson MP, Schoenfuss HL, Blob RW. 2009a. Feeding kinematics and performance of Hawaiian stream gobies, *Awaous guamensis* and *Lentipes concolor*: linkage of functional morphology and ecology. J Morph 270:344-356.

Maie T, Schoenfuss HL, Blob RW. 2009b. Jaw lever analysis of Hawaiian gobioid stream fishes: a simulation study of morphological diversity and functional performance. 270:976-983.

Martin RF. 1978. Clutch weight/total body weight ratios of lizards (Reptilia, Lacertilia, Iguanidae): preservative induced variation. Journal of Herpetology 12:248-251.

McDowall RM. 1992. Diadromy: origins and definitions of terminology. Copeia 1992:248-251.

McDowall RM. 2003. Hawaiian biogeography and the islands' freshwater fish fauna. Journal of Biogeography 30:703-710.

McDowall RM. 2004. Ancestry and amphidromy in island freshwater fish faunas. Fish and Fisheries 5:75-85.

McDowall RM. 2009. Early hatch: a strategy for safe downstream larval transport in amphidromous gobies. Reviews in Fish Biology and Fisheries 19:1-8.

McDowall RM. 2010. Why be amphidromous: expatrial dispersal and the place of source and sink population dynamics? Reviews in Fish Biology and Fisheries 20:87-100.

McKaye KR, Weiland DJ, Lim TM. 1979. The effect of luminance upon the distribution and behavior of the eleotrid fish *Gobiomorus dormitor*, and its prey. Rev Can Biol 38:27-36.

Miller PJ. 1973. The osteology and adaptive features of *Rhyacichthys aspro* (Teleostei: Gobioidei) and the classification of gobioid fishes. J Zool Lond 171:397-434.

Miller PJ. 1998. The West African species of *Eleotris* and their systematic affinities (Teleostei: Gobioidei). Natural History 32:273-296.

Nishimoto RT, Kuamo'o DGK. 1997. Recruitment of goby postlarvae into Hakalau stream, Hawai'i island. Micronesica 30:41-49.

Nordlie FG. 1981. Feeding and reproductive biology of eleotrid fishes in a tropical estuary. Journal of Fish Biology 18:97-110.

Parenti LR, Maciolek JA. 1993. New sicydiine gobies from Ponape and Palau, Micronesia, with comments on systematics of the subfamily Sicydiinae (Teleostei: Gobiidae). Bulletin of Marine Science 53:945-972.

Pezold F, Cage B. 2002. A review of the spinycheek sleepres, genus *Eleotris* (Teleostei: Eleotridae), of the western hemisphere, with comparison to the West African species. Tulane Studies in Zoology and Botany 31:19-63.

Radtke RL, Kinzie RA III, Folsom SD. 1988. Age at recruitment of Hawaiian freshwater gobies. Environmental Biology of Fishes 23:205-213.

Regan CT. 1911. The osteology and classification of the gobioid fishes. The annals and Magazine of Natural History 8:729-733.

Rüber L, Van Tassell JL, Zardoya R. 2003. Rapid speciation and ecological divergence in the American seven-spined gobies (Gobiidae, Gobiosomatini) interred from a molecular phylogeny. Evolution 57:1584-1598.

Schoenfuss HL, Blob RW. 2003. Kinematics of waterfall climbing in Hawaiian freshwater fishes (Gobiidae): vertical propulsion at the aquatic-terrestrial interface. J Zool Lond 261:191-205.

Schoenfuss HL, Blob RW. 2007. The importance of functional morphology for fishery conservation and management: applications to Hawaiian amphidromous fishes. Bishop Museum Bulletin in Cultural and Environmental Studies 3:125-141.

Schoenfuss HL, Maie T, Kawano SM, Blob RW. 2011. Performance across extreme environments: comparing waterfall climbing among amphidromous gobioid fishes from Caribbean and Pacific islands. Cybium 35:361-369.

Springer VG. 1983. Tyson belos, new genus and species of western Pacific fish (Gobiidae, Xenisthminae), with discussions of gobioid osteology and classification. Smithsonian Contributions to Zoology 390:1-40.

Swain DP. 1992. Selective predation for vertebral phenotype in *Gasterosteous aculeatus*: reversal in the direction of selection at different larval sizes. Evolution 46:998-1013.

Takagi K. 1950. On the glossohyal bone of the gobioid fishes of Japan, with some phylogenetic considerations. Jpn J Ichthyol 1:37-52.

Takagi K. 1988. Cephalic sensory canal system of the gobioid fishes of Japan: comparative morphology with special reference to phylogenetic significance. Journal of the Tokyo University of Fisheries 75:499-568.

Tate DC. 1997. The role of behavioral interactions of immature Hawaiian stream fishes (Pisces: Gobioidei) in population dispersal and distribution. Micronesica 30:51-70.

Thacker CE. 2003. Molecular phylogeny of the gobioid fishes (Teleostei: Perciformes: Gobioidei). Molecular Phylogenetics and Evolution 26:354-368.

Thacker CE. 2005. Unusual gonad structure in the paedomorphic teleotsts *Schindleria praematura* (Teleostei: Gobioidei): a comparison with other gobioid fishes. Journal of Fish Biology 66:378-391.

Van Wassenbergh S, Aerts P, Adriaens D, Herrel A. 2005. A dynamic model of mouth closing movements in clariid catfishes: the role of enlarged jaw adductors. Journal of Theoretical Biology 234:49-65.

Wainwright PC, Reilly SM. 1994. Ecological morphology: integrative organismal biology. Chicago, The University of Chicago Press.

Wainwright PC, Richard BA. 1995. Predicting patterns of prey use from morphology with fishes. Environmental Biology of Fishes 44:97-113.

Wainwright PC, Shaw SS. 1999. Morphological basis of kinematic diversity in feeding sunfishes. Journal of Experimental Biology 202:3101-3110.

Wainwright PC, Bellwood DR, Westneat MW, Grubich JR, Hoey AS. 2004. A functional morphospace for the skull of labrid fishes: patterns of diversity in a complex biomechanical system. Biological Journal of the Linnean Society 82:1-25.

Watson W, Walker HJ. 2004. The world's smallest vertebrate, *Schindleria brevipinguis*, a new paedomorphic species in the family Schindleriidae (Perciformes: Gobioidei). Records of the Australian Museum 56:139-142.

Westneat MW. 1990. Feeding mechanics of teleost fishes (Labridae: Perciformes): a test of four-bar linkage models. J Morph 205:269-295.

Westneat MW. 1994. Transmission of force and velocity in the feeding mechanisms of labrid fishes (Teleostei, Perciformes). Zoomorph 114:103-118.

Winemiller KO, Ponwith BJ. 1998. Comparative ecology of eleotrid fishes in Central American coastal streams. Environmental Biology of Fishes 53:373-384.

Westneat MW. 2003. A biomechanical model for analysis of muscle force, power output and lower jaw motion in fishes. Journal of Theoretical Biology 223:269-281.

Yamamoto MN, Tagawa AW. 2000. Hawai'i's Native and Exotic Freshwater Animals. Honolulu: Mutual Publishing.

Zink RM, Fitzsimons JM, Dittmann DL, Reynolds DR, Nishimoto RT. 1996. Evolutionary genetics of Hawaiian freshwater fish. Copeia 1996:330-335.

CHAPTER TWO

PERFORMANCE AND SCALING OF A NOVEL LOCOMOTOR STRUCTURE: ADHESIVE CAPACITY OF CLIMBING GOBIID FISHES

SUMMARY

Many species of gobiid fishes adhere to surfaces using a sucker formed from fusion of the pelvic fins. Juveniles of many amphidromous species use this pelvic sucker to scale waterfalls during migrations to upstream habitats after an oceanic larval phase. However, adults may still use suckers to re-scale waterfalls if displaced. If attachment force is proportional to sucker area and if growth of the sucker were isometric, then increases in the forces that climbing fish must resist might outpace adhesive capacity, causing climbing performance to decline through ontogeny. To test for such trends, I measured pressure differentials and adhesive suction forces generated by the pelvic sucker across wide size ranges in six goby species, including climbing and non-climbing taxa. Suction was achieved via two distinct growth strategies: (1) small suckers with isometric (or negatively allometric) scaling among climbing gobies, vs (2) large suckers with positively allometric growth in non-climbing gobies. Species using the first strategy show a high baseline of adhesive capacity that may aid climbing performance throughout ontogeny, with pressure differentials and suction forces much greater than expected if adhesion were a passive function of sucker area. In contrast, large suckers possessed by non-climbing species may help compensate for reduced pressure differentials, thereby producing suction sufficient to support body weight. Climbing *Sicyopterus* species also use oral suckers during climbing waterfalls, which exhibited scaling patterns similar to

those for pelvic suction. However, oral suction force was considerably lower than that for pelvic suckers, reducing the ability for these fish to attach to substrates by the oral sucker alone.

INTRODUCTION

The environment in which animals live exposes them to numerous physical forces that can impose a wide range of functional demands (Denny, 1993; Vogel, 1994; Wainwright and Reilly, 1994; Herrel et al., 2006). In addition, the significance of such demands often varies substantially with the body size of animals (Carrier, 1996; McMahon, 1975; Schmidt-Nielsen, 1984; Maie et al., 2007). For example, through the course of growth the forces to which animals are exposed may change, potentially requiring compensatory allometric changes in the size or performance of support or propulsive structures if functional capacities are to be maintained as juveniles mature into adults (McGuire, 2003; McHenry and Lauder, 2006). Without such changes, the ability of adults to perform some tasks may be impaired, unless initial performance levels were sufficiently high to absorb size-related declines (Carrier, 1996; Blob et al., 2007).

Gobiid stream fishes from oceanic islands provide a particularly interesting system in which to examine interspecific and ontogenetic differences in functional performance and habitat, and to test the potential for allometric changes in functional performance to compensate for growth related changes in the forces to which animals are exposed. Gobies are a speciose lineage characterized by the fusion of the paired pelvic fins into a single ventral sucker that is used to adhere to substrates (Nelson, 1994). Many

species living in the streams of oceanic islands exhibit an amphidromous life history, in which larvae are swept downstream to the ocean upon hatching (e.g., Maciolek, 1977; Radtke et al., 1988; Kinzie, 1988; Fitzsimons and Nishimoto, 1995; Yamasaki and Tachihara, 2007; Maeda et al., 2008; McDowall, 2009). After growing for several months, postlarvae return to stream habitats where they undergo metamorphosis and grow to reproductive individuals (Radtke et al., 1988; Bell, 1994; Shen et al., 1998; Radtke et al., 2001). But whereas some species remain in the nearshore estuarine reaches of streams during maturation and adulthood, other species embark on migrations further upstream that may entail climbing major waterfalls, several tens of meters (or more) in height (Ford and Kinzie, 1982; Bell, 1994; Keith et al., 2002; Voegtlé et al., 2002; Keith, 2003; McDowall, 2003, 2004; Schoenfuss and Blob, 2003, 2007). Though present even in non-climbing gobies, the ventral sucker is a particularly critical component of the performance of species that climb, allowing them to remain attached to vertical rock surfaces even in the face of rushing water (Ford and Kinzie, 1982; Voegtlé et al., 2002; Schoenfuss and Blob, 2003).

Use of the ventral sucker is exhibited most dramatically among juvenile gobies returning from the ocean, and the adhesive capacity of climbing species would be expected to exceed that of non-climbing species because climbing species must face the additional demand of resisting gravity, as well as flowing water (Maie et al., 2007). Adhesion can also be used by adults to resist dislodgement by currents, or to climb back to upstream habitats after dislodgement (Fukui, 1979; Fitzsimons and Nishimoto, 1995; Maie et al., 2007; Blob et al., 2007). How might growth to adult size affect adhesive

performance in gobies? The pelvic sucker has been proposed to generate an adhesive force by means of suction, based on the flattening of the bowl-shaped 'disc' to form a seal on wet surfaces during climbing (Schoenfuss and Blob, 2003; Maie et al., 2007). In suction, the force of attachment is proportional to the attached area of the sucker (Kier and Smith, 1990), which is dimensionally proportional to the square of length (i.e., L^2). For non-climbing species, the primary force that adhesion by the sucker would need to resist would be drag from flowing water. Because drag is proportional to the frontal or wetted surface area of an animal (Vogel, 1994), it would also be proportional to L^2; thus, non-climbing gobies might be able to maintain adequate adhesive performance from juvenile through adult life stages even if they exhibited isometric growth, because the forces to which they are exposed and their ability to resist those forces are expected to increase in equal proportion. In contrast, climbing gobies encounter different functional demands. Because much of the body is out of the water when they climb (Blob et al., 2007; Maie et al., 2007), the pelvic sucker would need to resist the force of gravity on the body, which would be proportional to its mass, or L^3 (Maie et al., 2007). If these fish grew isometrically, increases in gravitational force would outpace increases in adhesion through growth of sucker surface area, suggesting that either positively allometric growth of the sucker relative to mass, or other compensatory mechanisms, would be required if climbing performance were to be prevented from declining among adults (Maie et al., 2007).

In this study, I measured adhesive performance (pressure differential and force of attachment) across wide ranges of body size in six species of stream gobies from the

islands of Hawai'i and Honshu (Mainland, Japan) in the Pacific Ocean, as well as Dominica in the Caribbean Sea, that differ in climbing ability, patterns of climbing mechanics, and penetration of upstream habitats. My first goal was to experimentally verify that suction is the adhesive mechanism exhibited in the pelvic suckers of these species. More broadly, My comparisons across taxa and body size allowed me to test several additional predictions. First, I compared adhesion in a non-climbing species, *Stenogobius hawaiiensis* (Watson 1991), and a species that does not climb as an adult, *Awaous guamensis* (Valenciennes 1837) with the performance of four species from the sicydiine lineage that retain climbing performance as adults: *Lentipes concolor* (Gill 1860), *Sicydium punctatum* (Perugia 1896), *Sicyopterus japonicus* (Tanaka 1909), and *Sicyopterus stimpsoni* (Gill 1860). Data from non-climbing *St. hawaiiensis* allow me to evaluate whether non-climbing species cannot adhere sufficiently to support the body on an inclined climbing surface, and provide a comparative baseline for evaluating the extent to which the performance of climbing species is elevated above an unspecialized condition. In addition, while *A. guamensis*, *L. concolor*, and *S. punctatum* all have only a single adhesive structure (the pelvic sucker) and, as juveniles, use strong undulations of the body axis during climbing (a behavior termed "powerburst climbing": Schoenfuss and Blob, 2003), both species of *Sicyopterus* possess an additional oral adhesive structure (the oral sucker) formed from a velum on the upper lip, and 'inch up' surfaces via alternate attachment of the oral and pelvic suckers (Fukui, 1979; Schoenfuss, 1997; Schoenfuss and Blob, 2003). Comparisons across my focus species will, therefore, allow me to assess the relative adhesive capacities of these two climbing mechanisms. Finally,

my comparisons both across species and through variation in body size within species will allow me to test how well the size of the pelvic sucker predicts its adhesive capacity (e.g., Maie et al., 2007). If size is the primary determinant of the strength of goby suckers, then the scaling patterns of the sucker should provide substantial insight into how climbing capacity can be maintained as fish grow.

MATERIALS AND METHODS

Fish collection

Fish from all species were collected with a prawn net while snorkeling in their native streams (see Table 2.1 for localities and body size ranges). After collection, fish were kept in aerated stream water at ambient temperature (18-21^{o}C) until transport to local research facilities for testing (see below).

Species	Climbing Style	N	Body Mass (g)	Locality	Island	Year
Stenogobius hawaiiensis	non-climbing	19	0.11 - 8.97 (82-fold)	Hakalau stream, Waiakea pond	Island of Hawai'i, Hawai'i	2011
*Sicyopterus stimpsoni**	climbing, "inch-up"	16	0.11 - 15.36 (140-fold)	Hakalau & Maili streams	Island of Hawai'i, Hawai'i	2011
Awaous guamensis	climbing juvenile only, "power-burst"	7	0.035 - 1.505 (43-fold)	Hakalau, Honoli'i, Maili, & Nanue streams	Island of Hawai'i, Hawai'i	2009, 2010
*Sicyopterus stimpsoni**	climbing, "inch-up"	21	0.11 - 16.49 (150-fold)	Great crack, Maili & Nanue streams	Island of Hawai'i, Hawai'i	2009
Lentipes concolor	climbing, "power-burst"	12	0.040 - 5.02 (126-fold)	Manoloa & Nanue streams	Island of Hawai'i, Hawai'i	2009
Sicydium punctatum	climbing, "power-burst"	15	0.077 - 14.58 (189-fold)	Check Hall & Batalie rivers	Dominica, West Indies	2008
Sicyopterus japonicus	climbing, "inch-up"	11	0.14 - 12.67 (91-fold)	Koza river	Wakayama, Japan	2009

Table 2.1: Characteristics of gobiid stream fishes examined in this study, including climbing behaviors, body size, and collection data. *Two sets of the climbing species *Sicyopterus stimpsoni* were used for adhesive pressure recordings, in addition to a third set of *Si. stimpsoni* (N=32; 1.67 - 15.12g from Nanue stream, Island of Hawai'i, 2009) used for calculation of the coefficient of friction of the climbing surface. (see text)

Pressure and force measurement

Evaluation of passive adhesive suction – To assess how the area and surface of the pelvic sucker might passively contribute to adhesion, independent of the action of associated structures (e.g. extrinsic pelvic muscles), I evaluated the suction generated by anesthetized individuals (hereafter referred to as 'passive adhesion') of non-climbing *St. hawaiiensis*, and the climbing species *Si. stimpsoni* [tricaine methanesulfonate (MS-222), 0.26 g L^{-1} (Lumb, 1963)]. Immediately after anesthesia (submerging fish into MS-222 solution until the cessation of movement), fish were lightly blotted and placed with the pelvic sucker over a hole drilled in a hinged Plexiglas plate coated with fine sand attached by spray glue (Figure 2.1A). A 1 mm cannula fitted tightly into the hole was connected to a pressure transducer with a data acquisition interface (SensorDAQ, Vernier Software & Technology, Beaverton, OR, USA). A hinge was used to adjust the angle of the cannulated surface so that suction pressures could be recorded (200 Hz; LabView 8.5, National Instruments, Austin, TX, USA) at each of three inclinations (45°, 90°, >90°: Figure 2.1A). The inclination greater than 90^{o}, indicated as $>90^{o}$, was the angle above which the fish could not hold or support their body on the testing surface, and varied among individuals for both species (ranging $90\text{-}180^{o}$). Prior to each trial, ambient atmospheric pressure was recorded for 10 seconds, and the average pressure from this period was used to calculate suction pressure differentials ($\Delta P = P_{ATM} - P_{SUCTION}$). For each individual, area of the pelvic sucker was calculated as an ovoid from maximum width and length measurements collected directly (Area = Width*Length*π/4: Schoenfuss and Blob, 2003; Blob et al., 2006; Maie et al., 2007); pressure differentials were then multiplied by this value to calculate adhesive suction forces generated by the

pelvic sucker (Force = Area*ΔP). For each individual, I collected 17-22 pressure recordings for each inclination, and selected the five highest values at each inclination to represent maximum adhesive capacity. After data collection, individuals used in this portion of the study were placed in an aerated tank for recovery and returned back to stream sites where they were captured.

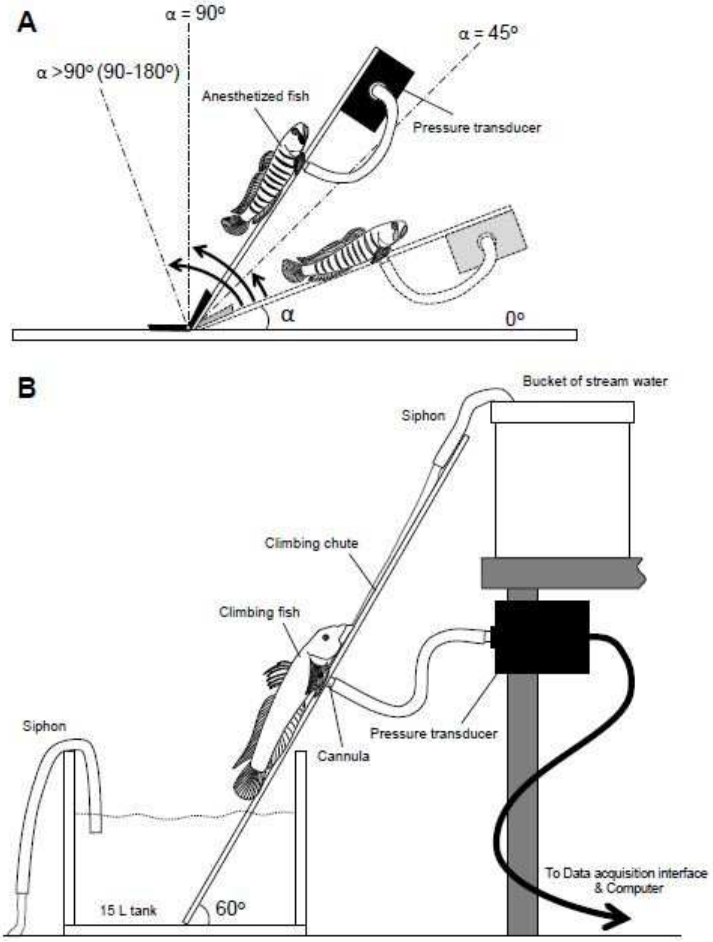

Figure 2.1: Schematic illustrations of pressure recording setups. (A) Testing surface with adjustable inclination (45, 90, and >90°) for evaluating passive adhesive suction by anesthetized individuals of non-climbing vs. climbing gobiids. (B) Experimental setup with 60° inclined climbing chute (using the same surface from A) for evaluating adhesive suction by climbing gobiids.

Evaluation of adhesive suction during climbing – To measure suction produced during climbing, I inserted the cannula of the pressure transducer snuggly into a hole 20 cm from the bottom of a sand-coated, Plexiglas climbing chute angled at 60° from the horizontal (e.g., Blob et al., 2006, 2007) and placed in a small (15 L) tank (Figure 2.1B). Stream water from a bucket was released over the climbing surface by siphon at 250 mL/min, producing a sheet 1 mm in depth (Figure 2.1B). As individual fish in the tank climbed up the surface over the cannula (see Figures 2.1B, 2.2), pressure differentials (Figure 2.3) were collected and suction forces calculated as in the evaluations of passive adhesive suction described above, with two additions. First, because the fish needed to climb directly over the cannulated portion of the chute to obtain a valid reading, the position of each fish during climbing was closely monitored using a high-speed camera (250 Hz; Redlake, Tucson, AZ, USA). Second, pressure measurements (20-30 recordings collected from each individual) and force calculations were obtained from the oral sucker as well as the pelvic sucker in both species of *Sicyopterus* (*Si. stimpsoni* and *Si. japonicus*), with a calculated oval area of the oral sucker (e.g., Schoenfuss and Blob, 2003) as 45% of the area of the pelvic sucker based on data from *Si. stimpsoni* (N=5; 45±1%).

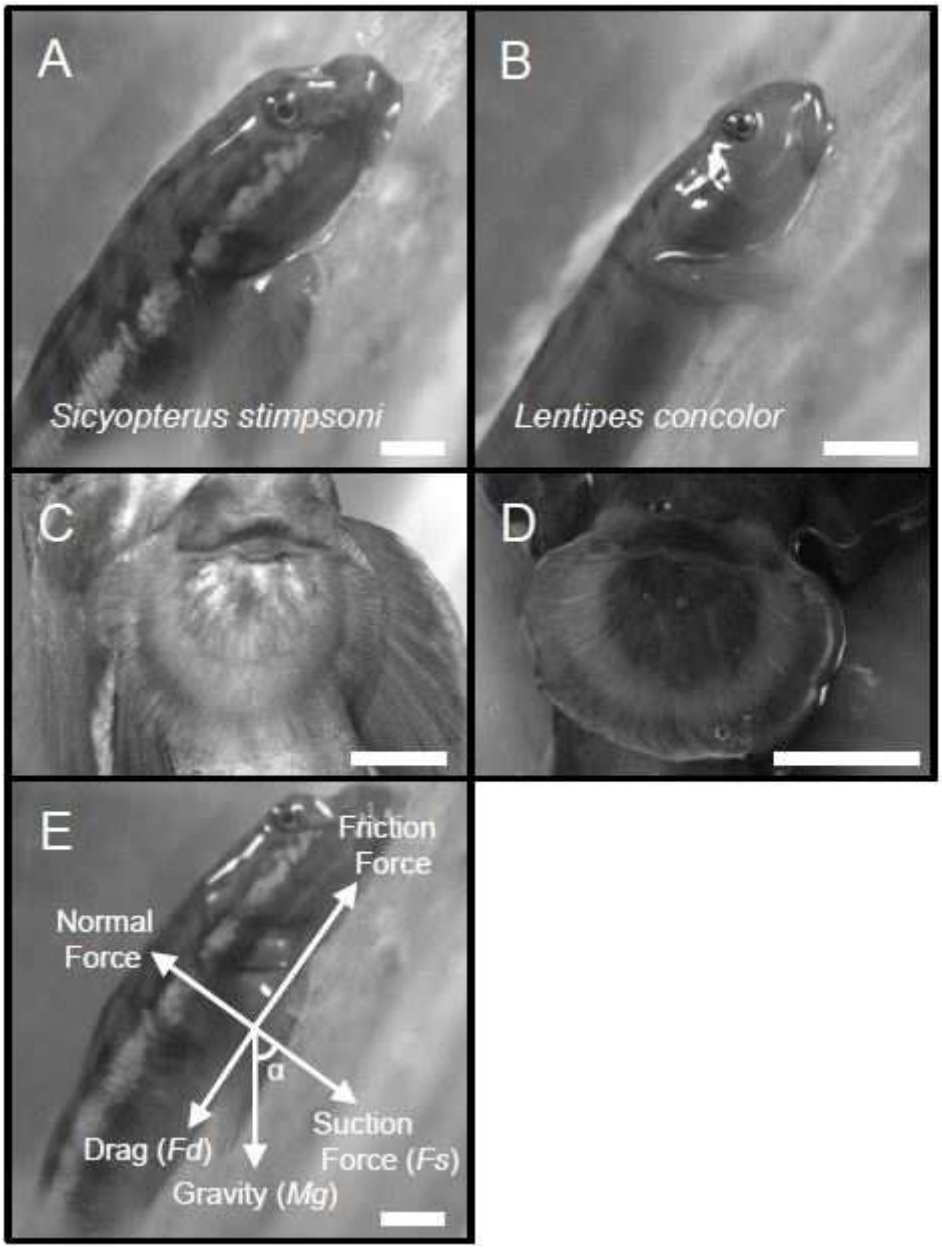

Figure 2.2: Lateral and ventral views of adult *Sicyopterus stimpsoni* (A, C, and E) and adult *Lentipes concolor* (B and D). Lateral views (A and B) show their pectoral fins (pelvic suckers can be seen behind the pectoral fins). Ventral views (C and D) show their pelvic suckers. Arrows in (E) represent forces these climbing gobies experience while climbing on the inclined surface. Each scale bar represents 5 mm.

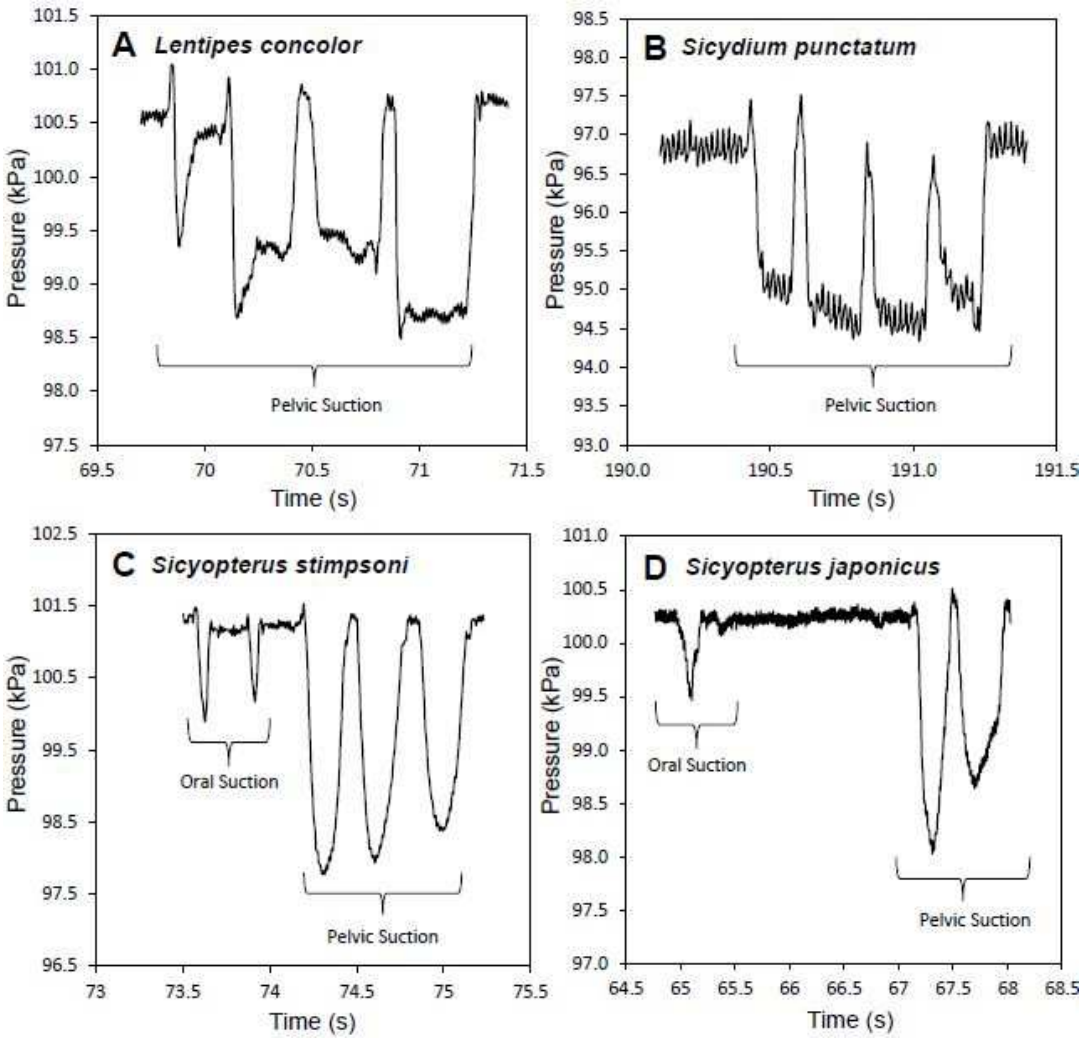

Figure 2.3: Examples of pressure profile, extracted from representative (A) *Lentipes concolor* (body mass = 5.04g), (B) *Sicydium punctatum* (body mass = 10.07g), (C) *Sicyopterus stimpsoni* (body mass = 11.19g), and (D) *Sicyopterus japonicus* (body mass = 7.43g). Two smaller peaks in the profile from *Si. stimpsoni* and *Si. japonicus* represent suction by the mouth (oral suction) and three larger peaks represent suction by the pelvic sucker (pelvic suction).

Measurements of suction pressure were placed in the context of the minimum forces required for gobies to adhere during climbing. For gobies to establish static equilibrium on a surface, they must resist both gravitational force and hydrodynamic drag

using their adhesive suckers. As they create a pressure differential for adhesion, they would experience the normal reaction force perpendicular to the climbing surface (Figure 2.2E). With this model, the minimum suction force sufficient for gobies to adhere to a climbing surface can be calculated as $F_s = (F_d + Mg*\sin\alpha)/\mu - Mg*\cos\alpha$, where F_s is the suction force, F_d is the drag from water flowing over the body, Mg is gravitational force, α is the incline of the climbing surface, and μ is the static coefficient of friction between the fish and the surface (Figure 2.2E). In this study, I made a simplifying assumption that, during climbing, the effect of drag could be neglected because gobies (particularly species of *Sicyopterus*) typically choose routes with minimal water depth, and their bodies are predominantly out of the water (Schoenfuss and Blob, 2003; Blob et al., 2007; Maie, pers. obs.): this reduced the equation to $F_s = (Mg/\mu)*(\sin\alpha - \mu*\cos\alpha)$. The static coefficient of friction (μ) of the climbing surface (Plexiglas coated with fine sand) used for all of my experiments was measured as the tangent of the incline (tan α') at which a fish placed on its side (i.e., with no adhesive sucker contacting the substrate) began to slide down the surface. A sample of *Si. stimpsoni* from the Island of Hawai'i (Nanue stream), collected in 2009 separately from those used for other experiments (N=32; 1.67–15.12g), was used to generate the evaluation of the static coefficient of friction.

It is possible that my assumptions of negligible hydrodynamic drag and constant coefficient of friction on the climbing surface could affect my estimates of adhesive performance, potentially leading to underestimation of the suction force required for adhesion. For example, any hydrodynamic drag experienced during climbing would be expected to increase the suction force required for adhesion. In addition, accounting for

the potential of fish to slide down along the climbing surface would require me to convert the static coefficient of friction to a kinetic coefficient, which is lower than the value of the static coefficient and would also lead to a greater suction force being required for adhesion. Also, due to specimen availability my static coefficient of friction was evaluated from only one species (e.g., *Si. stimpsoni*), but this value might vary among species; in particular, *Lentipes concolor* lacks scales on its body and, thus, might incur a lower coefficient of friction that would require greater adhesive force. Nonetheless, given the general similarity across my study species in patterns of body scalation and tendency to climb while emergent from water, I believe that my assumptions are reasonable simplifications that provide a repeatable baseline for standardized minimum estimates of required adhesive performance across my study species, facilitating my comparative analysis.

Statistical Analysis

Statistical analyses were performed using JMP 9.0 for Windows (SAS Institute Inc., Cary, NC, USA). For each species, I evaluated four scaling relationships between: 1) body mass and pelvic sucker area; 2) body mass and pressure differential by the pelvic sucker; 3) body mass and adhesive suction force by the pelvic sucker; and 4) pelvic sucker area and suction force. For the two *Sicyopterus* species, I evaluated three additional scaling relationships between: 1) body mass and pressure differential achieved by the oral sucker; 2) body mass and adhesive suction force produced by the oral sucker; and 3) the area of the oral sucker and suction force. For these analyses, all data were log

(base 10)-transformed and used to generate model II reduced major axis (RMA) regressions, which account for structural relationships between variables when both are subjected to error (Rayner, 1985; McArdle, 1988; LaBarbera, 1989). A scaling relationship was considered allometric if the 95% confidence interval (e.g., Jolicoeur and Mosimann, 1968) for its RMA slope failed to overlap the slope predicted for isometry. In addition, I used Tsutakawa's non-parametric quick test (Tsutakawa and Hewett, 1977) to evaluate differences in each structural and functional variable between species while accounting for differences in body mass and pelvic sucker size among species (Swartz, 1997; Blob, 2000). In these comparisons, a pooled RMA regression line was calculated for the two groups being compared, and the numbers of points above and below the line were counted for each group, producing a 2x2 contingency table to which Fisher's Exact test ($\alpha<0.05$) was applied (Tsutakawa and Hewett, 1977; Swartz, 1997; Blob, 2000; Maie et al., 2007).

Because of the range of both morphological and functional variables I considered and their differing dimensionalities, I will briefly clarify my expectations for isometry in my comparisons. First, as briefly noted earlier, under isometric growth the area of an adhesive pelvic sucker would be expected to increase as body length $(L)^2$, whereas body mass would be expected to increase as L^3, producing an expected slope of 0.667. My model for how pressure differentials are expected to scale with isometric increases in body size requires more explanation. Pressure is a force divided by an area. For pelvic suckers in suction, the area considered is the area of the sucker, and with isometric growth of the body this would be expected to scale as L^2. But what force contributes to

the generation of pressure differentials in the sucker? Sub-ambient pressures in the pelvic sucker must be achieved by increasing the volume inside the sucker, which would decrease the pressure relative to the outside environment (Kier and Smith, 1990). In fish using active adhesion, a primary mechanism expected to increase the volume under the sucker would be the use of extrinsic retractor muscles of the pelvic fins to pull upward on the sucker after a seal had been formed between the sucker and the substrate. These muscles would then contribute to the primary force-generating adhesive, sub-ambient pressures (i.e., pressure differentials). Because the force produced by a muscle can be modeled as proportional to the cross-sectional area of the muscle (e.g., Hill, 1950), then the force contributing to the pressure differential also could be modeled as proportional to an area, or L^2. As a result, pressure differentials of climbing gobies can be modeled to increase in proportion to the ratio of an area (L^2) over an area (L^2) – in other words, with an exponent or slope of zero, or independent of body size. Without the use of such muscles to generate suction (e.g. during passive adhesion), pressure differentials might even be expected to decrease as body size increased. Conversely, if pressure differentials show a positive increase in slope as fish increase in size, then it is possible that the cross-sectional areas of fin retractor muscles grow with positive allometry relative to body mass rather than isometry, or that size-related changes in the lever mechanics of these muscles could amplify their potential for force production. Moreover, based on this expectation for the scaling of pressure differentials under isometry, the scaling of suction forces (sucker area*pressure differential) can also be considered. If pressure differentials scale independently from body size, then under isometric growth suction forces should

scale in direct proportion to the area of the sucker (1.0), or by L^2/L^3 (0.667) relative to body mass.

RESULTS

Passive adhesion by the pelvic suckers of non-climbing and climbing gobies

For the fish from my sample used to evaluate passive adhesion (i.e., adhesion by the pelvic sucker of anesthetized fish), Tsutakawa's quick test indicated that non-climbing *St. hawaiiensis* have larger pelvic suckers than climbing *Si. stimpsoni* at any given body size ($P<0.0001$: Figure 2.4A). Moreover, I found strong positive allometry of pelvic sucker area relative to body mass for non-climbing *St. hawaiiensis* (slope 95% CI = 0.745-0.933: Table 2.2), but isometric growth of pelvic sucker area relative to body mass for climbing *Si. stimpsoni* (slope 95% CI of 0.601-0.987 overlaps isometric slope of 0.667: Table 2.2) consistent with previous findings for this species (Maie et al., 2007).

x	y	species	incline°	n	r^2	RMA intercept ± 95% CL	RMA slope (95% CI)	*Expected RMA by isometry*	*Allometry*
BM	MSA	*St. hawaiiensis*	n/a	19	0.951	1.792 ± 0.061	0.834 (0.745 - 0.933)	0.667	+
BM	ΔPps	*St. hawaiiensis*	45	95	0.130	-0.740 ± 0.034	-0.277 (- 0.336 - -0.229)	0.000	-
BM	Fps	*St. hawaiiensis*	45	95	0.850	-2.122 ± 0.040	0.773 (0.714 - 0.838)	0.667	+
MSA	Fps	*St. hawaiiensis*	45	95	0.890	-3.757 ± 0.127	0.927 (0.866 - 0.993)	1.000	-
BM	ΔPps	*St. hawaiiensis*	90	95	0.042	-0.595 ± 0.026	-0.195 (-0.239 - -0.160)	0.000	-
BM	Fps	*St. hawaiiensis*	90	95	0.916	-1.924 ± 0.032	0.808 (0.761 - 0.857)	0.667	+
MSA	Fps	*St. hawaiiensis*	90	95	0.946	-3.596 ± 0.094	0.970 (0.924 - 1.017)	1.000	0 (near -)
BM	ΔPps	*St. hawaiiensis*	>90	95	0.062	-0.488 ± 0.016	-0.116 (-0.142 - -0.095)	0.000	-
BM	Fps	*St. hawaiiensis*	>90	95	0.920	-1.794 ± 0.030	0.816 (0.770 - 0.865)	0.667	+
MSA	Fps	*St. hawaiiensis*	>90	95	0.980	-3.481 ± 0.058	0.980 (0.952 - 1.009)	1.000	0 (near -)
BM	MSA	*Si. stimpsoni*	n/a	16	0.809	2.351 ± 0.099	0.770 (0.601 - 0.987)	0.667	0
BM	ΔPps	*Si. stimpsoni*	45	80	0.560	-0.739 ± 0.046	0.589 (0.508 - 0.684)	0.000	+
BM	Fps	*Si. stimpsoni*	45	80	0.879	-2.407 ± 0.048	1.210 (1.118 - 1.308)	0.667	+
MSA	Fps	*Si. stimpsoni*	45	80	0.841	-5.117 ± 0.229	1.569 (1.434 - 1.717)	1.000	+
BM	ΔPps	*Si. stimpsoni*	90	80	0.541	-0.618 ± 0.050	0.627 (0.538 - 0.730)	0.000	+
BM	Fps	*Si. stimpsoni*	90	80	0.885	-2.239 ± 0.048	1.227 (1.136 - 1.324)	0.667	+
MSA	Fps	*Si. stimpsoni*	90	80	0.814	-5.307 ± 0.251	1.593 (1.445 - 1.755)	1.000	+
BM	ΔPps	*Si. stimpsoni*	>90	80	0.568	-0.498 ± 0.058	0.762 (0.657 - 0.883)	0.000	+
BM	Fps	*Si. stimpsoni*	>90	80	0.888	-2.082 ± 0.052	1.345 (1.247 - 1.450)	0.667	+
MSA	Fps	*Si. stimpsoni*	>90	80	0.772	-6.190 ± 0.305	1.746 (1.568 - 1.944)	1.000	+

Table 2.2: Scaling coefficients (RMA intercept ± 95% confidence limits, CL) and exponents (RMA slope, with asymmetric 95% confidence interval, CI) for maximum pelvic sucker area (MSA), pelvic suction pressure differential (ΔPps), and pelvic suction force (Fps) for adhesion predicted from body mass (BM) of *Stenogobius hawaiiensis* and *Sicyopterus stimpsoni* at three incline levels (45°, 90° and >90°) of climbing slope. Five maximum performance values for pressure differential and suction force from each anesthetized individual (passive adhesion) were used for the analysis.

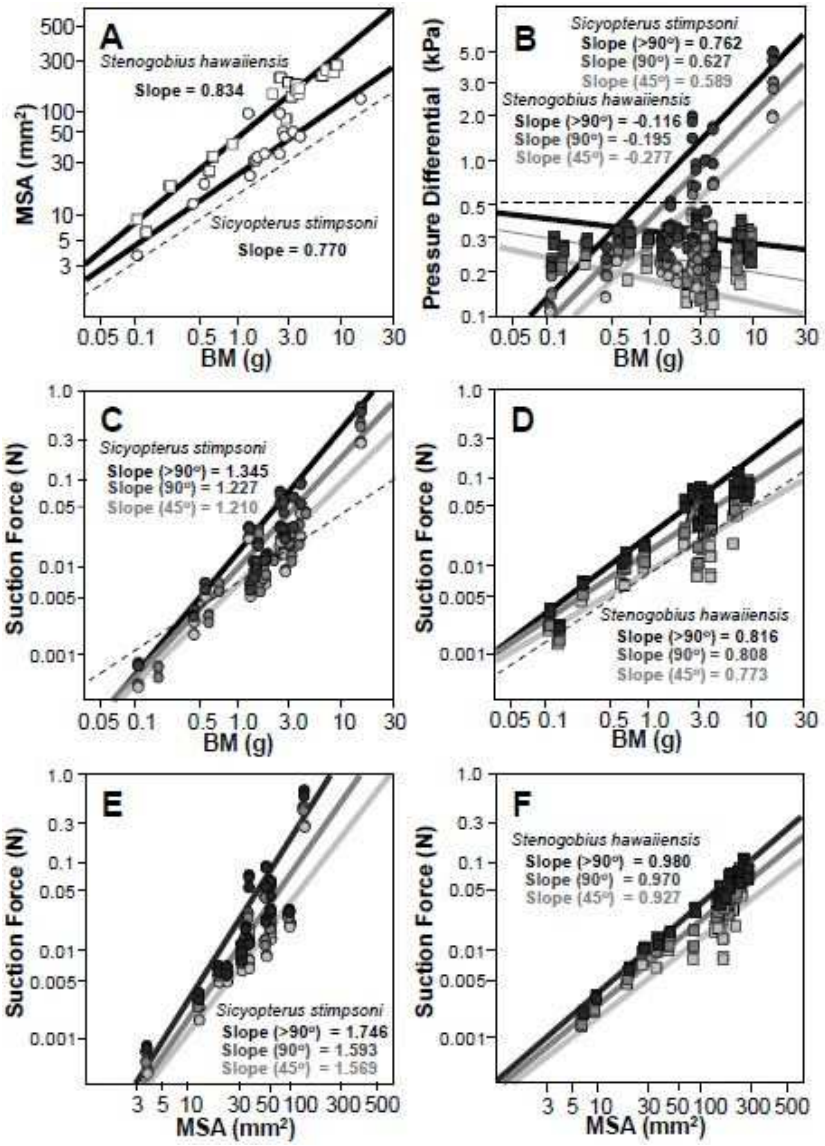

Figure 2.4: Log-log plots of reduced major axis (RMA) regression based on morphological and performance data for climbing goby, *Sicyopterus*

stimpsoni (circle), and non-climbing goby, *Stenogobius hawaiiensis* (square), on a hinged climbing surface with three distinct inclines (45^{o}, 90^{o}, and >90^{o}) upon anesthesia: (A) maximum pelvic sucker area (MSA) versus body mass (BM) for both species; (B) pressure differential versus BM for both species; (C) suction force versus BM for *Si. stimpsoni* and (D) *St. hawaiiensis*; (E) suction force versus MSA for *Si. stimpsoni* and (F) *St. hawaiiensis*. Inclines are differentiated by gray colors (lighter to darker; 45^{o} to >90^{o}). For each panel A-F, an expected line for isometry is indicated as a dotted line. (See Table 2.2 for parameters of scaling equations.

At all incline levels of the climbing surface, both non-climbing *St. hawaiiensis* and climbing *Si. stimpsoni* showed strong correlations between morphological variables (body mass and pelvic sucker size) and most functional variables (Table 2.2, Figure 2.4A-F), though most scaling patterns were significantly different between the two species. In both species, scaling exponents for pressure differential with respect to body mass became greater as the incline of the surface increased (Table 2.2, Figure 2.4B). These increases in scaling exponent with incline are generally significant: confidence intervals for regression slopes showed some overlap for *Si. stimpsoni* between 45° and 90°, but almost no overlap (0.010) between these inclines for *St. hawaiiensis*, and no overlap between 90° and >90° for either species (Table 2.2). However, while slopes indicated negative allometry for *St. hawaiiensis* (with fairly weak correlation coefficients and near-zero slopes), slopes indicated positive allometry for *Si. stimpsoni* (Table 2.2, Figure 2.4B). In addition, Tsutakawa's quick test indicated that pressure differentials generated at 45^{o} did not differ between the two species (P=0.1938), but the pelvic sucker of *Si. stimpsoni* exhibited a much greater pressure differential than *St. hawaiiensis* at 90^{o} (P<0.0001) and at the greater incline (>90^{o}; P=0.0096).

Scaling exponents for adhesive suction force relative to body mass indicated positive allometry for both species (i.e., 95% CI>0.667: Table 2.2), and also tended to increase as the incline increased (Table 2.2, Figures 2.4C, 2.4D). However, although scaling exponents of *Si. stimpsoni* were much greater than those of *St. hawaiiensis*, Tsutakawa's quick test indicated that, at any given body size, the pelvic sucker of *St. hawaiiensis* could generate greater magnitudes of suction force at both 45^o ($P<0.0001$) and 90^o inclines ($P=0.0365$), and generated comparable forces to *Si. stimpsoni* at $>90^o$ ($P=0.1319$).

My trials to evaluate the static coefficient of friction (μ) of the climbing surface resulted in a size-independent ($r^2=0.0055$) μ of 0.494±0.088, a value that falls in a range between rough surfaces and viscoelastic materials (e.g., 0.4–0.8: Persson, 2001; Mofidi et al., 2008). I used this value to assess minimum required adhesive suction forces as $F_s = 2.023*Mg*(\sin\alpha - 0.494*\cos\alpha)$ for $0<\alpha<180^o$. On such a climbing surface, inclinations between 52.6^o and 180^o would require a fish to generate suction force greater than their body weight (up to about twice body weight at maximum incline). In addition, for static adhesion on the 45^o and 90^o inclined surface used in my trials, the required F_s was $0.723*Mg$ or 0.723*body weight, and $2.023*Mg$ or 2.023*body weight, respectively. The pelvic sucker of *Si. stimpsoni* could support 0.72 times its body weight at 45^o incline, 0.99 times at 90^o incline, and 1.5 times at $>90^o$ incline (Table 2.3). The pelvic sucker of *St. hawaiiensis* could support 0.98 times its body weight at 45^o incline, 1.3 times at 90^o incline, and 1.7 times at $>90^o$ incline (Table 2.3). The presence of values below the required performance is noteworthy, indicating that, since the fish did not come off the

testing surface, other factors beyond just passive adhesive suction must have contributed to adhesion in such instances (see discussion).

Species	Incline°	Suction force per BM (N/g)	Support capacity (Body Weight)	
St. hawaiiensis	45	0.00956 ± 0.00051	0.976 ± 0.052	P < 0.0001*
Si. stimpsoni	45	0.00704 ± 0.00046	0.719 ± 0.047	
St. hawaiiensis	90	0.0126 ± 0.00059	1.287 ± 0.060	P = 0.0365*
Si. stimpsoni	90	0.00969 ± 0.00065	0.989 ± 0.066	
St. hawaiiensis	>90	0.0164 ± 0.00071	1.678 ± 0.073	P = 0.1319
Si. stimpsoni	>90	0.0147 ± 0.00108	1.501 ± 0.110	

Table 2.3: Pelvic suction force (for passive adhesion) generated by the anesthetized pelvic sucker of *Stenogobius hawaiiensis* and *Sicyopterus stimpsoni* on three incline (45°, 90° and >90°) of climbing slope, and capacity to support their body weight at each incline. Values indicate mean ± s.e.m.

The scaling of adhesive suction force relative to sucker area showed different allometric patterns than scaling relative to body mass. *St. hawaiiensis* showed negative allometric or nearly negative isometric scaling of adhesive suction force relative to area for all inclines, whereas *Si. stimpsoni* showed positively allometric patterns for these variables at all inclines (Table 2.2, Figures 2.4E, 2.4F). In addition, Tsutakawa's quick tests indicated *St. hawaiiensis* could generate a greater suction force, at any given sucker size, at 45° incline (P=0.0191) than *Si. stimpsoni*, but, *Si. stimpsoni* generated greater forces at both 90° and greater inclines than *St. hawaiiensis* (P<0.0001 for both comparisons).

Adhesive performance and scaling pattern among waterfall climbing gobies

All collected size classes of the sicydiine species, *Lentipes concolor*, *Sicyopterus stimpsoni*, *Sicydium punctatum*, and *Sicyopterus japonicus*, and also the closely related species *Awaous guamensis*, were able to climb on the inclined (60^{o}) artificial waterfall surface using their pelvic suckers **(**Figure 2.3**)**, and all species showed strong correlations between morphological and adhesive performance variables (Table 2.4, Figure 2.5A). The sucker areas of *S. punctatum* and *Si. japonicus* exhibited negative allometry with respect to body mass (0.559 and 0.460, respectively; 95% CI<0.667: Table 2.4, Figure 2.5A), whereas isometric scaling was indicated for the three species of climbing goby native to Hawai'i (*L. concolor*, 0.641; *Si. stimpsoni*, 0.659; *A. guamensis*, 0.730: Table 2.4, Figure 2.5A).

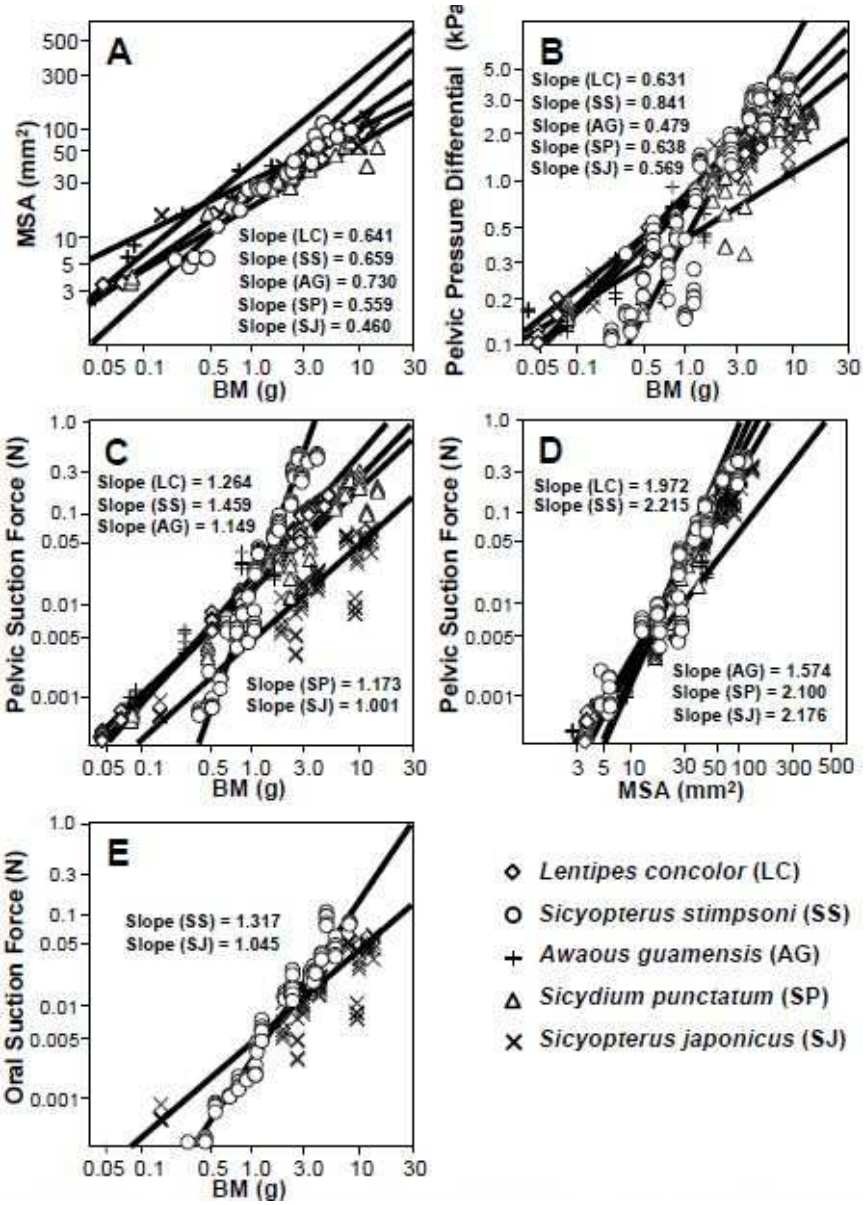

Figure 2.5: Log-log Plots of RMA regression based on morphological and performance data for waterfall-climbing gobies (*Lentipes concolor*, LC; *Sicyopterus stimpsoni*, SS; *Awaous guamensis*, AG; *Sicydium punctatum*, SP; *Sicypterus japonicus*, SJ): (A) maximum pelvic sucker area (MSA) versus body mass (BM); (B) pelvic pressure differential versus BM; (C) Pelvic suction force versus BM; (D) Pelvic suction force versus MSA; and (E) Oral suction force versus BM. Scaling coefficients for each plot are indicated accordingly with corrected regression lines. For each panel A-E, an expected line for isometry is indicated as a dotted line. See Table 2.4 for parameters of scaling equations.

Tsutakawa's quick test indicated that the sicydiine goby species examined in my study did not differ significantly in the size of the pelvic sucker at any given body size ($P>0.05$); however, the weakly climbing, non-sicydiine species *A. guamensis* has a significantly larger pelvic sucker than *L. concolor* ($P=0.0198$) and *Si. stimpsoni* ($P=0.0286$) at any given body size, and does not show a significant difference in size from the large pelvic sucker exhibited by non-climbing *St. hawaiiensis* (Tsutakawa's test, $P>0.9999$).

x	y	Species	n	r^2	RMA intercept ± 95% CL	RMA slope (95% CI)	*Expected RMA by isometry*	*Allometry*
BM	MSA	*L. concolor*	12	0.989	1.417 ± 0.033	0.641 (0.595 - 0.690)	0.667	0
BM	ΔPps	*L. concolor*	60	0.975	-0.104 ± 0.018	0.631 (0.605 - 0.658)	0.000	+
BM	Fps	*L. concolor*	60	0.995	-1.688 ± 0.016	1.264 (1.241 - 1.288)	0.667	+
MSA	Fps	*L. concolor*	60	0.987	-4.494 ± 0.090	1.972 (1.914 - 2.032)	1.000	+
BM	MSA	*Si. stimpsoni*	21	0.953	1.361 ± 0.046	0.659 (0.594 - 0.731)	0.667	0
BM	ΔPps	*Si. stimpsoni*	105	0.869	-0.266 ± 0.040	0.841 (0.784 - 0.903)	0.000	+
BM	ΔPos	*Si. stimpsoni*	105	0.876	-0.624 ± 0.032	0.700 (0.653 - 0.750)	0.000	+
BM	Fps	*Si. stimpsoni*	105	0.956	-1.986 ± 0.040	1.459 (1.401 - 1.521)	0.667	+
BM	Fos	*Si. stimpsoni*	105	0.971	-2.635 ± 0.030	1.317 (1.274 - 1.362)	0.667	+
MSA	Fps	*Si. stimpsoni*	105	0.932	-6.331 ± 0.175	2.215 (2.105 - 2.330)	1.000	+
MOA	Fos	*Si. stimpsoni*	105	0.937	-4.915 ± 0.119	2.000 (1.903 - 2.099)	1.000	+
BM	MSA	*A. guamensis*	7	0.950	1.637 ± 0.162	0.730 (0.566 - 0.942)	0.667	0
BM	ΔPps	*A. guamensis*	35	0.616	-0.326 ± 0.089	0.479 (0.385 - 0.595)	0.000	+
BM	Fps	*A. guamensis*	35	0.896	-1.801 ± 0.114	1.149 (1.026 - 1.288)	0.667	+
MSA	Fps	*A. guamensis*	35	0.937	-4.337 ± 0.173	1.574 (1.441 - 1.720)	1.000	+
BM	MSA	*S. punctatum*	15	0.944	1.314 ± 0.063	0.559 (0.485 - 0.644)	0.667	-
BM	ΔPps	*S. punctatum*	75	0.875	-0.215 ± 0.042	0.638 (0.588 - 0.693)	0.000	+
BM	Fps	*S. punctatum*	75	0.945	-2.007 ± 0.050	1.173 (1.110 - 1.239)	0.667	+
MSA	Fps	*S. punctatum*	75	0.954	-4.973 ± 0.163	2.100 (1.997 - 2.208)	1.000	+
BM	MSA	*Si. japonicus*	12	0.898	1.521 ± 0.080	0.460 (0.368 - 0.575)	0.667	-
BM	ΔPps	*Si. japonicus*	60	0.855	-0.164 ± 0.044	0.569 (0.515 - 0.629)	0.000	+
BM	ΔPos	*Si. japonicus*	60	0.572	-0.800 ± 0.088	0.664 (0.559 - 0.788)	0.000	+
BM	Fps	*Si. japonicus*	60	0.924	-1.654 ± 0.056	1.001 (0.931 - 1.076)	0.667	+
BM	Fos	*Si. japonicus*	60	0.804	-2.968 ± 0.094	1.045 (0.930 - 1.174)	0.667	+
MSA	Fps	*Si. japonicus*	60	0.933	-4.981 ± 0.266	2.176 (2.033 - 2.329)	1.000	+
MOA	Fos	*Si. japonicus*	60	0.808	-5.956 ± 0.380	2.275 (2.028 - 2.552)	1.000	+

Table 2.4: Scaling coefficients (RMA intercept ± 95% confidence limits, CL) and exponents (RMA slope, with asymmetric 95% confidence interval, CI) for maximum pelvic sucker area (MSA), pelvic suction pressure differential (ΔPps), pelvic suction force (Fps), for adhesion predicted accordingly from body mass (BM) and MSA from *Lentipes concolor*, *Sicyopterus stimpsoni*,*Awaous guamensis*, *Sicydium punctatum*, and *Sicyopterus*

japonicus. Oral sucker area (MOA), oral suction pressure differential (ΔPos), and oral suction force (Fos) were additionally examined from *Si. stimpsoni* and *Si. japonicus*. Five maximum performance values for pressure differential and suction force from each climbing individual on the 60^{o} artificial climbing surface were used for the analysis. Calculations were obtained from RMA regressions of log-transformed measurements: x, regression abscissa; y, regression ordinate, n, sample size. Scaling pattern is indicated as either isometric (0), positively allometric (+), or negatively allometric (-).

For the pelvic sucker, all climbing species showed positive allometry of pressure differential relative to body mass, and all species showed positive allometry of suction force relative to both sucker area and body mass (Table 2.4, Figures 2.5B-D), although the weakly climbing species *A. guamensis* generally showed exponents that were closest to isometric values among the species compared (Table 2.4). Tsutakawa's quick test indicated that *Si. stimpsoni*, at any given body size, generated a maximum pressure differential equivalent to that shown by other Hawaiian "power-burst" climbing gobies (*L. concolor*, P=0.6237; *A. guamensis*, P=0.8424). However, between Hawaiian "power-burst" climbers, *L. concolor* generated a greater maximum pressure differential than *A. guamensis* (P<0.0001) at any given body size. In addition, *S. punctatum* and *Si. japonicus* did not differ from Hawaiian climbing species in pressure differentials at any given body size (P>0.05). For comparisons of pelvic suction force, Tsutakawa's quick test indicated that Hawaiian "power-burst" climbing gobies (*L. concolor* and *A. guamensis*) generated pelvic suction force equivalent to each other (P=0.3977) at any given body size, and both greater than the "power-burst" species, *S. punctatum* (P<0.05), and both of the "inching" species *Si. stimpsoni* and *Si. japonicus* (P<0.05). In addition, *Si. japonicus* generated pelvic suction force greater than *S. punctatum* (P=0.0014), but *Si.*

stimpsoni did not (P=0.0876). Between Hawaiian "power-burst" climbing gobies, it appears that larger suckers of *A. guamensis* (similar in size as *St. hawaiiensis*) compensate for their lower pressure differential compared to *L. concolor* and, thereby, generate equivalent suction force.

Based on the minimum required adhesive suction forces calculated, climbing on the 60^{o} incline would require a fish to generate suction force greater than their body weight (1.253**Mg* or 1.253*body weight). All climbing species tested could generate suction forces with their pelvic suckers well exceeding this minimum required force. On average, *L. concolor* could support 2.4 times body mass, *Si. stimpsoni* could support 2.2 times its body mass with the pelvic sucker, and *A. guamensis* could support 1.8 times its body mass (Table 2.5). *Si. stimpsoni* and *S. punctatum* generated an equivalent magnitude of suction force (Tsutakawa's test, P=0.1526), and both species exhibited greater force than *L. concolor* at any given sucker size (Tsutakawa's test, P=0.00349 and P=0.0006, respectively). Between *Sicyopterus* species, *Si. stimpsoni* generated greater pelvic suction force than *Si. japonicus* at any given sucker size (Tsutakawa's test, P=0.0009). On average, *Si. japonicus* could support 2.5 times its body mass with the pelvic sucker and *S. punctatum* could support 1.7 times its body mass (Table 2.5).

Species	Incline°, Sucker type	Suction force per BM (N/g)	Support capacity (Body Weight)
L. concolor	60, pelvic	0.0239 ± 0.0011	2.436 ± 0.115
Si. stimpsoni	60, pelvic	0.0213 ± 0.0014	2.176 ± 0.140
Si. stimpsoni	60, oral	0.0034 ± 0.0002	0.352 ± 0.021
A. guamensis	60, pelvic	0.0174 ± 0.0018	1.773 ± 0.185
S. punctatum	60, pelvic	0.0166 ± 0.0008	1.689 ± 0.086
Si. japonicus	60, pelvic	0.0249 ± 0.0011	2.545 ± 0.111
Si. japonicus	60, oral	0.0043 ± 0.0002	0.435 ± 0.023

Table 2.5: Suction force generated by waterfall-climbing goby species, *Lentipes concolor*, *Sicyopterus stimpsoni*, *Awaous guamensis*, *Sicydium punctatum*, and *Sicyopterus japonicus*, and capacity to support their body weight while climbing on the 60^{o} artificial waterfall surface. Values indicate mean ± s.e.m.

In addition to the use of pelvic suckers, both inching *Sicyopterus* species, *Si. stimpsoni* and *Si. japonicas*, also use the oral suckers for adhesion (Figures 2.3C, 2.3D), although pressure differentials during oral suction (ΔPos) were less than half those generated during pelvic suction (43.9 ± 2.4% for *Si. stimpsoni*; 41.9 ± 2.1% for *Si. japonicus*; P=0.9539, Mann-Whitney *U* test), and forces from oral suction (Fos) were 19-20% of pelvic suction (19.8 ± 1.1% for *Si. stimpsoni*; 18.9 ± 1.0% for *Si. japonicus*; P=0.96, Mann-Whitney *U* test). By oral suction alone, on average, *Si. stimpsoni* could support only 35% of body weight, and *Si. japonicus* could support 43.5% of body weight (Table 2.5). Oral suction for adhesion in *Si. stimpsoni* and *Si. japonicus* exhibited scaling patterns similar to those exhibited for their pelvic suction (Table 2.3, Figures 2.5C, 2.5E). In addition, Tsutakawa's quick test indicated that both species generated similar pressure differentials (P>0.9999) and forces (P=0.3310) by oral suction at any given body size. However, with an adhesive capacity much less than half that of pelvic suction, these gobies seem unlikely to be able to support their body weight by their mouth alone. The capacity to support body weight shows a slight increase with body size only in *Si. stimpsoni* (r^2=0.3243) but is independent of size in *Si. japonicus* (r^2=0.0037), despite the similarity in both scaling pattern and magnitude of adhesion by the oral suction discs (the mouth) in both *Sicyopterus* species (Table 2.4).

DISCUSSION

Growth and functional performance of pelvic suckers in goby species

The primary variation in patterns of sucker growth among the species I examined was between the non-climbing species *St. hawaiiensis* and the climbing species, particularly the sicydiines *S. punctatum* and *Si. japonicus*. Among the six species I examined, only the non-climbing *St. hawaiiensis* exhibited positively allometric growth of sucker area relative to body mass (Tables 2.2,2.4; Figures 2.4A, 2.5A). In contrast, climbing species exhibited isometric sucker growth or, in *S. punctatum* and *Si. japonicus*, negatively allometric growth with respect to mass (Table 2.4; Figure 2.5A). When compared in the context of adhesive performance measurements, these patterns indicate divergent strategies for the maintenance of adhesive performance through growth.

Non-climbing *St. hawaiiensis* typically do not use the sucker during locomotion along the substrate, which commonly consists of sand and gravel in its habitat (Schoenfuss and Blob, 2007). It is possible that patterns observed in this species may reflect primitive retentions of features that characterize the majority of gobiid species that do not leave water in their life history. In this non-climbing species, with positively allometric sucker growth, passive pressure differentials counterintuitively decrease as body size increases (Figure 2.4B). This pattern is what might be predicted if the generation of sub-ambient pressures depends strongly on the contraction of fin retractor muscles on the sucker and increase the volume it contains, but those muscles could not perform that function due to anesthesia. However, *St. hawaiiensis* maintains positive allometry of suction force relative to body mass (Figure 2.4D), indicating that positive

allometry of sucker area compensates for negative allometry of pressure differentials. With this maintenance of the force across body sizes, even adults were able to remain attached to the inclined substrates of my experiments, indicating that a low adhesive capacity is likely not the only factor limiting the ability of this species to climb. In addition, the relationship of pressure differential to body mass shifted closer to isometry in *St. hawaiiensis* as the inclination of the substrate increased (Figure 2.4B). This might result as the shift to a more vertical orientation of the substrate and body allowed the force of gravity to pull the body away from the substrate and expand sucker volume (producing greater pressure differentials), rather than compressing the sucker towards the substrate.

In contrast to patterns in the non-climbing species I examined, changes in sucker proportions relative to body size do not help maintain adhesive performance in climbing species as they grow, and in some cases (*S. punctatum*, *Si. japonicus*) actually work against it with negatively allometric growth. However, both pressure differentials and adhesive suction forces scale with strong positive allometry in all climbing species, indicating that other factors must contribute to allow these species to maintain climbing performance as they grow. One possibility may be positively allometric increases in the force output of pelvic fin retractor muscles that retract or adduct the sucker to increase its enclosed volume. Such force output allometry might be achieved either through increases in muscular cross sectional area, or allometric changes in the skeletal lever system through which retractor forces are applied. Comparisons of these features across

the climbing species I examined, in a phylogenetic context, could determine the extent to which their performance reflects the common inheritance of an ancestral trait, functional convergence, or, alternatively, an example of many-to-one mapping (Wainwright et al., 2005) in which different combinations of structures produce similar functional output. Available phylogenies (Parenti and Thomas, 1998; Thacker, 2003; Keith et al., 2011) indicate that four of the species I examined (*Si. stimpsoni*, *Si. japonicus*, *S. punctatum*, and *L. concolor*) are closely related within the clade Sicydiinae, but it is unresolved whether the climbing genus *Awaous* or the non-climbing genus *Stenogobius* is more closely related to this group. Thus, even if the structural basis for their performance were similar, the scaling patterns I identified may have evolved independently between *A. guamensis* and other climbing taxa. Although formal analyses of musculoskeletal leverage have not yet been performed in these taxa, the base of the pelvic sucker is much more heavily muscularized in all climbing species compared with non-climbing *St. hawaiiensis*, even though my Tsutkawa's quick test results indicate that the absolute sucker areas of climbing species are generally smaller than those of *St. hawaiiensis* at any given body size. Such muscularization indicates an important role for the fin retractor muscles among effectively climbing species, but why do such species not also exhibit positive allometry of sucker size, particularly since the tissues comprising the fins might be expected to be less energetically demanding than enlarged muscles? It is possible that excessively large pelvic suckers might actually impede functional performance in waterfall climbing, if increased drag or mass of the sucker made it more difficult to advance, or if large sucker size increased the chance of encountering a heterogeneous

climbing surface, making it difficult for the sucker to form an effective seal on the substrate (Blob et al., 2006). Some support for such hypotheses is indicated by selection experiments that required juvenile *Si. stimpsoni* to climb artificial waterfalls, which found significant selection for suckers that were larger in width, but smaller in length (Blob et al., 2010). Nonetheless, enhanced pelvic fin retractor muscles do not appear to be the sole contributor to the adhesive performance of climbing gobies compared to non-climbing species, since Tsutkawa's quick tests indicate that even anesthetized *Si. stimpsoni*, in which the retractors were not active, exhibit greater pressure differentials than non-climbing *St. hawaiiensis* at almost all inclines and body sizes (Figure 2.4B).

Functional capacity of the oral sucker during adhesion

Adhesive capacities of oral suckers were similar between *Si. stimpsoni* and *Si. japonicus*, and were considerably lower than those shown by the pelvic suckers of these species, averaging less than one half the pressure differential (Table 2.5) and less than one fifth the suction force in each taxon. With such limited adhesive performance, it might be difficult for either species to remain attached to substrates by the oral sucker alone. However, previous kinematic studies of climbing by *Si. stimpsoni* have described the 'inching' mode of climbing as involving the alternating attachment of the oral and pelvic suckers to the substrate (Schoenfuss and Blob, 2003; Blob et al., 2007), implying that the oral sucker must provide the sole suction force during some portions of the climbing cycle. How would fish avoid sliding off substrates during such periods? One critical factor may be friction enhancement, which is also provided by the body and

pectoral fins. Although the pectoral fins are used sparingly, if at all, during climbing in juvenile *Si. stimpsoni* (Schoenfuss and Blob, 2003), they become a standard component of the climbing apparatus among adults (Blob et al., 2007). In fact, the pectoral fins are spread maximally over the climbing surface (conveying the greatest possible contact and friction) just as the oral sucker applies its greatest force at maximal expansion [see Fig. 3D in (Blob et al. 2007)]. Nonetheless, it seems likely that it is at this point in the climbing cycle that 'inching' climbers would be most vulnerable to dislodgement.

Pelvic suction performance in gobiids: overkill, precaution, or opportunity?

The adhesive performance of pelvic suckers in climbing gobiids was much greater than would have been predicted from the size of the suckers alone, indicating substantial contributions of the fin retractor muscles and potentially other factors to the adhesive performance of these species (e.g. epidermal microstructure or mucus secretion: Arita, 1967; Nachtigall, 1974; Branch and Marsh, 1978; Green, 1979; Emerson and Diehl, 1980; Grenon and Walker, 1981; Green and Barber, 1988; Das and Nag, 2004; Pinky et al., 2004; Cook et al., 2005; Das and Nag, 2005; Goodwyn et al., 2006; Adams and Reinhardt, 2008). In addition, the absolute performance of climbing gobiid suckers was high relative to the primary force that set the standard for my comparisons, which was the need to suspend the weight of the body against gravity. Across species and individuals of different sizes, the pelvic suckers of climbing gobies typically could support well over twice body weight.

My expectation for body weight to impose the most significant regular force that goby suckers would have to resist was based on video observations of climbing, in which fish chose paths in thin sheets of flowing water that left most of the body unsubmerged (Schoenfuss and Blob, 2003; Blob et al., 2007; Schoenfuss et al., 2011). If these were the only situations ever experienced by climbing gobies, then the adhesive capacities of their pelvic suckers might be regarded as excessive. However, in natural streams and waterfalls, conditions are likely much more unpredictable than the settings in which the preferred behaviors of gobies have been observed. Flash floods from massive rainstorms are known to have washed standing populations of gobies from several species completely out of streams on the island of Kaua'i during Hurricane Iniki (Fitzsimons and Nishimoto, 1995), and one proposed advantage of the amphidromous life style exhibited by these species is to provide an oceanic population reservoir that can re-establish stream populations in the event of such disasters (McDowall, 2003, 2004). The high adhesive capacities of the pelvic suckers in climbing gobiids might be viewed as conveying a margin of safety (Alexander, 1981; Diamond and Hammond, 1992) to help ensure against dislodgement against less severe, but considerably more common, pulses of flow that might periodically expose gobies to much greater forces than body weight. In addition, for gravid females, this elevated adhesive capacity would also help to meet increased demands on performance compared to those experienced by non-gravid females or males (e.g., Scales and Butler, 2007). What might account for the specific range of 'safety factors' exhibited by goby species, or for characteristic variation in values across species, requires further study. However, evidence from systems as varied as limpets living in

tidal environments (Lowell, 1985) to vertebrate limb bones (Blob and Biewener, 1999; Butcher et al., 2008) indicates that higher safety factors become more advantageous as environmental unpredictability increases. Even with a margin of safety, given the potential surges of force to which these fishes can be exposed, it might be viewed as surprising why higher suction performance is not present in these species, and whether the performance they exhibit is subject to physiological constraints or tradeoffs (Blob et al., 2010). Such factors could take on increasing importance in the future, as factors such as global climate change and human use of water resources impact the flow environments of streams (Castro-Santos and Haro, 2006; Schoenfuss and Blob, 2007; Blob and Rivera, 2008). These contexts might provide fruitful future directions for studies of fish adhesive capacities across species and populations from regions with different flow characteristics.

LITERATURE CITED

Adams, R. D. and Reinhardt, U. G. (2008). Effects of texture on surface attachment of spawning-run sea lampreys *Petromyzon marinus*: a quantitative analysis. *J. Fish. Biol.* 73, 1464-1472.

Alexander, R. M. (1981). Factors of safety in the structure of animals. *Sci. Prog.* 67, 109-130.

Arita, G. S. (1967). A comparative study of the structure and function of the adhesive disc of the Cyclopteridae and Gobiesocidae. MS thesis. Univ. British Columbia, Vancouver, Brit. Col.

Bell, K. N. I. (1994). Life cycle, early life history, fisheries and recruitment dynamics of diadromous gobies of Dominica, W. I., emphasizing *Sicydium punctatum* Perugia. Unpubl. Ph.D. diss., Memorial University of Newfoundland, St. John's, Newfoundland, Canada.

Blob, R. W. (2000). Interspecific scaling of the hindlimb skeleton in lizard, crocodilians, felids and canids: does limb bone shape correlate with limb posture? *J. Zool. Lond.* 250, 507-531.

Blob, R. W. and Biewener, A. A. (1999). *In vivo* locomotor strain in the hindlimb bones of *Alligator mississipiensis* and *Iguana iguana*: implications for the evolution of limb bone safety factor and non-sprawling limb posture. *J. Exp. Biol.* 202, 1023-1046.

Blob, R. W. and Rivera, G. (2008). Going with the flow: ecomorphological variation across aquatic flow regimes: an introduction to the symposium. *Integr. Comp. Biol.* 48, 699-701.

Blob, R. W., Rai, R., Julius, M. L. and Schoenfuss, H. L. (2006). Functional diversity in extreme environments: effects of locomotor style and substrate texture on the waterfall climbing performance of Hawaiian gobiid fishes. *J. Zool. Lond.* 268, 315-324.

Blob, R. W., Wright, K. M., Becker, M., Maie, T., Iverson, T. J., Julius, M. L. and Schoenfuss, H. L. (2007). Ontogenetic change in novel functions: waterfall climbing in adult Hawaiian gobiid fishes. *J. Zool. Lond.* 273, 200-209.

Blob, R. W., Kawano, S. M., Moody, K. N., Bridges, W. C., Maie, T., Ptacek, M. B., Julius, M. L. and Schoenfuss, H. L. (2010). Morphological selection and the evaluation of potential tradeoffs between escape from predators and the climbing of waterfalls in the Hawaiian stream goby *Sicyopterus stimpsoni*. *Integr. Comp. Biol.* 50, 1185-1199.

Branch, G. M. and Marsh, A. C. (1978). Tenacity and shell shape in six *Patella* species: adaptive features. *J. Exp. Mar. Biol. Ecol.* 34, 111-130.

Butcher, M. T., Espinoza, N. R., Cirilo, S. R. and Blob, R. W. (2008). In vivo strains in the femur of river cooter turtles (*Pseudemys concinna*) during terrestrial locomotion: tests of force-platform models of loading mechanics. *J. Exp. Biol.* 211, 2397-2407.

Castro-Santos, T. and Haro, A. (2006). Biomechanics and fisheries conservation. In *Fish Physiology Volume 23: Fish Biomechanics* (ed. R. E. Shadwick and G. V. Lauder), pp. 469-523. New York: Academic Press.

Cediel, R. A., Blob, R. W., Schrank, G. D., Plourde, R. C. and Schoenfuss, H. L. (2008). Muscle fiber type distribution in climbing Hawaiian gobioid fishes: ontogeny and correlations with locomotor performance. *Zoology* 111, 114-122.

Carrier, D. R. (1996). Ontogenetic limits on locomotor performance. *Physiol. Zool.* 69, 467-488.

Cook, R. D., Hilliard, R. W. and Potter, I. C. (2005). Oral papillae of adults of the southern hemisphere lamprey *Geotria australis*. *J. Morphol.* 203, 87-96.

Das, D. and Nag, T. C. (2004). Adhesion by paired pectoral and pelvic fins in a mountain-stream catfish, *Pseudocheneis sulcatus* (Sisoridae). *Env. Biol. Fishes* 71, 1-5.

Das, D. and Nag, T. C. (2005). Structure of adhesive organ of the mountain-stream catfish, *Pseudocheneis sulcatus* (Teleostei: Sisoridae). *Acta Zool. Stockh.* 86, 231-237.

Denny, M. W. (1993). *Air and Water: The Biology and Physics of Life's Media.* Princeton, New Jersey: Princeton University Press.

Diamond, J. M. and Hammond, K. A. (1992). The matches, achieved by natural selection, between biological capacities and their natural loads. *Experientia* 48, 551-557.

Emerson, S. B. and Diehl, D. (1980). Toe pad morphology and mechanisms of sticking in frogs. *Biol. J. Linn. Soc.* 13, 199-216.

Fitzsimons, J. M. and Nishimoto, R. T. (1995). Use of fish behaviour in assessing the effects of Hurricane Iniki on the Hawaiian island of Kaua'i. *Env. Biol. Fish.* 43, 39-50.

Ford, J. I. and Kinzie, III. R. A. (1982). Life crawls upstream. *Nat. Hist.* 91, 60-67.

Fukui, S. (1979). On the rock-climbing behaviour of the goby, *Sicyopterus japonicus*. *Jpn. J. Ichthyol.* 26, 84-88.

Goodwyn, P. P., Peressadko, A., Schwarz, H., Kastner, V. and Gorb, S. (2006). Material structure, stiffness, and adhesion: why attachment pads of the grasshopper (*Tettigonia viridissima*) adhere more strongly than those of the locust (*Locusta migratoria*) (Insecta: Orthoptera). *J. Comp. Physiol. A* 192, 1233-1243.

Green, D. M. (1979). Tree frog toe pads: comparative surface morphology using scanning electron microscopy. *Can. J. Zool.* 57, 2033-2046.

Green, D. M. and Barber, D. L. (1988). The ventral adhesive disc of the clingfish *Gobiesox maeandricus*: integumental structure and adhesive mechanisms. *Can. J. Zool*. 66,1610-1619.

Grenon, J. F. and Walker, G. (1981). The tenacity of the limpet, *Patella vulgate* L.: an experimental approach. *J. Exp. Mar. Biol. Ecol.* 54, 277-308.

Herrel, A., Speck, T. and Rowe, N. P. (2006). *Ecology and Biomechanics: A Mchanical Approach to the Ecology of Animals and Plants.* Boca Raton, FL: CRC Press.

Hill, A. V. (1950). The dimensions of animals and their muscular dynamics. *Sci. Prog.* 38, 209-230.

Jolicoeur, R. and Mosimann, J. E. (1968). Intervalles de confiance pour la pente de l'axe majeur d'une distribution normale bidimensionelle. *Biometrie-Praximetrie* 9,121-140.

Keith, P. (2003). Biology and ecology of amphidromous Gobiidae of the Indo-Pacific and Caribbean regions. *J. Fish. Biol.* 63, 831-847.

Keith, P., Vigneux, E. and Marquet, G. (2002). *Atlas des poissons et des crustaces d'eau douce de Polynesie francaise*. Patrimoines naturels, 55. Paris: Museum National d'Histoire Naturelle.

Keith, P., Lord, C., Lorion, J., Watanabe, S., Tsukamoto, K., Couloux, A., and Dettai, A. (2011). Phylogeny and biogeography of Sicydiinae (Teleostei: Gobiidae) inferred from mitochondrial and nuclear genes. *Mar. Biol.* 158, 311-316.

Kier, W. M. and Smith, A. M. (1990). The morphology and mechanics of octopus suckers. *Biol. Bull.* 178, 126-136.

Kinzie, III. R. A. (1988). Habitat utilization by Hawaiian stream fishes with reference to community structure in oceanic island streams. *Env. Biol. Fish.* 22, 179-192.

LaBarbera, M. (1989). Analyzing body size as a factor in ecology and evolution. *Ann. Rev. Ecol. Syst.* 20, 97-117.

Lowell, R. B. (1985). Selection for increased safety factors of biological structures as environmental unpredictability increases. *Science* 228, 1009-1011.

Lumb, W. V. (1963). *Anesthesia of laboratory and zoo animals. In: Small animal anesthesia.* Philadelphia: Lea & Febiger.

Maciolek, J. A. (1977). Taxonomic status, biology, and distribution of Hawaiian *Lentipes*, a diadromous goby. *Pac. Sci.* 31, 355-362.

Maeda, K., Yamasaki, N., Kondo, M. and Tachihara, K. (2008). Reproductive biology and early development of two species of sleeper, *Eleotris acanthopoma* and *Eleotris fusca* (Teleostei: Eleotridae). *Pac. Sci.* 62, 327-340.

Maie, T., Schoenfuss, H. L. and Blob, R. W. (2007). Ontogenetic scaling of body proportions in waterfall-climbing gobiid fishes from Hawai'i and Dominica: implications for locomotor function. *Copeia* 2007, 755-764.

McArdle, B. H. (1988). The structural relationship: regression in biology. *Can. J. Zool.* 66, 2329-2339.

McDowall, R. M. (2003). Hawaiian biogeography and the islands' freshwater fish fauna. *J. Biogeog*. 30, 703-710.

McDowall, R. M. (2004). Ancestry and amphidromy in island freshwater fish faunas. *Fish. Fisheries* 5, 75-85.

McDowall, R. M. (2009). Early hatch: a strategy for safe downstream larval transport in amphidromous gobies. *Rev. Fish. Biol. Fisheries* 19, 1-18.

McGuire, J. A. (2003). Allometric prediction of locomotor performance: an example from southeast Asian flying lizards. *Am. Nat.* 161, 337-349.

McHenry, M. J. and Lauder, G. V. (2006). Ontogeny of form and function: locomotor morphology and drag in zebrafish (*Danio rerio*). *J. Morphol.* 267, 1099-1109.

McMahon, T. A. (1975). Using body size to understand the structural design of animals: quadrupedal locomotion. *J. Appl. Physiol.* 39, 619-627.

Mofidi, M., Prakash, B., Persson, B. N. J. and Albohr, O. (2008). Rubber friction on (apparently) smooth lubricated surfaces. *J. Phys. Cond. Matter* 20, 1-8.

Nachtigall, W. (1974). *Biological Mechanisms of Attachment.* Berlin, Heidelberg, New York: Springer-Verlag.

Nelson, J. S. (1994). *Fishes of the world, 3rd edn.* New York: Wiley.

Ojha. J. and Singh, S. K. (1992). Functional morphology of the anchorage system and food scrapers of a hillstream fish, *Garra lamta* (Ham.) (Cyprinidae, Cypriniformes). *J. Fish. Biol.* 41, 159-161.

Parenti, L. R. and Thomas, K. R. (1998). Pharyngeal jaw morphology and homology in sicydiine gobies (Teleostei: Gobiidae) and allies. *J. Morphol.* 237, 257-274.

Persson, B. N. J. (2001). Theory of rubber friction and contact mechanics. *J. Chem. Phys.* 115, 3840-3841.

Persson, B. N. J. (2007). Wet adhesion with application to tree frog adhesive toe pads and tires. *J. Phys. Cond. Matter* 19, 1-16.

Pinky, Mittal, S., Yashpal, M., Ojha, J. and Mittal, A. K. (2004). Occurrence of keratinization in the structures associated with lips of a hill stream fish *Garra lamta* (Hamilton) (Cyprinidae, Cypriniformes). *J. Fish. Biol.* 65, 1165-1172.

Radtke, R. L., Kinzie, III. R. A. and Folsom, S. D. (1988). Age at recruitment of Hawaiian freshwater gobies. *Environ. Biol. Fish.* 23, 205-213.

Radtke, R. L., Kinzie, III. R. A. and Shafer, D. J. (2001). Temporal and spatial variation in length of larval life and size at settlement of the Hawaiian amphidromous goby *Lentipes concolor*. *J. Fish. Biol*. 59, 928-938.

Rayner, J. M. V. (1985). Linear relations in biomechanics: the statistics of scaling functions. *J. Zool. Lond*. 206, 415-439.

Scales, J. and Butler, M. (2007). Are powerful females powerful enough? Acceleration in gravid green iguanas (*Iguana iguana*). *Integr. Comp. Biol.* 47, 285-294.

Schmidt-Nielsen, K. (1984). *Scaling: Why is Animal Size so Important?* Cambridge: Cambridge University Press.

Schoenfuss, H. L. (1997). Metamorphosis of the Hawaiian stream goby, Sicyopterus stimpsoni: a structural, functional, and behavioral analysis. Unpubl. Ph.D. diss., Louisiana State University, Baton Rouge, Louisiana.

Schoenfuss, H. L. and Blob, R. W. (2003). Kinematics of waterfall climbing in Hawaiian freshwater fishes (Gobiidae): vertical propulsion at the aquatic-terrestrial interface. *J. Zool. Lond.* 261,191-205.

Schoenfuss, H. L. and Blob, R. W. (2007). The importance of functional morphology for fishery conservation and management: application to Hawaiian amphidromous fishes. *Bishop Mus. Bull. Cult. Environ. Stud.* 3, 125-141.

Schoenfuss, H. L., Maie, T., Kawano, S. M. and Blob, R. W. (2011). Performance across extreme environments: comparing waterfall climbing among amphidromous gobioid fishes from Caribbean and Pacific Islands. *Cybium* 35, 361-369.

Shen, K. N., Lee, Y. C. and Tzeng, W. N. (1998). Use of otolith microchemistry to investigate the life history pattern of gobies in a Taiwanese stream. *Zool. Stud.* 37, 322-329.

Swartz, S. M. (1997). Allometric patterning in the limb skeleton of bats: implications for the mechanics and energetics of powered flight. *J. Morphol.* 234, 277-294.

Thacker, C. E. (2003). Molecular phylogeny of the gobioids fishes (Teleostei: Perciformes: Gobioidei). *Mol. Phylo. Evol.* 26, 354-368.

Tsutakawa, R. K. and Hewett, J. E. (1977). Quick test for comparing two populations with bivariate data. *Biometrics* 33, 215-219.

Voegtlé, B., Larinier, M. and Bosc, P. (2002). Étude sur les capacités de franchissement des cabots bouche-rondes (*Sicyopterus lagocephalus*, Pallas, 1770) en vue de la conception de dispositifs adaptés aux prises d'eau du transfert Salazie (Ile de La Réunion). *Bull. Fr. Peche. Piscie.* 364, 109-120.

Vogel, S. (1994). *Life in Moving Fluids: The Physical Biology of Flow, 2nd edn.* Princeton, New Jersey: Princeton University Press.

Wainwright, P. C. and Reilly, S. M. (1994). *Ecological Morphology: Integrative Organismal Biology.* Chicago: University of Chicago Press.

Wainwright, P. C., Alfaro, M. E., Bolnick, D. I. and Hulsey, C. D. (2005). Many-to-one mapping of form to function: a general principle in organismal design? *Integr. Comp. Biol.* 45, 256–262.

Yamasaki, N. and Tachihara, K. (2007). Eggs and larvae of *Awaous melanocephalus* (Teleostei: Gobiidae). *Ichthyol. Res.* 54, 89-91.

CHAPTER THREE

MUSCULOSKELETAL DETERMINANTS OF PELVIC SUCKER FUNCTION IN HAWAIIAN STREAM GOBIID FISHES: INTERSPECIFIC COMPARISONS AND ALLOMETRIC SCALING

SUMMARY

Gobiid fishes possess a distinctive ventral sucker, formed from fusion of the pelvic fins. This sucker is used to adhere to a wide range of substrates including, in some species, the vertical cliffs of waterfalls that are climbed during upstream migrations. Previous studies of waterfall-climbing goby species have found that pressure differentials and adhesive forces generated by the sucker increase with positive allometry as fish grow in size, despite isometry or negative allometry of sucker area. To produce such scaling patterns for pressure differential and adhesive force, waterfall-climbing gobies might exhibit allometry for other muscular or skeletal components of the pelvic sucker that contribute to its adhesive function. In this study, I used anatomical dissections and modeling to evaluate the potential for allometric growth in the cross-sectional area, effective mechanical advantage, and force generating capacity of major protractor and retractor muscles of the pelvic sucker (protractor ischii and retractor ischii) that help to expand the sealed volume of the sucker to produce pressure differentials and adhesive force. I compared patterns for three Hawaiian gobiid species: a non-climber (*Stenogobius hawaiiensis*), a poor climber (*Awaous guamensis*), and a proficient climber (*Sicyopterus stimpsoni*). Scaling patterns were relatively similar for all three species, typically exhibiting isometric or negatively allometric scaling for the muscles and lever

systems examined. Although these scaling patterns do not help to explain the positive allometry of pressure differentials and adhesive force as climbing gobies grow, the best climber among the species I compared, *S. stimpsoni*, does exhibit the highest calculated estimates of effective mechanical advantage, muscular input force, and output force for pelvic sucker retraction at any body size, potentially facilitating its adhesive ability.

INTRODUCTION

Animals must resist a wide range of physical forces imposed by the environment in which they live (Denny, 1993; Vogel, 1994; Wainwright and Reilly, 1994; Herrel et al., 2006). As animals grow, those forces may change as a function of their increase in size (Carrier, 1996; McMahon, 1975; Schmidt-Nielsen, 1984; Maie et al., 2007). To accommodate such changes in forces, many species exhibit compensatory allometric changes in the size or performance of anatomical structures (McGuire, 2003; McHenry and Lauder, 2006). However, in many cases, performance depends on input from multiple structures with a range of anatomical configurations that can lead to equivalent functional performance – a pattern described as 'many-to-one mapping of structure to function' (Wainwright et al., 2005). In such cases, functional equivalence could be maintained through the course of growth via allometric changes in multiple potential structures or combinations of structures.

Gobiid stream fishes from oceanic islands provide an interesting opportunity to explore the potential for allometry of multiple candidate structures to contribute to the maintenance of functional performance through the course of growth. Gobies possess a

diagnostic ventral sucker that forms from fusion of the pelvic fins (Figure 3.1: Nelson, 1994). This pelvic sucker can be used to adhere to a wide range of substrates including, in some amphidromous species, the vertical cliffs of waterfalls. This use of the pelvic sucker to climb waterfalls is particularly dramatic among juveniles of several species that climb during upstream migrations, returning to adult habitats after completing an oceanic larval phase (Radtke et al., 1988; Bell, 1994; Shen et al., 1998; Radtke et al., 2001; Schoenfuss and Blob, 2003; Maie et al., 2007). In general, the adhesive capacity of a sucker would be expected to scale in proportion to the size of the sucker (Emerson and Diehl, 1980; Kier and Smith, 1990; Maie et al., 2007). In a test of this expectation, I previously compared size-related changes in pelvic sucker adhesive capacity across several species of amphidromous gobies, including the non-climbing species *Stenogobius hawaiiensis*, which remains in the near shore estuarine regions of streams during maturation and adulthood after completing its oceanic phase, and several waterfall-climbing species (including *Sicyopterus stimpsoni*, *Sicyopterus japonicus*, *Sicydium punctatum*, *Awaous guamensis*, and *Lentipes concolor*: Maie et al., 2012). I found that, as expected, the non-climber *S. hawaiiensis* exhibited positive allometry of sucker force production that was achieved through positive allometry of its sucker area (Maie et al., 2012). However, my measurements of pressure differentials and adhesive forces generated by the pelvic suckers of waterfall-climbing species indicated that these aspects of performance increased with positive allometry as fish grew in size, despite isometric or even negatively allometric growth of sucker area (Maie et al., 2012). These results raised the question: how do climbing gobies achieve is relative improvement of adhesive

performance under the anatomical constraint of isometric or negative allometric growth in sucker area?

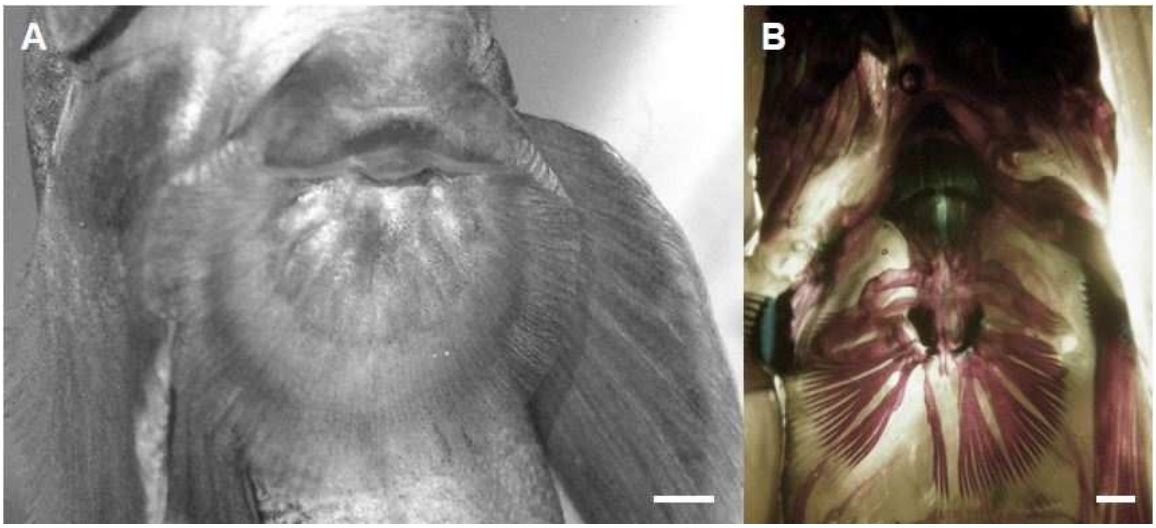

Figure 3.1: Pelvic sucker of Hawaiian stream gobiid, *Sicyopterus stimpsoni*, (A) in the ventral view and (B) clear-and-stained pelvic sucker in the ventral view. Scale bars indicate 5 mm.

To produce positively allometric scaling patterns for pressure differential and adhesive force, waterfall-climbing gobies might exhibit positive allometry for muscular and/or skeletal components of the sucker, other than its surface area, that contribute to its adhesive function. In this study, I used anatomical dissections and modeling to evaluate musculoskeletal factors that could help enhance suction force in climbing gobies even with relatively smaller suckers than non-climbing species. In particular, I evaluated the potential for allometric growth in the cross-sectional area, mechanical advantage, and force generating capacity of major protractor and retractor muscles of the pelvic sucker (protractor ischii and retractor ischii) that act to expand the sealed volume of the sucker

to produce pressure differentials and adhesive force. I compared patterns for three Hawaiian gobiid species: a proficient climber (*Sicyopterus stimpsoni*), a poor climber (*Awaous guamensis*), and a non-climber (*Stenogobius hawaiiensis*). Phylogenetic relationships among these three gobiid species have not been resolved yet, but comparisons of these features across these species, which likely invaded island stream habitats independently (Parenti and Thomas, 1998; Thacker, 2003; Keith et al., 2011), could determine the extent to which their performance reflects the potential for many-to-one mapping to have produced similar functional outputs through differences in scaling patterns across components of the pelvic sucker (Wainwright et al., 2005).

MATERIALS AND METHODS

Specimen Collection

Specimens of three Hawaiian gobiid species (*Sicyopterus stimpsoni* Gill 1860, *Awaous guamensis* Valenciennes 1837, and *Stenogobius hawaiiensis* Watson 1991) were captured while snorkeling using a prawn net in their native stream habitat. Collections were made on the Hawaiian Islands during field seasons between 2004-2011 (see Table 3.1 for localities and body mass ranges, which ranged from nearly 50-fold in *S. hawaiiensis* to over 100-fold in *S. stimpsoni* and *A. guamensis*).

Species	N	Body Mass (g)	Locality	Year
Sicyopterus stimpsoni	15	0.12 - 13.35	Hakalau & Nanue (Hawai'i); Waimea (Kaua'i)	2004 - 2011
Awaous guamensis	18	0.17 - 17.85	Hakalau & Nanue (Hawai'i); Waimea (Kaua'i)	2004 - 2005
Stenogobius hawaiiensis	9	0.14 - 6.32	Honoli'i & Waiakea (Hawai'i); Waimea (Kaua'i)	2009 - 2011

Table 3.1: Hawaiian stream gobiid fishes and their collection localities.

Simulation of Pelvic Sucker Movement

The movements of the pelvic sucker of gobiid fishes are controlled by six distinctive muscles (Winterbottom, 1974). Of these muscles, I focused on two of the largest and most prominent pelvic extrinsic muscles that are responsible for transmitting force and powering the angular motions (Westneat, 1994; 2003) of the pelvic bone (basipterygium) deep to the base of the pelvic sucker: the protractor ischii muscle and the retractor ischii muscle (Figures 3.1B, 3.2, 3.3). These muscles are also known as the infracarinalis anterior and the infracarinalis medius, respectively (Winterbottom, 1974); however, in this paper I have retained the functionally descriptive terminology for these muscles used by Shelden (1937) in order to clearly distinguish their functional roles. The protractor ischii originates at the cleithral arch and inserts onto the ventral face of the pelvic bone (Figures 3.2, 3.3). Protraction of the pelvic sucker and ventral rotation at the pelvico-cleithral joint (formed by the cleithrum and the ossified intercleithral cartilage of the pelvic bone) is powered by the protractor ischii in a third-order lever mechanism, in which input force is applied on the lever between the pelvico-cleithral joint as the fulcrum and a point where the output force results (Figure 3.3D). This motion helps initiate and establish an attachment of the pelvic sucker onto the substrate. The retractor ischii originates at the base of the anal fin spine caudal to the urogenital papilla and inserts onto the dorso-caudal face of the pelvic bone (Figures 3.2, 3.3). Retraction of the pelvic sucker and dorsal rotation at the pelvico-cleithral joint is powered by the retractor ischii also in a third-order lever mechanism (Figure 3.3E). After the attachment of the

pelvic sucker is established, this retractor muscle exerts force to expand the sealed space formed between the pelvic sucker and the substrate, which results in increased pressure differentials and adhesion for withstanding current flow (and gravity for waterfall-climbing species).

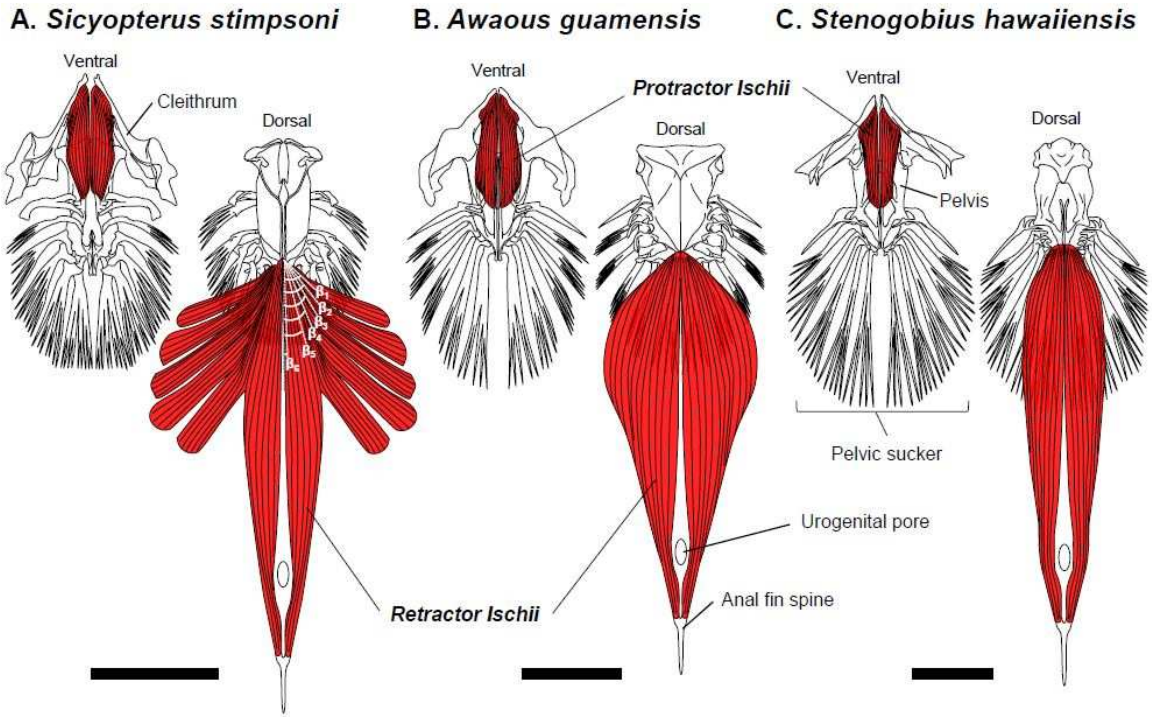

Figure 3.2: Pelvic musculoskeletal structure of Hawaiian stream gobiid species, (A) *Sicyopterus stimpsoni*, (B) *Awaous guamensis* and (C) *Stenogobius hawaiiensis* (ventral and dorsal views). Scale bars indicate 5 mm.

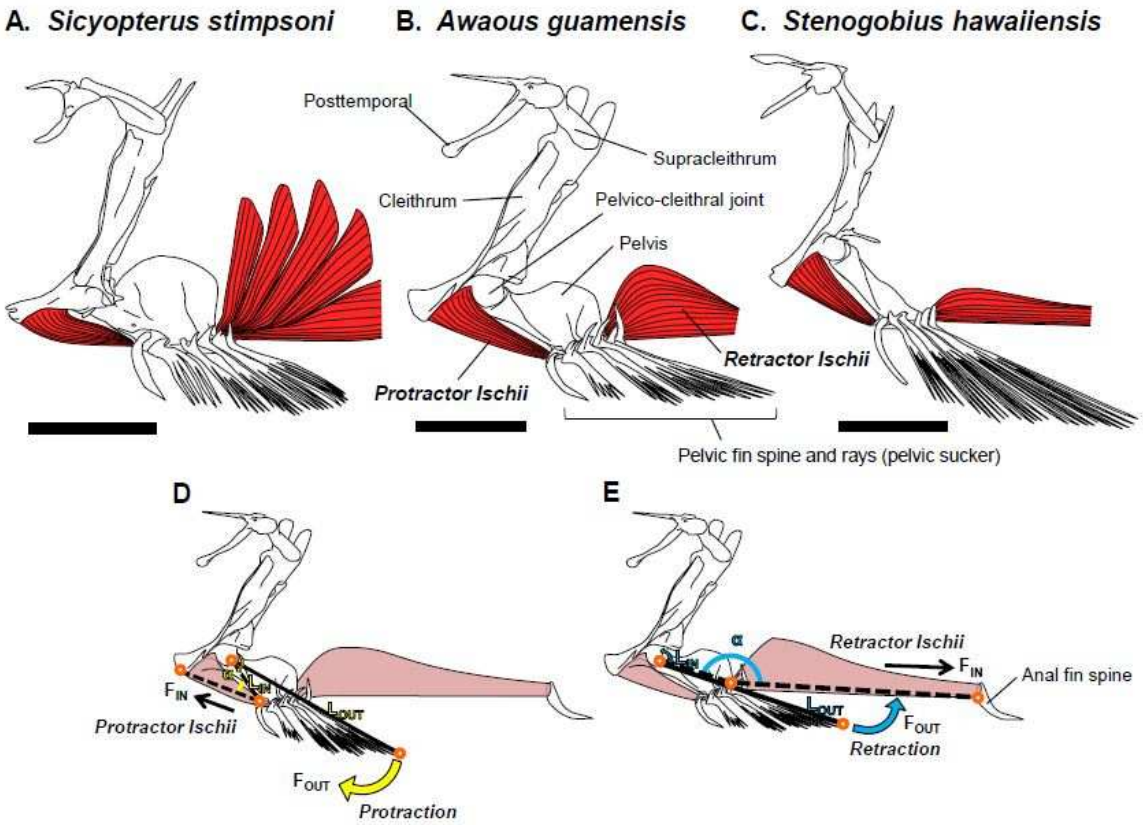

Figure 3.3: Pelvic musculoskeletal structure of Hawaiian stream gobiid species, (A) *Sicyopterus stimpsoni*, (B) *Awaous guamensis* and (C) *Stenogobius hawaiiensis* (lateral view) with the cleithro-pelvic lever system of the pelvic sucker. (D, E) Schematic diagrams (based on *A. guamensis*) of (D) the protractor ischii muscle with a third-order lever mechanism and (E) the retractor ischii muscle with a third-order lever mechanism. F_{IN} is the muscular input force. F_{OUT} is the output force produced at the pelvic sucker. L_{IN} is the in-lever arm. L_{OUT} is the out-lever arm. α is the insertion angle of each muscle. Scale bars indicate 5 mm.

To evaluate how pelvic musculoskeletal components contribute to sucker performance, the pelvic muscles and skeleton of specimens spanning a broad size range in each species were dissected under a dissecting scope (Nikon SMZ 1000) and photographed using a digital camera (Nikon CoolPix P5100) and Image J (Abramoff et al., 2004). Morphological measurements were collected from these photographs,

including muscle fiber length, in-lever arm (L_{IN}), out-lever arm (L_{OUT}), muscle insertion angle *in situ* (α', at dissection), and length of the "opposite" (i.e., a distance between the pelvico-cleithral joint and the origin of the muscle opposite to its insertion angle). Body mass (BM) and the mass of each muscle were weighed to the nearest 0.0001 g (Denver Instruments).

These anatomical measurements were used as the input for simulations of functional performance based on models derived by Westneat (2003) for jaw lever systems in fishes. I simulated a series of changes in the insertion angle of the protractor and retractor ischii muscles, and examined their consequences for protraction and retraction of the pelvic sucker. When each muscle contracts (e.g., muscle fiber shortens in an unloaded fashion), its insertion angle and anatomical cross-sectional area (CSA) change. The insertion angle (α) was calculated as: $\alpha = \arccos((L_{IN}^2 + \text{Fiber Length}^2 - \text{Opposite}^2)/(2*\text{Fiber Length}*L_{IN}))$. CSA was calculated as: CSA = (Muscle Mass/Fiber Length)($\cos\beta$/Muscle density), where β is the pinnation angle of muscle fibers (Alexander, 1974; Westneat, 2003). I assumed muscle density to be 1.05 g/cm^3 (Lowndes, 1955) and β to be 0 in *A. guamensis* and *S. hawaiiensis* because no pinnation was found in either protractor or retractor muscles in these species. However, the retractor ischii of *S. stimpsoni* has five subdivisions originating from the ribs and one subdivision from the anal fin spine (Figure 3.2A) with pinnation angles as follows: 44.65 ± 2.63^o (β_1), 36.83 ± 2.18^o (β_2), 30.04 ± 1.38^o (β_3), 22.96 ± 1.14^o (β_4), 16.51 ± 1.22^o (β_5), and 0^o (β_6). CSA, therefore, was calculated as a sum of CSAs from all subdivisions, and insertion angle was calculated using an average fiber length for the group.

For both protraction and retraction of the pelvic sucker with simulated changes in the insertion angle, the following performance variables were computed throughout the fiber contraction-induced angular excursion of the structure: effective mechanical advantage (EMA, calculated as EMA = $(L_{IN}/L_{OUT})*\sin\alpha$: Biewener, 1989), maximum muscular input force (F_{IN} max) normalized to BM, and maximum output force (F_{OUT} max) normalized to BM. Size-normalized F_{IN} max (unilateral) was calculated as: F_{IN} max = P_C*CSA/BM, where P_C (maximum isometric stress) = 20 N/cm^2 or 200 kPa (Altringham and Johnston, 1982; Powell et al., 1984). Size-normalized F_{OUT} max was calculated as: F_{OUT} max = $2*P_C*CSA*EMA/BM$. This is equivalent to F_{OUT} max = $2*F_{IN}$ max*EMA/BM, and considers the output force as the result of symmetrical, bilateral contraction of each pelvic muscle on the respective lever mechanism. In my simulation, the angular excursion of the pelvic sucker ranges over 20-35^o for its protraction (35^o = fully protracted position) and over 145-160^o for its retraction (160^o = fully retracted position). To evaluate the significance of differences in performance across species, I compared performance values at extremes of each movement (35^o for protraction and 160^o for retraction) using one-way ANOVA and Fisher's LSD *post hoc* tests (0.05 level).

Scaling Analysis

For each species, I evaluated the following scaling relationships for both the protractor and retractor ischii: (1) between *in situ* CSA (at dissection) and body mass, (2) between EMA and body mass, and (3) between F_{OUT} max and body mass. For these analyses, all data were $\log_{10}$-transformed and used to generate model II reduced major

axis (RMA) regressions, which account for structural relationships between variables when both are subject to error (Rayner, 1985; McArdle, 1988; LaBarbera, 1989). A scaling relationship was considered allometric if the 95% confidence interval (e.g., Jolicoeur and Mosimann, 1968) for its RMA slope failed to overlap the slope predicted for isometry based on dimensional analysis. In addition, I used Tsutakawa's non-parametric quick test (Tsutakawa and Hewett, 1977) to evaluate differences in each variable between species while accounting for differences in body mass across the size range of individuals compared (Swartz, 1997; Blob, 2000). In these comparisons, a pooled RMA regression line was calculated for the two groups being compared, and the numbers of points above and below this line were counted for each group, producing a 2x2 contingency table to which I applied Fisher's Exact test with significance at the 0.05 level (Tsutakawa and Hewett, 1977; Swartz, 1997; Blob, 2000; Maie et al., 2007).

Under isometric growth, CSA of muscles would be expected to increase as body length $(L)^2$, whereas body mass would be expected to increase as L^3, producing an expected isometric slope of 0.667 between these variables. As a unitless variable, EMA would be expected to increase as L^0 (i.e., independently with respect to body mass), producing an expected isometric slope of 0 between these variables. Finally, under isometric growth, forces (both maximum input force and output force) would be expected to scale in direct proportion to the CSA of muscles, thus scaling as an area (L^2) relative to body mass (L^3) for an expected slope of 0.667.

RESULTS

Analysis of Pelvic Sucker Movements

As the pelvic sucker protracted (rotated through increasing angles from 20 to 35^{o}), EMA of protractor levers for all species increased in a similar fashion from 0.05 to 0.10 (Figure 3.4A), with no significant difference across species at the fully protracted position ($\alpha = 35^{o}$) of the sucker (Table 3.2). Maximum input force (F_{IN} max) from the protractor ischii muscle increased slightly through the course of protraction (Figure 3.4C) and did not differ across species at $\alpha = 35^{o}$ (Table 3.2). Maximum output force (F_{OUT} max) transmitted at the pelvic sucker increased more substantially than F_{IN} max during protraction (Figure 3.4E), but also did not differ significantly across species at full protraction (Table 3.2).

Variables		*Sicyopterus stimpsoni* (n = 15)	*Awaous guamensis*(n = 18)	*Stenogobius hawaiiensis* (n = 9)	*P* - value
Protraction ($\alpha = 35^{o}$)	EMA	0.099 ± 0.005	0.100 ± 0.004	0.092 ± 0.006	0.5302
	F_{IN} max/BM (N/g)	0.129 ± 0.035	0.078 ± 0.032	0.136 ± 0.045	0.4312
	F_{OUT} max/BM (N/g)	0.028 ± 0.007	0.014 ± 0.006	0.021 ± 0.009	0.3321
Retraction ($\alpha = 160^{o}$)	EMA	0.200 ± 0.004, **a**	0.145 ± 0.003, **b**	0.094 ± 0.005, **c**	<0.0001*
	F_{IN} max/BM (N/g)	0.089 ± 0.020, **a**	0.024 ± 0.007, **b**	0.036 ± 0.009, **b**	0.0024*
	F_{OUT} max/BM (N/g)	0.037 ± 0.009, **a**	0.007 ± 0.002, **b**	0.006 ± 0.004, **b**	0.0010*

Table 3.2: Comparison of performance variables at fully protracted ($\alpha = 35^{o}$) and fully retracted ($\alpha = 160^{o}$) position of the pelvic sucker in the simulation for *Sicyopterus stimpsoni*, *Awaous guamensis* and *Stenogobius hawaiiensis*. For the variable significantly different indicated in ANOVA, species are ranked (a, b, and c) based on Fisher's LSD (0.05 level) post hoc tests. Values are means ± SEM.

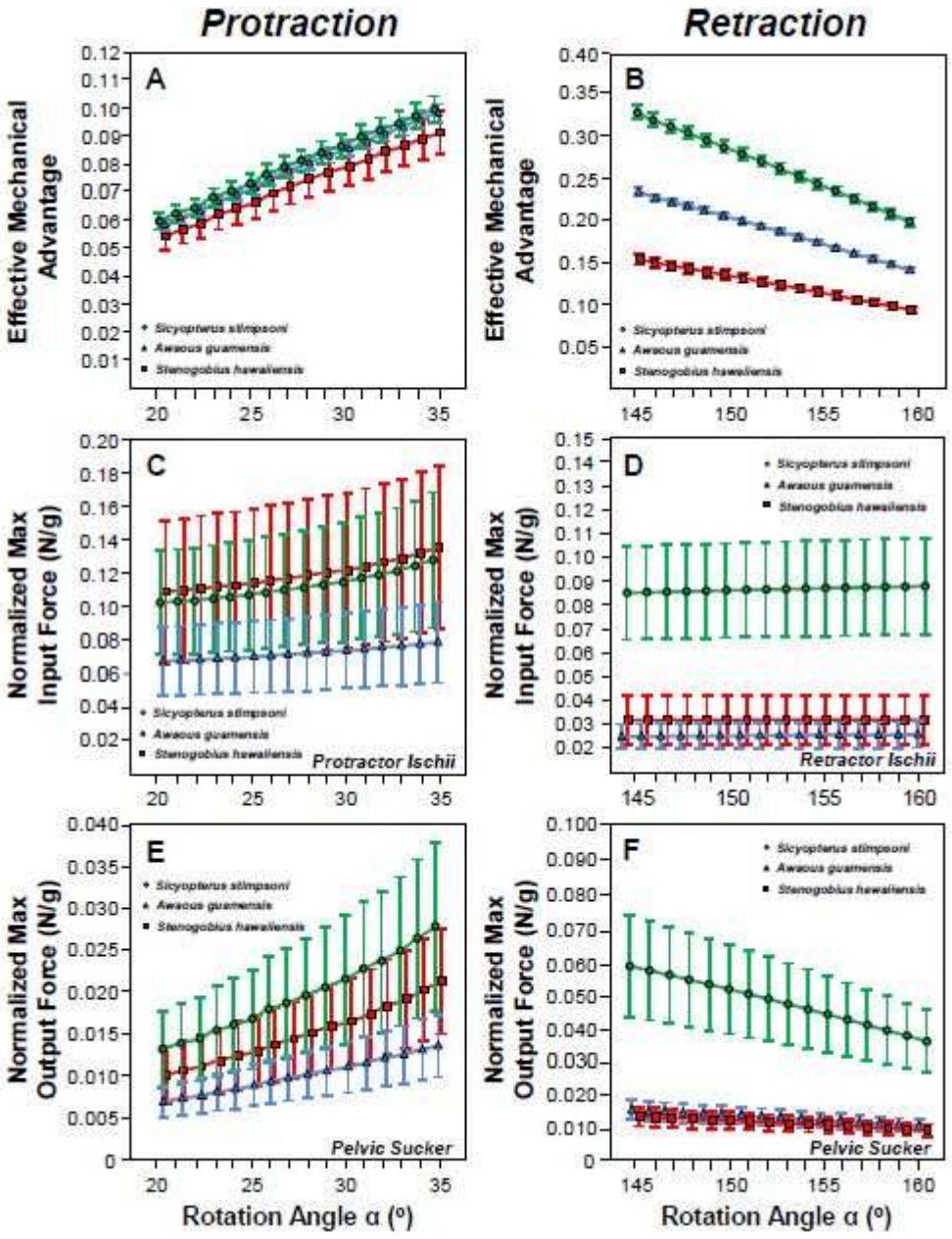

Figure 3.4: Profile of (A and B) effective mechanical advantage (EMA), (C and D) mass-normalized maximum input force (F_{IN} max/BM) and (E and F) mass-normalized maximum output force (F_{OUT} max/BM) during simulated $\Delta\alpha = 15^{o}$ rotations (for protraction and retraction) of the pelvic suckers of Hawaiian stream gobiid species, *Sicyopterus stimpsoni* (circles), *Awaous guamensis* (triangles), and *Stenogobius hawaiiensis* (squares).

As the pelvic sucker retracted (rotated through increasing angles from 145 to 160^{o}), EMA of retractor levers decreased from 0.33 to 0.20 in *S. stimpsoni*, from 0.24 to 0.15 in *A. guamensis*, and from 0.15 to 0.09 in *S. hawaiiensis* (Figure 3.4B). *S. stimpsoni* exhibited a significantly greater retractor lever EMA than both *A. guamensis* ($P < 0.0001$, Fisher's LSD *post hoc* test) and *S. hawaiiensis* ($P < 0.0001$, Fisher's LSD *post hoc* test) at the fully retracted position ($\alpha = 160^{o}$: Table 3.2, Figure 3.4B). *A. guamensis* exhibited a significantly greater EMA than *S. hawaiiensis* at this fully retracted position ($P < 0.0001$, Fisher's LSD *post hoc* test: Table 3.2, Figure 3.4B). Retractor lever EMA at the beginning of retraction ($\alpha = 145^{o}$) showed a similar statistical pattern ($P < 0.0001$ for *S. stimpsoni* vs. *A. guamensis*; $P < 0.0001$ for *S. stimpsoni* vs. *S. hawaiiensis;* $P < 0.0001$ for *A. guamensis* and *S. hawaiiensis*). F_{IN} max from the retractor ischii muscle increased slightly (e.g., 0.45 – 3.15%) during retraction. *S. stimpsoni* exhibited the highest values among the species ($P = 0.0007$ for *S. stimpsoni* vs. *A. guamensis*; $P = 0.0101$ for *S. stimpsoni* vs. *S. hawaiiensis*: Table 3.2, Figure 3.4D). However, *A. guamensis* and *S. hawaiiensis* did not significantly differ with respect to muscular input force ($P = 0.7363$: Table 3.2, Figure 3.4D). F_{OUT} max transmitted at the pelvic sucker decreased in retraction (Figure 3.4F) in all three species (from 0.059 to 0.037 N/g in *S. stimpsoni*, from 0.012 to 0.007 N/g in *A. guamensis*, and from 0.010 to 0.006 N/g in *S. hawaiiensis*). *S. stimpsoni* exhibited a significantly greater F_{OUT} max than both *A. guamensis* ($P = 0.0006$, Fisher's LSD *post hoc* test) and *S. hawaiiensis* ($P = 0.0029$, Fisher's LSD *post hoc* test) at the fully retracted position ($\alpha = 160^{o}$: Table 3.2, Figure 3.4F). However, *A. guamensis* and *S. hawaiiensis* did not differ in F_{OUT} max at the fully retracted position ($P = 0.9169$:

Table 3.2, Figure 3.4F). Maximum output force at the beginning of retraction ($\alpha = 145^{o}$) showed the same statistical pattern (P = 0.0006 for *S. stimpsoni* vs. *A. guamensis*; P = 0.0027 for *S. stimpsoni* vs. *S. hawaiiensis*; P = 0.9215 for *A. guamensis* vs. *S. hawaiiensis*, Fisher's LSD *post hoc* test).

Ontogenetic Scaling Patterns

All three gobiid species showed strong positive correlations between CSA of both the protractor and retractor ischii muscles and body mass (Table 3.3, Figures 3.5A, 3.5B). Scaling exponents for CSA of the protractor ischii with respect to body mass indicated negative allometry for all species examined (i.e., 95% Confidence Interval, CI < 0.667: Table 3.3, Figure 3.5A). For the protractor ischii, Tsutakawa's quick test indicated no significant differences in CSA across species (P = 0.3028 for *S. stimpsoni* vs. *A. guamensis*; P = 0.0894 for *S. stimpsoni* vs. *S. hawaiiensis*; P = 0.4197 for *A. guamensis* vs. *S. hawaiiensis*: Fisher's Exact test) at any given body size. In contrast, scaling exponents for CSA of the retractor ischii indicated isometry for *S. stimpsoni* and *S. hawaiiensis* (i.e., 95% CI of regression slope for both species overlap predicted slope of 0.667 for isometry) and slightly negative, nearly isometric scaling for *A. guamensis* (Table 3.3, Figure 3.5B). In addition, for the retractor ischii, Tsutakawa's quick test indicated larger CSA in *S. stimpsoni* than the other species (P < 0.0001 for *S. stimpsoni* vs. *A. guamensis*; P = 0.0005 for S. stimpsoni vs. *S. hawaiiensis*) at given any body size. However, no significant difference in CSA of the retractor ischii was found between *A. guamensis* and *S. hawaiiensis* (P = 0.4197).

x	y	Species	n	r^2	RMA intercept ± 95% CL	RMA slope (95% CI)	*Expected RMA by isometry*	*Allometry*
BM	Protractor Ischii CSA	*Sicyoterus stimpsoni*	15	0.477	-2.510 ± 0.112	0.417 (0.274 - 0.635)	0.667	-
		Awaous guamensis	18	0.767	-2.431 ± 0.085	0.435 (0.337 - 0.560)	0.667	-
		Stenogobius hawaiiensis	9	0.645	-2.512 ± 0.134	0.377 (0.217 - 0.654)	0.667	-
BM	Retractor Ischii CSA	*Sicyoterus stimpsoni*	15	0.860	-2.450 ± 0.097	0.695 (0.556 - 0.868)	0.667	0
		Awaous guamensis	18	0.890	-2.867 ± 0.074	0.559 (0.469 - 0.665)	0.667	- (near 0)
		Stenogobius hawaiiensis	9	0.823	-2.946 ± 0.147	0.585 (0.393 - 0.871)	0.667	0
BM	Protractor Lever EMA ($\alpha = 35^o$)	*Sicyoterus stimpsoni*	15	0.013	n.s.	n.s.	0.000	0
		Awaous guamensis	18	0.404	-1.051 ± 0.031	0.100 (0.067 - 0.149)	0.000	+
		Stenogobius hawaiiensis	9	0.372	n.s.	n.s.	0.000	0
BM	Retractor Lever EMA ($\alpha = 160^o$)	*Sicyoterus stimpsoni*	15	0.561	-0.688 ± 0.027	-0.069 (-0.101 - -0.047)	0.000	-
		Awaous guamensis	18	0.332	-0.816 ± 0.023	-0.053 (-0.080 - -0.035)	0.000	-
		Stenogobius hawaiiensis	9	0.633	-1.031 ± 0.050	0.085 (0.049 - 0.149)	0.000	+
BM	Protraction F_{OUT} max ($\alpha = 35^o$)	*Sicyoterus stimpsoni*	15	0.406	-1.896 ± 0.126	0.445 (0.284 - 0.695)	0.667	0
		Awaous guamensis	18	0.688	-1.938 ± 0.119	0.529 (0.395 - 0.708)	0.667	0
		Stenogobius hawaiiensis	9	0.699	-1.957 ± 0.193	0.587 (0.353 - 0.979)	0.667	0
BM	Retraction F_{OUT} max ($\alpha = 160^o$)	*Sicyoterus stimpsoni*	15	0.807	-1.575 ± 0.109	0.670 (0.517 - 0.869)	0.667	0
		Awaous guamensis	18	0.891	-2.077 ± 0.092	0.525 (0.441 - 0.625)	0.667	-
		Stenogobius hawaiiensis	9	0.871	-2.349 ± 0.226	0.647 (0.459 - 0.912)	0.667	0

Table 3.3: Scaling coefficients (RMA Intercept ± 95% Confidence Limits, CL) and exponents (RMA slope, with asymmetric 95% Confidence Interval, CI) for cross-sectional area (CSA) of the protractor ischii muscle and retractor ischii muscle with respect to body mass (BM), effective mechanical advantage (EMA) and maximum force output (F_{OUT} max) at simulated phases of muscle contraction ($\alpha = 35^o$ for protractor ischii; $\alpha = 160^o$ for retractor ischii) with respect to BM of Hawaiian stream gobiid species, *Sicyopterus stimpsoni*, *Awaous guamensis*, and *Stenogobius hawaiiensis*. Calculations were obtained from reduced major axis (RMA) regressions of log10-transformed measurements: x, regression abscissa; y, regression ordinate; n, sample size. Scaling pattern (allometry) is indicated as either isometric (0), negatively allometric (-), or positively allometric (+). For BM vs CSA, muscle insertion angles at dissection *in situ* were $\alpha' = 31.8 \pm 4.9^o$ for the protractor ischii; $\alpha' = 161.8 \pm 8.9^o$ for the retractor ischii.

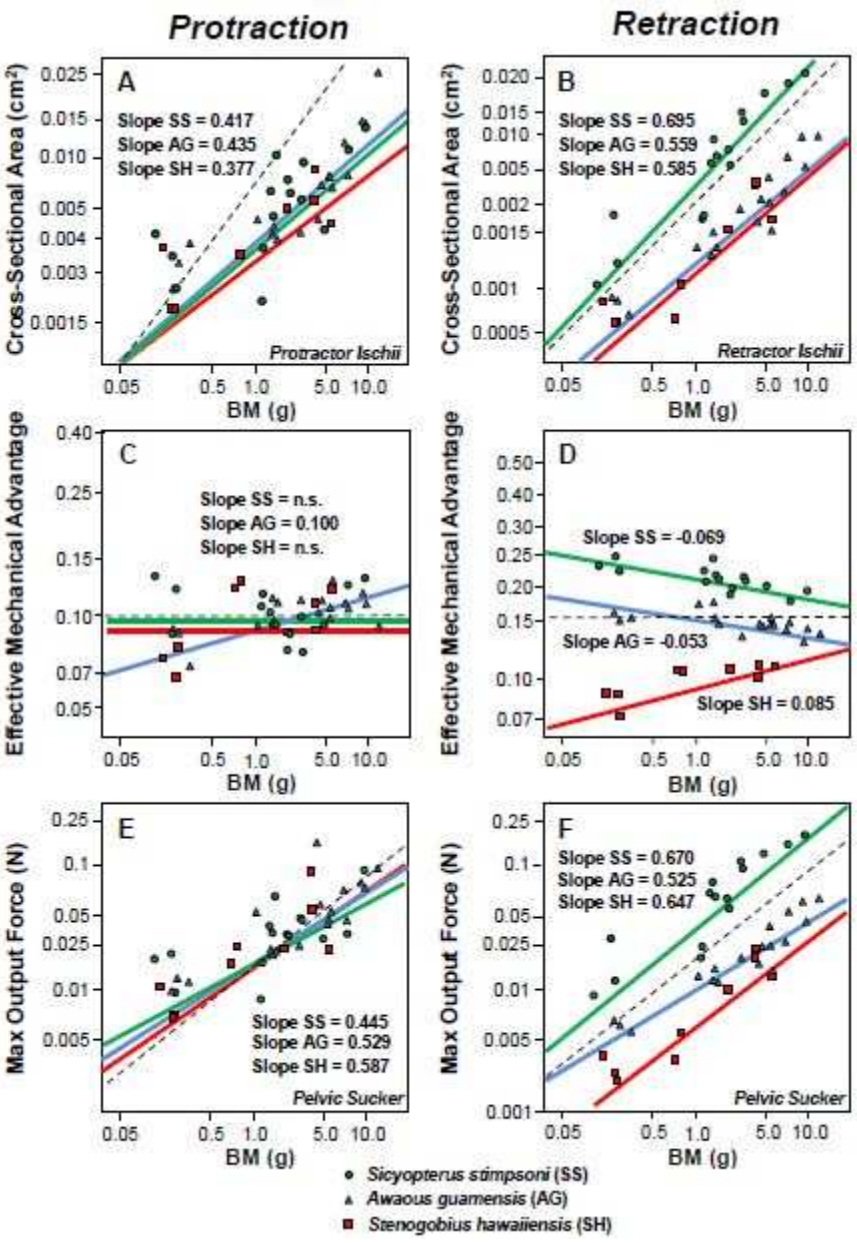

Figure 3.5: Log-log plots of reduced major axis (RMA) regression comparing cross-sectional area (CSA) of the protractor ischii muscle (A) and retractor ischii muscle (B) *in situ* ($\alpha' = 31.8 \pm 4.9^{o}$ for protractor ischii; $\alpha' = 161.8 \pm 8.9^{o}$ for retractor ischii), effective mechanical advantage (EMA: C, protractor lever; D, retractor lever), and maximum output force (E, sucker protraction; F, sucker retraction) at simulated phases of muscle contraction ($\alpha = 35^{o}$ for protractor ischii; $\alpha = 160^{o}$ for retractor ischii) with respect to body mass (BM) in Hawaiian stream gobiid species, *Sicyopterus stimpsoni* (circle), *Awaous guamensis* (triangle), and *Stenogobius hawaiiensis*

(square). For each scaling relationship, an expected line for isometry is indicated as a dashed line. See Table 3 for parameters of scaling equations.

Effective mechanical advantage (EMA) of the protractor lever at its fully protracted position ($\alpha = 35^{o}$) did not change in proportion to body mass for *S. stimpsoni* or *S. hawaiiensis*, with P-values for RMA regressions of 0.6921 and 0.0812 respectively (Table 3.3, Figure 3.5C). Only in *A. guamensis* did the scaling exponent for the protractor lever EMA at its fully protracted position indicate positive allometry with respect to body mass (Table 3.3, Figure 3.5C). Despite these differences in scaling pattern, however, Tsutakawa's quick test failed to produce a significant result for comparisons of protractor lever EMA at $\alpha = 35^{o}$ ($P > 0.9999$ for all Fisher's Exact tests). Scaling exponents for the retractor lever EMA with respect to body mass at its fully retracted position ($\alpha = 160^{o}$) indicated negative allometry for *S. stimpsoni* and *A. guamensis* but positive allometry for *S. hawaiiensis* (Table 3.3, Figure 3.5D). However, Tsutakawa's quick test indicated *S. stimpsoni* at any given body size had a greater retractor lever EMA at $\alpha = 160^{o}$ than both *A. guamensis* ($P < 0.0001$) and *S. hawaiiensis* ($P < 0.0001$). Further, *A. guamensis* had a greater EMA than *S. hawaiiensis* ($P < 0.0001$) at any given body size.

All three species showed strong positive correlations between maximum output force (F_{OUT} max) and body mass for both fully protracted ($\alpha = 35^{o}$) and retracted ($\alpha = 160^{o}$) positions (Table 3.3, Figures 3.5E, 3.5F). Scaling exponents for F_{OUT} max of the pelvic sucker at its fully protracted position ($\alpha = 35^{o}$) indicated isometry for all three species (Table 3.3, Figure 3.5E). Tsutakawa's quick test indicated no significant difference in protractor output force across species ($P = 0.4939$ for *S. stimpsoni* vs. *A.*

guamensis; P = 0.6752 for *S. stimpsoni* vs. *S. hawaiiensis*; P = 0.6946 for *A. guamensis* vs. *S. hawaiiensis*) at any given body size. Scaling exponents for retractor F_{OUT} max at its fully retracted position ($\alpha = 160^{o}$) indicated isometry for *S. stimpsoni* and *S. hawaiiensis*, and a nearly isometric, negative allometry for *A. guamensis* (Table 3.3, Figure 3.5F). Tsutakawa's quick test indicated *S. stimpsoni* at any given body size would have a greater maximum output force from the pelvic sucker than both *A. guamensis* ($P < 0.0001$) and *S. hawaiiensis* ($P < 0.0001$). Further, *A. guamensis* had a greater output force at maximum retraction than *S. hawaiiensis* ($P = 0.0115$) at any given body size.

DISCUSSION

My simulation of pelvic sucker performance in Hawaiian stream gobies was driven by input motions to the pelvic lever system (e.g., the pelvis rotating around the pelvico-cleithral joint) powered by the protractor ischii and retractor ischii muscles. I estimated force output for these muscles in species with three different levels of climbing proficiency, including strong (*S. stimpsoni*), poor (*A. guamensis*) and non-climbing (*S. hawaiiensis*) taxa. My analysis shows a strong anatomical basis for the adhesive performance of *S. stimpsoni*, as well as evidence for many-to-one mapping of structure to function between *A. guamensis* and *S. hawaiiensis* (e.g., Wainwright et al., 2005). However, these results did not explain the different patterns of ontogenetic scaling for adhesion between climbing and non-climbing species (Maie et al., 2012), leaving the basis for the positive allometry of adhesive force in climbing gobiids unresolved.

Anatomical factors contributing to interspecific differences in goby adhesive performance

Although both *S. hawaiiensis* and *A. guamensis* have larger pelvic suckers than *S. stimpsoni* at any given body size, *S. stimpsoni* has been shown to produce pressure differentials equal or greater in magnitude, and to generate comparable adhesive forces (Maie et al., 2012). Based on my comparative analyses of the pelvic musculoskeletal system, the anatomical factors that may contribute to the ability of *S. stimpsoni* to achieve these levels of performance appear to be concentrated in one of the two major muscle groups that contract to expand pelvic sucker volume. The mechanical advantage, input force, and output force for the protractor ischii show no significant differences across species throughout the range of pelvic motion (Figures 3.4A, 3.4C, 3.4E). In contrast, *S. stimpsoni* shows a greater mechanical advantage for the retractor ischii than both of the other two species throughout its range of motion (Figure 3.4B). In combination with its greater size-normalized input force generated by the retractor ischii, due in part to its pinnate configuration (Figure 3.4D), *S. stimpsoni* produces a significantly greater size-normalized output force than both *A. guamensis* and *S. hawaiiensis* (Figure 3.4F). This additional force output might help to compensate for the smaller sucker size exhibited by *S. stimpsoni* by facilitating sucker volume expansion and the generation of pressure differentials.

The poorly climbing species *A. guamensis* also shows a greater mechanical advantage for the retractor ischii than non-climbing *S. hawaiiensis* throughout the range of motion of this muscle (Figure 3.4B). However, input forces from this muscle are

greater in *S. hawaiiensis* (Figure 3.4D). As a result, the output force for this muscle does not differ between *A. guamensis* and *S. hawaiiensis* (Figure 3.4F). This similarity in performance is achieved through different pathways and could be viewed as an example of many-to-one mapping of structure to function (Wainwright et al., 2005). However, these two pathways may bear different energetic costs. The amplification of force output via mechanical advantage in *A. guamensis* should be more energetically efficient than producing the same force output via higher input forces (as in *S. hawaiiensis*), which must be generated by larger muscle cross-sectional areas with their consequent metabolic demands. The enhancement of force by leverage could be advantageous for a species like *A. guamensis* that makes use of its sucker in demanding exertions such as climbing, in contrast to non-climbing *S. hawaiiensis* which lives in predominantly estuarine habitats with slow flow (Schoenfuss and Blob, 2007). It is even possible that such energetic restrictions could contribute to the lack of climbing ability in *S. hawaiiensis*.

Musculoskeletal allometry and performance allometry

My previous work showed that the non-climbing gobiid *S. hawaiiensis* achieved positive allometry of suction force production via positive allometry of sucker area, whereas climbing species (including *A. guamensis* and *S. stimpsoni*) produced positive allometry of suction force despite isometric sucker growth (Maie et al., 2012). I hypothesized that climbing species might be able to enhance suction performance as they grew by means of positive allometry of either the size or lever arms of the muscles that move the sucker and increase the volume it encloses during adhesion. However, my

musculoskeletal scaling analyses did not provide clear explanations for the positive allometry of *in vivo* suction performance in climbing species. Muscle cross-sectional areas scaled with either isometry (for the retractor ischii) or negative allometry (for the protractor ischii) in both climbing and non-climbing species (Figure 3.5). Patterns of scaling for mechanical advantage differed between the protractor and retractor ischii, but also appeared unlikely to contribute to relative increases in suction performance with size; in fact, for the retractor ischii, both climbing species showed negative allometry of EMA, suggesting size-related increases in velocity advantage, rather than mechanical advantage (Figure 3.5D). As a result, neither muscle showed positive allometry in predicted output force for either climbing or non-climbing species (Figures 3.5E, 3.5F).

Explanations for the positive allometry of suction pressure differentials and forces among climbing goby taxa with isometric (or, in some cases, negatively allometric) sucker areas must, therefore, depend on other anatomical or physiological factors. For example, while my simulation examined the two largest pelvic muscles, I did not account for intrinsic muscles associated with the fin spine and rays of the sucker (e.g., abductor and adductor pelvicus complexes), which might synergistically contribute to the suction performance. Changes in fiber type composition (e.g., Cediel et al., 2008; Maie et al., 2011), neural activation of the protractor and retractor muscles, or mechanical property of the fin rays (e.g., Lundberg and March, 1976) with size could also influence functional performance. Such factors have yet to be evaluated, but the results of this study provide a motivation for such examinations if the underpinnings of gobiid sucker function are to be clarified.

LITERATURE CITED

Abramoff MD, Magelhaes PJ, Ram SJ. 2004. Image Processing with ImageJ. Biophotonics Int 11:36-42.

Alexander RM. 1974. The mechanics of a dog jumping, *Canis familiaris*. J Zool Lond 173:549-573.

Altringham JD, Johnston IA. 1982. The pCa-tension and force-velocity characteristics of skinned fibers isolated from fish fast and slow muscles. J Physiol 333:421-449.

Bell KNI. 1994. Life cycle, early life history, fisheries and recruitment dynamics of diadromous gobies of Dominica, W. I., emphasizing *Sicydium punctatum* Perugia. PhD dissertation, Memorial University of Newfoundland, St. John's Newfoundland, Canada.

Biewener AA. 1989. Scaling body support in mammals: limb posture and muscle mechanics. Science 245:45-48.

Blob RW. 2000. Interspecific scaling of the hindlimb skeleton in lizards, crocodilians, felids and canids: does limb bone shape correlate with limb posture? J Zool Lond 250:507-531.

Carrier DR. 1996. Ontogenetic limits on locomotor performance. Physiol Zool 69:467-488.

Cediel RA, Blob RW, Schrank GD, Plourde RC, Schoenfuss HL. 2008. Muscle fiber type distribution in climbing Hawaiian gobioid fishes: Ontogeny and correlations with locomotor performance. Zoology 111:114-122.

Denny MW. 1993. Air and Water: The Biology and Physics of Life's Media. Princeton: Princeton University Press.

Emerson SB, Diehl D. 1980. Toe pad morphology and mechanisms of sticking in frogs. Biol J Linn Soc Lond 13:199-216.

Herrel A, Speck T, Rowe NP. 2006. Ecology and Biomechanics: A Mechanical Approach to the Ecology of Animals and Plants. Boca Raton: CRC Press.

Jolicoeur R, Mosimann JE. 1968. Intervalles de confiance pour la pente de l'axe majeur d'une distribution normale bidimensionelle. Biometrie-Praximetrie 9:121-140.

Keith P, Lord C, Lorion, J, Watanabe S, Tsukamoto K, Couloux A, Dettai, A. 2011. Phylogeny and biogeography of Sicydiinae (Teleostei: Gobiidae) inferred from mitochondrial and nuclear genes. Mar Biol 158:311-316.

Kier WM, Smith AM. 1990. The morphology and mechanics of octopus suckers. Biol Bull 178:126-136.

LaBarbera M. 1989. Analyzing body size as a factor in ecology and evolution. Ann Rev Ecol Syst 20:97-117.

Lowndes AG. 1955. Density of fishes. Some notes on the swimming of fish to be correlated with density, sinking factor and the load carried. Ann Mag Nat Hist 8:241-256.

Lundberg JG, March E. 1976. Evolution and functional anatomy of the pectoral fin rays in cyprinoid fishes, with emphasis on the suckers (Family Catostomidae). Am Midland Nat 96:332-349.

Maie T, Schoenfuss HL, Blob RW. 2007. Ontogenetic scaling of body proportions in waterfall-climbing gobiid fishes from Hawai'i and Dominica: implications for locomotor function. Copeia 2007:755-764.

Maie T, Schoenfuss HL, Blob RW. 2012. Performance and scaling of a novel locomotor structure: adhesive capacity of climbing gobiid fishes. J Exp Biol 215:3925-3936.

Maie T, Meister AB, Leonard GL, Schrank GD, Blob RW, Schoenfuss HL. 2011. Jaw muscle fiber type distribution in Hawaiian gobioid stream fishes: Histochemical correlations with feeding ecology and behavior. Zoology 114:340-347.

McArdle BH. 1988. The structural relationship: regression in biology. Can J Zool 66:2329-2339.

McGuire JA. 2003. Allometric prediction of locomotor performance: An example from southeast Asian flying lizards. Am Nat 161:337-349.

McHenry MJ, Lauder GV. 2006. Ontogeny of form and function: Locomotor morphology and drag in zebrafish (*Danio rerio*). J Morph 267:1099-1109.

McMahon TA. 1975. Using body size to understand the structural design of animals: Quadrupedal locomotion. J Appl Physiol 39:619-627.

Nelson JS. 1994. Fishes of the World, 3rd edn. New York: Wiley.

Parenti LR, Thomas KR. 1998. Pharyngeal jaw morphology and homology in sicydiine gobies (Teleostei: Gobiidae) and allies. J Morph 237:257-274.

Powell PL, Roy RR, Kanim P, Bello MA, Edgerton VR. 1984. Predictability of skeletal muscle tension from architectural determinations in guinea pig hindlimbs. J Appl Physiol 57:1715-1721.

Radtke RL, Kinzie RW III, Folsom SD. 1988. Age at recruitment of Hawaiian freshwater gobies. Environ Biol fishes 23:205-213.

Radtke RL, Kinzie RW III, Shafer DJ. 2001. Temporal and spatial variation in length of larval life and size at settlement of the Hawaiian amphidromous goby *Lentipes concolor*. J Fish Biol 59:928-938.

Rayner JMV. 1985. Linear relations in biomechanics: the statistics of scaling functions. J Zool Lond 206:415-439.

Schmidt-Nielsen K. 1984. Scaling: Why is Animal Size so Important? Cambridge: Cambridge University Press.

Schoenfuss HL, Blob RW. 2003. Kinematics of waterfall climbing in Hawaiian freshwater fishes (Gobiidae): Vertical propulsion at the aquatic-terrestrial interface. J Zool Lond 261:191-205.

Schoenfuss HL, Blob RW. 2007. The importance of functional morphology for fishery conservation and management: application to Hawaiian amphidromous fishes. Bishop Mus Bull Cult Environ Stud 3:125-141.

Shelden FF. 1937. Osteology, myology, and probable evolution of the nematognath pelvic girdle. Annal New York Acad 37:1-96.

Shen KN, Lee YC, Tzeng WN. 1998. Use of otolith microchemistry to investigate the life history pattern of gobies in a Taiwanese stream. Zool Stud 37:322-329.

Swartz SM. 1997. Allometric patterning in the limb skeleton of bats: implications for the mechanics and energetics of powered flight. J Morphol 234:277-294.

Thacker CE. 2003. Molecular phylogeny of the gobioid fishes (Teleostei: Perciformes: Gobioidei). Mol Phylog Evol 26:354-368.

Tsutakawa RK, Hewett JE. 1977. Quick test for comparing two populations with bivariate data. Biometrics 33:215-219.

Vogel S. 1994. Life in Moving Fluids: The Physical Biology of Flow, 2nd Edn. Princeton: Princeton University Press.

Wainwright PC, Reilly SM. 1994. Ecological morphology: integrative organismal biology. Chicago: University of Chicago Press.

Wainwright PC, Alfaro ME, Bolnick DI, Hulsey CD. 2005. Many-to-one mapping of form to function: A general principle in organismal design? Integr Comp Biol 45:256-262.

Westneat MW. 1994. Transmission of force and velocity in the feeding mechanisms of labrid fishes (Teleostei, Perciformes). Zoomorph 114:103-118.

Westneat MW. 2003. A biomechanical model for analysis of muscle force, power output and lower jaw motion in fishes. J Theor Biol 223:269-281.

Winterbottom R. 1974. A descriptive synonymy of the striated muscle of the teleostei. Proc Acad Nat Sci Phil 125:225-317.

CHAPTER FOUR

FEEDING KINEMATICS AND PERFORMANCE BY THE HAWAIIAN SLEEPER, *ELEOTRIS SANDWICENSIS*, DURING PREDATORY STRIKES: MODULATION BETWEEN PREY SPECIES AND IMPLICATIONS FOR SELECTIVE PRESSURES ON HAWAIIAN STREAM ICHTHYOFAUNA

SUMMARY

A species of piscivorous eleotrid, *Eleotris sandwicensis*, inhabits lower reaches of streams in the Hawaiian Archipelago, where it feeds on postlarvae of native amphidromous gobiid fishes migrating upstream from the ocean. As an ambush predator, *E. sandwicensis* relies on suction to capture its prey. Anatomical measurements and mathematical models have indicated the potential for elevated suction performance relative to other Hawaiian gobioids (e.g., high velocity advantage for jaw movements) as well as high output forces for jaw closing by the adductor mandibulae muscles. However, feeding kinematics and performance of eleotrids have never been measured directly, making the risk they pose to migrating juvenile gobies unclear. I used high-speed video and geometric modeling of the feeding apparatus to evaluate the kinematics and performance of *E. sandwicensis* suction feeding on free swimming gobiid juveniles, comparing performance between successful and unsuccessful strikes, and testing the extent to which *E. sandwicensis* modulates its predatory behavior between prey species (*S. stimpsoni* and *A. guamensis*) that differ in size, behavior, and physiology. With fast jaw movements and a large but well-controlled expansive buccal cavity, *E. sandwicensis* achieves high performance in suction feeding that enables the capture of elusive prey. Comparisons of predator-prey distance between successful and unsuccessful strikes

indicated that the species with larger juveniles (*S. stimpsoni*) could be captured from up to 18.6% body length (BL) away from the mouth, but capture of the smaller species (*A. guamensis*) required a closer distance to the predator (12.2% BL). Predator-prey distance appears to be the predominant factor determining strike outcome during feeding on juvenile *A. guamensis* because *E. sandwicensis* showed no difference in jaw kinematics or performance between successful and unsuccessful strikes. However, during feeding on juvenile *S. stimpsoni*, *E. sandwicensis* demonstrates a capacity to modulate strike behavior, showing faster gape cycles and jaw closing, greater premaxillary protrusion and hyoid retraction, and smaller cranial elevation and opercular expansion during successful strikes. Beyond these specific comparisons, the ability of *E. sandwicensis* to capture larger prey fish from longer distances suggests a potential biomechanical basis underlying observations of predation by eleotrids to impose selection against large body size in juvenile gobies.

INTRODUCTION

The stream habitats of the Hawaiian Archipelago present numerous challenges to juveniles of native amphidromous gobiid fishes. These include physical challenges such as rapidly flowing water and waterfall obstacles (e.g., Schoenfuss & Blob, 2003, 2007; Blob et al., 2008), as well as biological challenges. During their life cycle, postlarval amphidromous gobies migrate from the ocean into streams, entering a habitat populated by an endemic (and also amphidromous) species of piscivorous eleotrid, *Eleotris sandwicensis* (Tate, 1997; Ziegler, 2002). Eleotrids, commonly known as sleepers, are

the sister taxon of the gobiids (hereafter 'gobies'), and as such are part of the broader gobioid lineage (Thacker, 2003). Sleepers are ambush predators that rely on suction to capture their prey: they have been documented to feed on fishes, including juvenile gobies, in the wild (McKaye et al., 1979; Nordlie, 1981; Kido, 1996; Tate, 1997; Winemiller & Ponwith, 1998; Yamamoto & Tagawa, 2000; Bacheler et al., 2004; Schoenfuss & Blob, 2007), and their predation on juvenile gobies has been shown to exert significant selection pressure on the morphology of prey in lab studies (Blob et al., 2010). Anatomical measurements and mathematical models have indicated the potential for *E. sandwicensis* to exhibit elevated suction performance relative to other Hawaiian gobioids (e.g., high velocity advantage for jaw movements), as well as high output forces for jaw closing by the adductor mandibulae (Maie et al., 2009a; Chapter 5). However, feeding kinematics and performance of eleotrids have never been measured directly, making the risk they pose to migrating juvenile gobies unclear.

Although *E. sandwicensis* is the only species of predatory eleotrid that inhabits Hawaiian streams, it may encounter incoming juveniles of four different species of goby as prey. Juveniles of three of these species (*Awaous guamensis*, *Lentipes concolor*, and *Stenogobius hawaiiensis*) typically range from 14 to 16 mm in BL, but juveniles of the fourth species, *Sicyopterus stimpsoni*, range from 20 to 24 mm in BL, a difference of as much as 67% (Schoenfuss & Blob, 2003, 2007). These prey species also exhibit behavioral differences (Tate, 1997). For example, while *S. hawaiiensis* cohabits with *E. sandwicensis* in lower stream reaches for its entire post-oceanic lifespan, the other species have the capacity, with differing degrees of proficiency, to climb waterfalls in

streams and escape the range of predators. Potentially in association with their differing climbing behaviors, there are also physiological differences between postlarvae of gobiid prey species, with the species that uses the slowest climbing movements (*S. stimpsoni*: Schoenfuss and Blob, 2003) having a significantly greater proportion of slow oxidative (red) fibers in their propulsive axial musculature than either *A. guamensis* or *L. concolor* (Cediel et al., 2008).

Because of the differences in size, behavior, and physiology across postlarvae of Hawaiian gobiid species, it is possible that these species may have differing abilities to avoid being captured by predatory *E. sandwicensis*. For example, size-dependent physical and hydrodynamic effects (e.g., Weihs, 1980; Müller et al., 2000; McHenry & Lauder, 2005; 2006; Wainwright & Day, 2007), including the tendency of small animals to move relatively more quickly than larger animals (Hill, 1950; Herrel et al., 2005; Van Wassenbergh et al., 2006), might lead to differences in escape velocity or acceleration between larger *S. stimpsoni* and other prey species (e.g., Domenici and Blake, 1993; 1997). Although *S. stimpsoni* might be more efficient in propulsive motion than smaller species (e.g., Webb et al., 1984; Archer et al., 1990), the greater proportion of axial red muscle in *S. stimpsoni* compared to other Hawaiian gobies (Cediel et al., 2008) might also be correlated with slower escapes in this species. Such differences in prey size or escape performance might elicit modulations of feeding kinematics or performance by *E. sandwicensis* in response to different types of prey (e.g., Coughlin & Strickler, 1990; Norton, 1991; Wainwright et al., 2001). However, the cryptic behavior (i.e., 'sit-and-wait' strategy and chromatic camouflage) used by *E. sandwicensis* during predation

might maximize its likelihood of coming in close proximity to its prey, a factor found in previous studies to improve capture success (Lauder & Clark, 1984; Ferry-Graham et al., 2003; Day et al., 2005; Higham et al., 2006a; Holzman et al., 2007). If predator-prey distance is limited, then even across prey species with different characteristics there may be little need for *E. sandwicensis* to modulate its predatory strikes.

My objectives in this study were to measure the feeding kinematics and performance of *E. sandwicensis* striking at gobiid postlarvae (juveniles), in order to (1) evaluate the characteristics of successful and unsuccessful strikes, and (2) compare *E. sandwicensis* performance across prey species with differing traits, testing the extent to which it modulates its predatory behavior. For the latter objective, I compared strikes on *S. stimpsoni*, which are larger and have a high proportion of axial red muscle, and on *A. guamensis*, which are smaller and have a significantly lower proportion of red muscle than *S. stimpsoni* (Cediel et al., 2008). Through such data on the predatory performance of *E. sandwicensis*, a further goal of this study is to provide insight into the selective pressure this species may apply to migratory juveniles of amphidromous Hawaiian gobies (Blob et al., 2010).

MATERIALS AND METHODS

Field Collection

During two field seasons (2010-2011), specimens of *Eleotris sandwicensis* Vaillant and Sauvage 1875 (140.25 ± 8.86 mm TBL; N = 4) were captured while snorkeling in the lowest reaches of Hakalau Stream on the Island of Hawai'i

(19°53’55.17’’N, 155°7’51.86’’W) using an o’pae net (prawn net). Individuals of similar size were selected to avoid potential scaling effects and differences in foraging behaviors across individuals in my comparisons (e.g., Winemiller and Ponwith, 1998; Chapter 5). Specimens of postlarval Hawaiian gobiid species, *Sicyopterus stimpsoni* (20-24 mm TBL) and *Awaous guamensis* (14-16 mm TBL), were collected as prey fish, also from Hakalau stream on the Island of Hawai’i, using dip nets. All fish collected for this study were kept in aerated stream water at its ambient temperature (18-21ºC) and transported within two hours of capture for housing at a research facility of the Hawai’i Department of Land and Natural Resources, Division of Aquatic Resources (DAR) in Hilo, Hawai’i.

Kinematic and Performance Analysis

All collected *E. sandwicensis* were starved over five days before filming of predatory strikes. During both acclimation and filming periods, each *E. sandwicensis* individual was placed in the center of a small Plexiglas tank (5.76 L; 36.0x16.0x10.0 cm^3) with a mild flow (0.002-0.003 m/s) to induce directionality of swimming of prey fish in front of the predator (Fitzsimons et al., 1997; Schoenfuss & Blob, 2003). During the filming period, 3-6 postlarvae of a single species were introduced into the tank. To evaluate kinematics of predatory feeding strikes on prey fish, each *E. sandwicensis* was filmed in digitally synchronized lateral and ventral views using two high-speed cameras (1000 fps; Phantom V4.1, Vision Research, Inc., Wayne, NJ). Both successful and unsuccessful sequences were filmed to allow evaluation of the factors contributing to capture success.

Anatomical landmark points on the head of the predator, as well as on prey fish, were digitized from high-speed videos of feeding sequences using the program DLTdv5 (Hedrick, 2008) in MatLab 7.12 (Mathworks, Inc.; Natick, MA, USA). Following conventions from Maie et al (2009b) for kinematic analyses of suction feeding of the Hawaiian gobiids *A. guamensis* and *L. concolor*, 11 points in lateral view and eight points in ventral view were selected for digitizing (Figure 4.1). For lateral landmarks, 10 points on the predator's feeding apparatus included: a, anterior tip of the premaxilla; b, anterior tip of the dentary; c, posterior edge of the joint between the maxilla and dentary; d, ventral border of the hyoid arch; e, center of the eye; f, anterior tip of the neurocranium (joint between the maxilla and neurocranium); g, top of the neurocranium (insertion point for the epaxialis muscle); h, posterior tip of the operculum; i, dorsal tip of the pectoral fin base; and j, ventral tip of the pectoral fin base (Figure 4.1A). One additional point on the postlarval fish's head (k) also was digitized (Figure 4.1A). For ventral landmarks, seven points on the predator's head included: l, the anterior tip of the premaxilla; m, anterior tip of the dentary; n, a point on the posterior border of the hyoid arch; lateral tips of the premaxilla (o, right; p, left); and lateral most tips of the operculum (q, right; r, left; t, midpoint between q and r) (Figure 4.1B). One additional point on the tip of the snout of *S. stimpsoni* or *A. guamensis* postlarvae (s) also was digitized (Figure 4.1B).

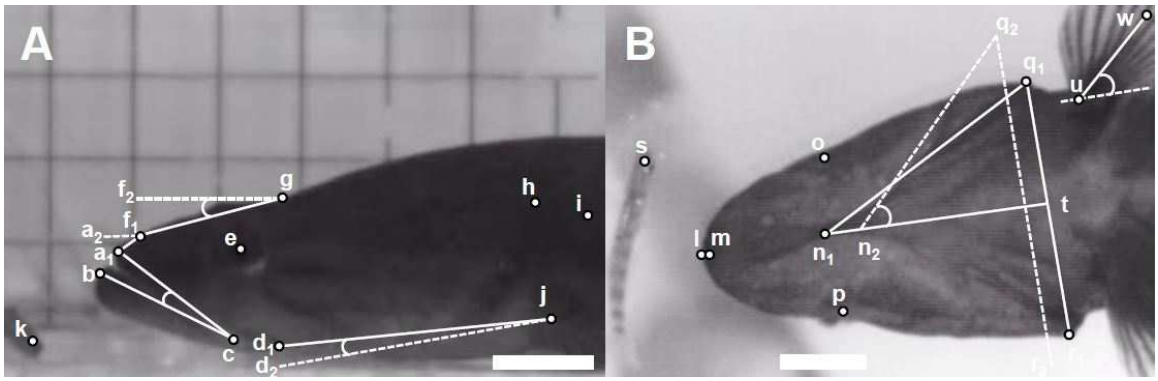

Figure 4.1: Lateral and ventral view of Hawaiian sleeper, *Eleotris sandwicensis*, illustrating 11 lateral anatomical landmarks (A), 10 ventral landmarks (B), and angular excursions between vectors formed by landmark points (angle a-c-b, gape angle; angle f_1-g-f_2, cranial elevation angle; angle d_1-j-d_2, hyoid depression angle; angle q-n-t, hyoid retraction angle), with t as mid point between q and r on the long axis of the head. Pectoral fin excursion angle is expressed by the angle formed by two vectors, w-u and n-t. Dashed lines represent positions of corresponding lines (solid lines) when each element is further moved toward full expansion of the buccal cavity. Scale bar indicates 10 mm.

Custom programs written in MatLab were used to calculate kinematic variables from the digitized coordinate data, including the angular and linear excursions of the upper and lower jaw, neurocranium, hyoid, operculum, as well as maximum values and timing variables associated with movement of the feeding apparatus (e.g., Maie et al., 2009b: Table 4.1). In addition to kinematics of the feeding apparatus, the angular excursion (i.e., adduction-abduction) of the predator's pectoral fin during the feeding strike (in the ventral view) was evaluated by digitizing the tip and base of the pectoral fin (w and u) and calculating the angle formed between this vector and the body axis (Table 4.1, Figure 4.1B). Fitting a quintic spline to the kinematic calculations, each feeding strike sequence was smoothed and interpolated to the same duration with 1% increments

through the gape cycle (101 equally spaced points) in order to obtain mean kinematic profiles for each variable.

Kinematic variable	Description
Gape	Angular/linear excursion between upper and lower jaws (Fig. 1: angle a-c-b; distance a-b)
Mandibular depression	Angular/linear excursion of the lower jaw from the beginning of the feeding strike
Premaxillary protrusion	Linear displacement of the premaxilla (Fig. 1: distance a-f)
Cranial elevation	Angular/linear excursion of a vector between the anterior tip of the neurocranium and the top of the neurocranium from the beginning of feeding strike (Fig. 1: angle f_1-g-f_2; distance f_1-f_2)
Hyoid depression	Angular/linear excursion of a vector between a point at the ventral border of the hyoid arch and a point at the ventral tip of the pectoral fin base from at the beginning of the feeding strike (Fig. 1: angle d_1-j-d_2; distance d_1-d_2)
Hyoid retraction	Angular excursion between the long axis of the head and the ceratohyal on the right side of the hyoid arch, with minimum angle subtracted (Fig. 1: angle q-n-t)
Opercular expansion	Linear excursion between the lateral-most tips of the two opercula, subtracted by its minimum distance (Fig. 1: distance q-r)
Pectoral fin adduction-abduction	Angular excursion of a vector between a point at the tip of the pectoral fin and a point at the base of the pectoral fin relative to the long axis of the head (Fig. 1: angle between w-u and n-t)
Gape cycle	Time between the beginning of feeding strike and the end of the strike
Time to max gape	Time from the beginning of feeding strike (i.e., first jaw movement to open the mouth) to maximum gape
Time to max mandibular depression	Time from the beginning of feeding strike to maximum mandibular depression
Time to max upper jaw protrusion	Time from the beginning of feeding strike to maximum upper jaw protrusion
Time to max cranial elevation	Time from the beginning of feeding strike to maximum cranial elevation
Time to max hyoid depression	Time from the beginning of feeding strike to maximum hyoid depression
Time to max hyoid retraction	Time from the beginning of feeding strike to maximum hyoid retraction angle
Time to max opercular expansion	Time from the beginning of feeding strike to maximum opercular expansion
Time to jaw closure from max gape	Time from maximum gape to the end of the feeding strike

Table 4.1: Kinematic variables calculated using landmarks digitized from suction feeding events by the Hawaiian sleeper, *Eleotris sandwicensis*.

Successful prey capture by suction feeding fishes requires the hydrodynamic capacity of the feeding apparatus (e.g., speed of buccal cavity expansion) to generate strong negative pressure relative to the ambient environment, which draws the mass of water and prey into the opening mouth (Osse, 1969; Muller et al., 1982; Lauder and Clark, 1984; Muller and Osse, 1984; Norton, 1991; Wilga and Motta, 2000; Sanford and Wainwright, 2002; Svanbäck et al., 2002; Day et al., 2005; Higham et al., 2006a, b; Wainwright and Day, 2007). Such functional capacity in prey capture behavior of *E. sandwicensis* is facilitated by well-developed cranial muscles and a lever mechanism that

produces movements of its highly kinetic feeding apparatus (Figure 4.2A: Maie et al., 2009a; Chapter 5). Using geometric modeling of changes in the volume of the buccal cavity (as a pair of conical frusta) through the time course of feeding strikes based on combined lateral and ventral kinematic data (Figure 4.2B: see Maie et al., 2009b for the formulas used in this study), I estimated values of the following variables for each strike for further comparisons of suction feeding performance: (1) buccal volume change; (2) suction flow speed; and (3) pressure differential.

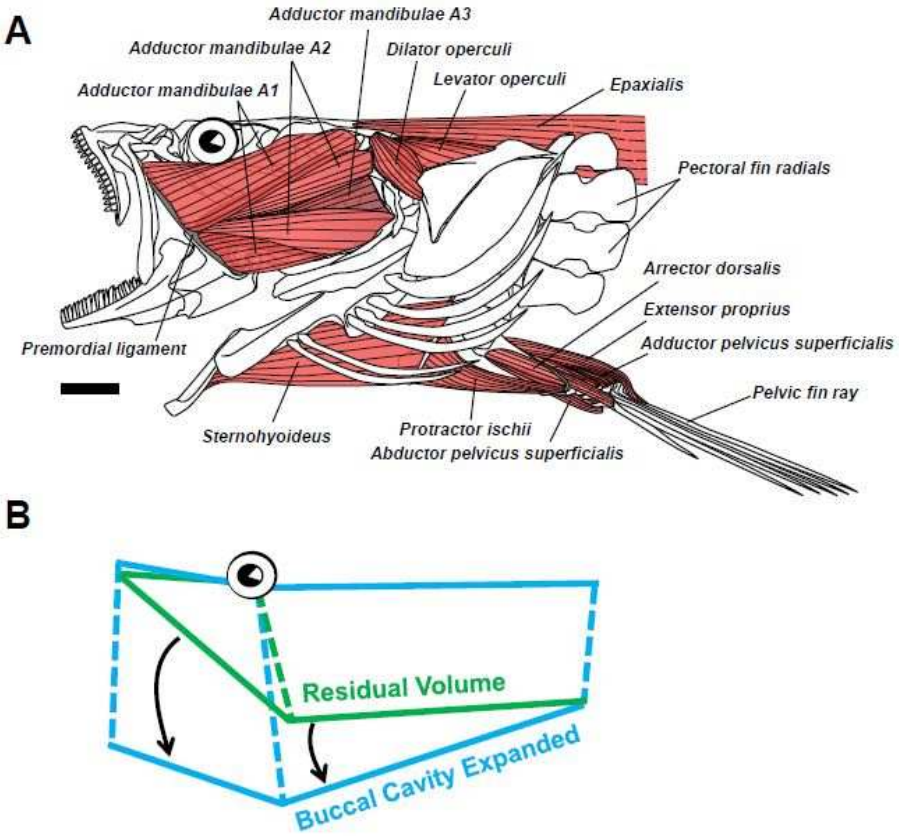

Figure 4.2: Feeding apparatus of *Eleotris sandwicensis* with major jaw opening expaxialis and sternohyoideus muscles, and jaw closing adductor mandibulae complex (A), and a simulated expansion of the buccal cavity (B) in lateral view.

Statistical Analysis

Statistical analyses were performed using JMP 10.0 Pro for Windows (SAS Institute, Cary, NC, USA). A total of 66 trials from four individuals of *E. sandwicensis* (24 successful and 16 failed strikes on juvenile *S. stimpsoni*; 18 successful and 8 failed strikes on juvenile *A. guamensis*) were analyzed in this study. Each category (successful strike on juvenile *S. stimpsoni*; failed strike on juvenile *S. stimpsoni*; successful strike on juvenile *A. guamensis*; failed strike on juvenile *A. guamensis*) was tested for individual variation in predator-prey distance at the beginning of feeding strikes using one-way analysis of variance (ANOVA). No categories showed significant differences between individual predators ($P = 0.1453$ for successful strike on juvenile *S. stimpsoni*; $P = 0.2077$ for unsuccessful strike on juvenile *S. stimpsoni*; $P = 0.8301$ for successful strike on *A. guamensis*; $P = 0.9406$ for successful strike on *A. guamensis*); therefore, all trials in each category were pooled together. In addition, on the pooled data for each category, Kolomogorov-Smirnov tests indicated that values of predator-prey distance were normally distributed, validating the use of parametric statistical tests in my study. Two-way ANOVAs followed by Fisher's PLSD post-hoc tests ($\alpha = 0.05$) were performed to evaluated differences in feeding kinematics and performance of *E. sandwichensis* between successful and unsuccessful (failed) prey captures, and between prey species. In addition, ANCOVAs were performed on one kinematic variable (maximum cranial elevation) and three timing variables (time to maximum premaxillary protrusion, time to maximum cranial elevation angle, time to maximum angular excursion of hyoid

retraction; see Results), with which predator-prey distance covaried, to account for the effect of predator-prey distance on comparisons of these variables across groups, A sequential Bonferroni correction was not applied to my data because some variables were not independent on one another, as well as to avoid the effect of increasing Type II error (Cabin and Mitchell, 2000; Moran, 2003).

RESULTS

General Characteristics of *E. sandwicensis* Feeding Kinematics and Performance

In typical suction feeding events by *E sandwicensis* (Figures 4.3A, 4.3B), gape angle, premaxillary protrusion, and hyoid depression reached their maxima at 32-50% of the gape cycle, followed by cranial elevation, hyoid retraction, and opercular expansion reaching their maxima (57-69% cycle: Table 4.3; Figure 4.4). Movements of these kinematic variables dictate the sequence of expansion of the eleotrid buccal cavity in the double-frustum-model (reaching a maximum at 53-65% gape cycle: Table 4.4; Figure 4.6) and, thereby, creating a unidirectional suction flow from the oral cavity to the opercular cavity. Although all *E. sandwicensis* individuals exhibited some degree of forward movement of the body during feeding strikes, prey fish were always drawn into the predator's mouth and no opening of the gill slits were detected in the predator during at least jaw opening duration in any feeding trials. This indicates that prey fish were captured primarily through suction, rather than by ram feeding (e.g., Maie et al., 2009b). In addition, *E. sandwicensis* exhibited maximum adduction of the pectoral fins (20-27^{o}) at 14-26% of the gape cycle, well before any other kinematic variables of the feeding

apparatus reached their maxima, and also showed a strong braking maneuver (maximum abduction: 102-108^{o}) at the end of the feeding strike (93-99%: Table 4.3; Figures 4.4O, 4.4P) well after other kinematic variables reached their maxima (Table 4.3; Figure 4.4). The transition between acceleration and deceleration occurred when the maximum gape was reached (Figures, 4.4O, 4.4P, 4.6A, 4.6B). Although the locomotor pattern of the pectoral fin maneuver was similar to that exhibited by centrarchid fishes feeding on elusive prey (e.g., Higham, 2007), *E. sandwicensis* showed greater angular excursion (73-85^{o}) with a mean rotational speed of 0.94-1.18 ^{o}/ms (e.g., ~50-60^{o} angular excursion achieved by largemouth bass, *Micropterus salmoides*: Higham, 2007).

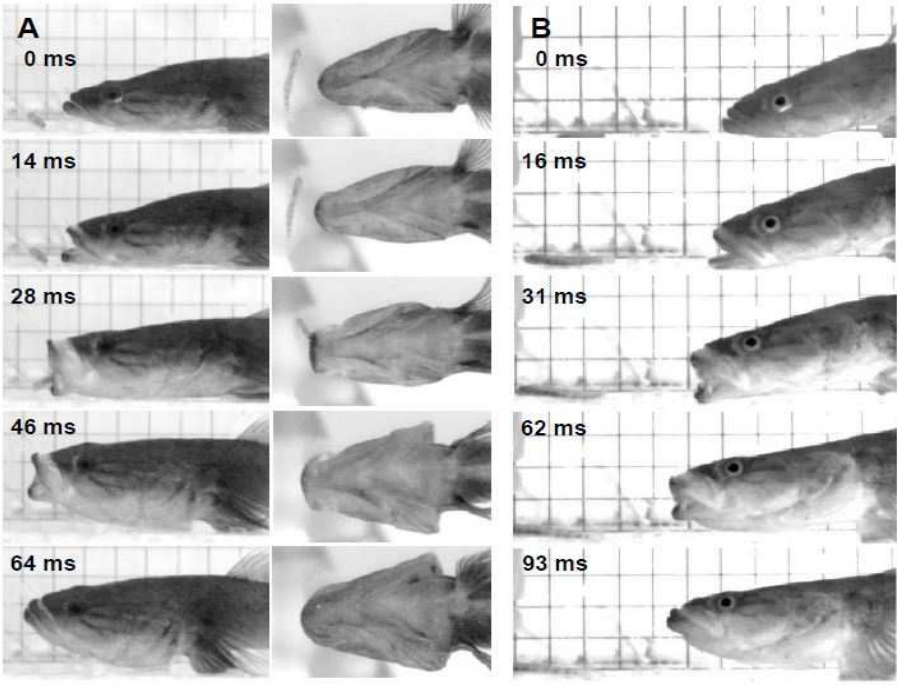

Figure 4.3: Selected frames from high-speed video of suction feeding behavior in *Eleotris sandwicensis* feeding successfully on juvenile Sicyopterus stimpsoni in lateral and ventral views (A), and unsuccessful strike on juvenile *S. stimpsoni* by *E. sandwicensis* in lateral view (B). The entire

gape cycle was completed in 64.17± 4.33 ms (maximum gape reached at 28.04 ± 1.30 ms) for successful feeding on juvenile *S. stimpsoni*, and 92.88 ± 11.33 ms (maximum gape reached at 30.63 ± 2.52 ms) for unsuccessful attempt on juvenile *S. stimpsoni*. Background in the aquarium is a 1 cm grid sheet.

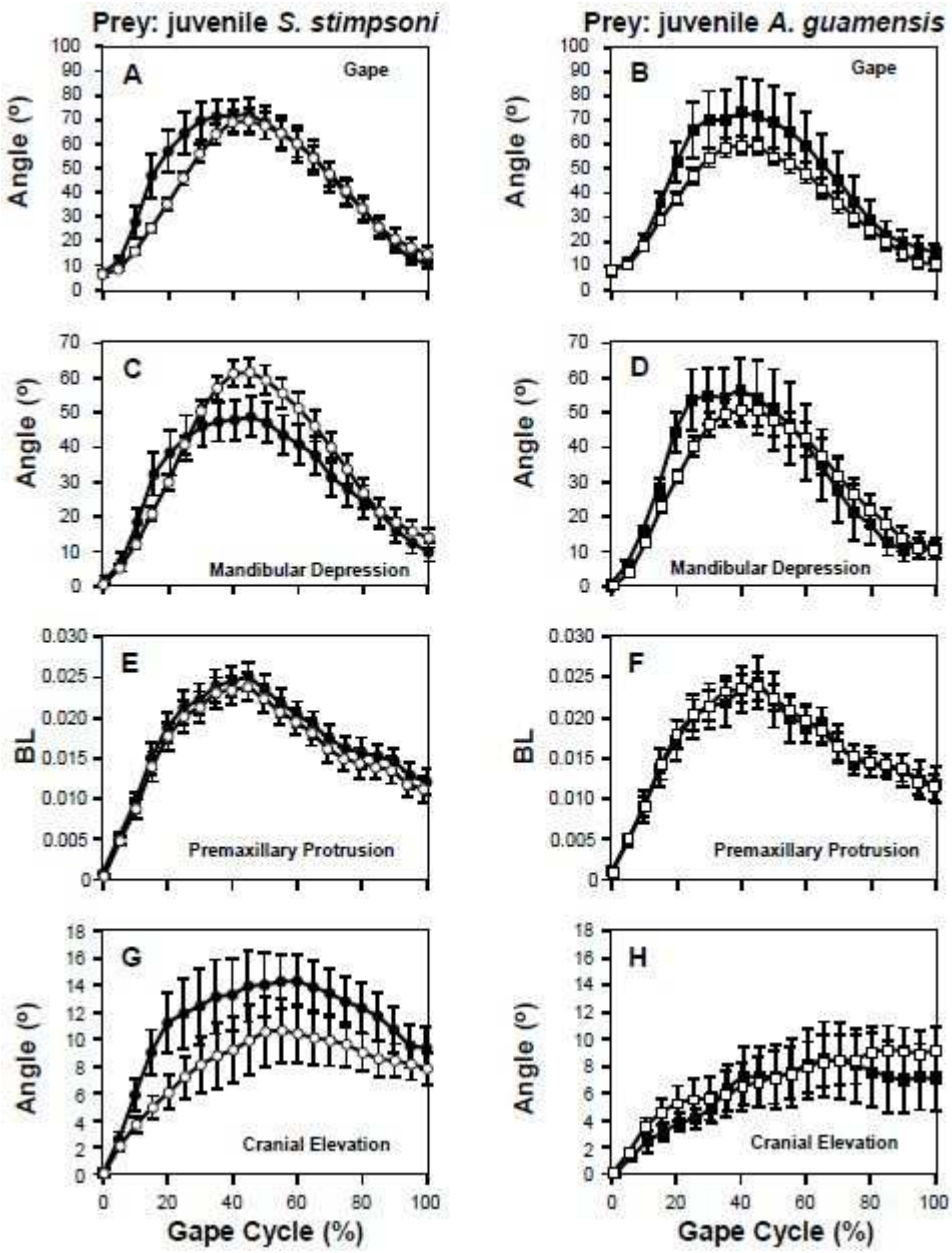

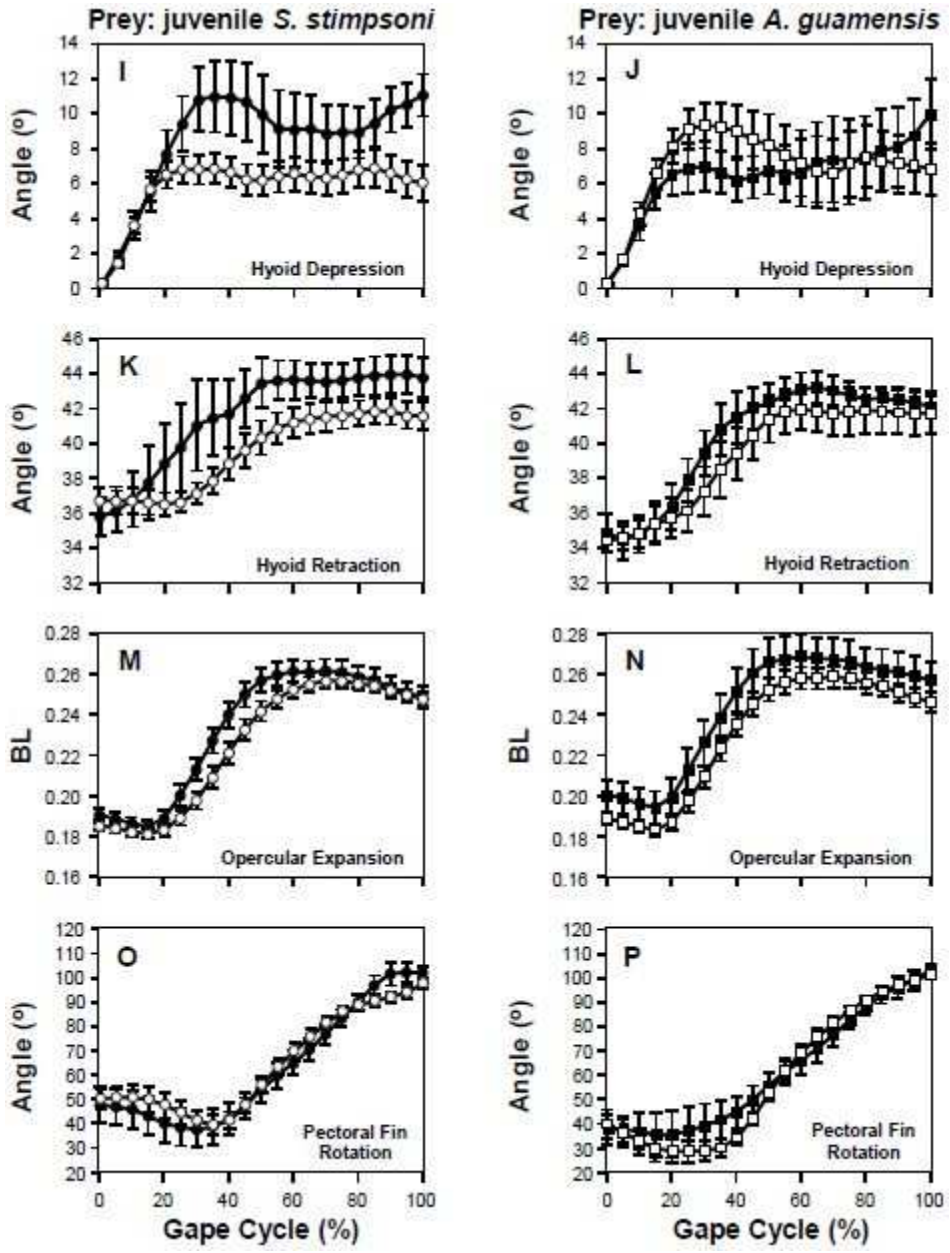

Figure 4.4: Average kinematic profiles across all analyzed trials for gape cycle (A, B), mandibular depression (C, D), premaxillary protrusion (E, F), cranial elevation (G, H), hyoid depression (I, J), hyoid retraction (K, L), opercular expansion (M, N), and pectoral fin rotation (O, P) during suction feeding behaviors in *Eleotris sandwicensis* (open circle and square: successful prey capture; closed circle and square: failed prey capture) with two different prey fish species (circle: juvenile *Sicyopterus stimpsoni*; square: juvenile *Awaous guamensis*). To construct profiles, all trials were

normalized to the same duration, and variable values for all trials for a given group were interpolated to evenly distributed percentage increments of the gape cycle, from which average values (points) and standard errors (error bars) were calculated for each time increment.

At the beginning of feeding strike, the predator generated a surge of water flow that reached its maximum of 36-84 BL/s at 11-30% gape cycle; as a result, the maximum pressure differential was established during this phase of the cycle (16.49-118.89 kPa: Table 4.4; Figures 4.6A-4.6F). By this point of the cycle, however, the mouth of the predator only reached approximately 20% of its maximum gape. Suction flow, immediately after reaching its peak, started to drop markedly until 33-44% gape cycle, when predators reached maximum gape area (Figures 4.6A-4.6F). From the time of maximum gape to maximum buccal volume at 53-65% gape cycle, suction flow decreased slowly and diminished to zero (Figures 4.6E, 4.6F). This flow pattern after the peak flow in suction feeding indicated that the predator must close its jaws quickly to secure prey trapped in the mouth. Reflecting this demand, the time during feeding cycles that *E. sandwicensis* spent during jaw closing was typically close to the time spent during the rapid jaw opening that generated suction, ranging from 56-67% of the cycle for al strikes, and 56-58% for successful prey capture. For comparison, *E. sandwicensis* had jaw closing durations only 1.2 times longer than jaw opening durations (Table 4.3), whereas other suction feeding gobiids (e.g. *L. concolor*: Maie et al., 2009b) had jaw closing durations as much as 2 times longer than jaw opening durations. Although back-flow was predicted from my model, unidirectional flow of water through the gill slits of

the predator would be induced due to opening of the operculum followed by compression of the buccal cavity after prey capture (Figures 4.6E, 4.6F).

Predator-Prey Distance

E. sandwicensis began suction feeding events at significantly closer distances to prey fish in successful strikes than in failed strikes, regardless of species of the prey (e.g., 49.2% closer for juvenile *S. stimpsoni*; 39.6% for juvenile *A. guamensis*: Table 4.2; Figure 4.5). *E. sandwicensis* also showed significant differences between prey species in the predator-prey distance that yielded successful and failed strikes. For successful prey capture as well as failed strikes, predators were closer to juvenile *A. guamensis* than juvenile *S. stimpsoni* (12.2% BL vs. 18.6% BL for successful prey capture; 20.2% BL vs. 36.6% BL for failed strike: Table 4.2, Figure 4.5).

Prey	Capture Result	N	Predator-Prey Distance at T = 0 (Mean ± SE)	P-value; F-ratio
Juvenile *S. stimpsoni*	Successful	24	0.186 ± 0.013 BL (25.82 ± 1.74 mm)	$P<0.0001^*$; $F_{1,38}=45.5336$
	Failed	16	0.366 ± 0.020 BL (53.72 ± 3.09 mm)	
Juvenile *A. guamensis*	Successful	18	0.122 ± 0.014 BL (17.57 ± 1.75 mm)	$P=0.0005^*$; $F_{1,24}=16.3284$
	Failed	8	0.222 ± 0.021 BL (32.91 ± 3.34 mm)	

Capture Result	Prey	N	Predator-Prey Distance at T = 0 (Mean ± SE)	P-value; F-ratio
Successful	Juvenile *S. stimpsoni*	24	0.186 ± 0.013 BL (25.82 ± 1.74 mm)	$P=0.0019^*$; $F_{1,40}=11.0731$
	Juvenile *A. guamensis*	18	0.122 ± 0.012 BL (17.57 ± 1.75 mm)	
Failed	Juvenile *S. stimpsoni*	16	0.366 ± 0.020 BL (53.72 ± 3.09 mm)	$P=0.0013^*$; $F_{1,22}=13.4696$
	Juvenile *A. guamensis*	8	0.222 ± 0.021 BL (32.91 ± 3.34 mm)	

Table 4.2: Predator-prey distance at the beginning (T = 0 ms) of feeding strike by the predator. Significant difference at $\alpha < 0.05^*$ (ANOVA).

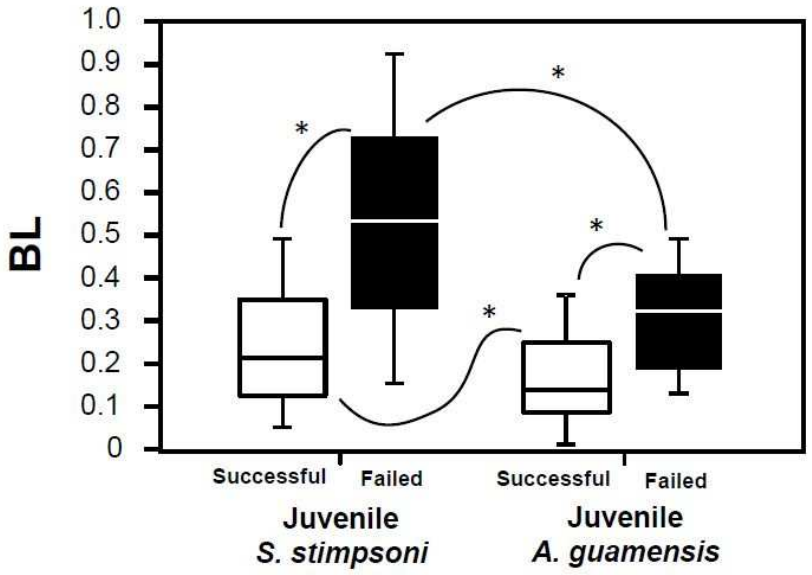

Figure 4.5: Box plots comparing distance between the predator (*Eleotris sandwicensis*) and prey (juvenile *Sicyopterus stimpsoni* and *Awaous guamensis*) in body lengths (BL) of the predator at the beginning (T = 0 ms) of feeding strikes for successful and failed prey captures. For each plot, the box ranges from the first to third quartiles (25-75%), and a line indicates the median. Significant difference at P<0.05* (ANOVA followed by Fisher's PLSD post-hoc tests, see Table 4.2).

Comparison of Feeding Kinematics and Performance Between Successful and Unsuccessful Events and Between Prey Species

Comparisons of maximum values of kinematic variables for *E. sandwicensis* between strikes that resulted in successful and failed prey capture indicated specific movements of the feeding apparatus that may have particular importance in contributing to successful feeding. Overall speed of the gape cycle was 30% faster (P = 0.0195: Table 4.3) during successful predation on juvenile *S. stimpsoni* than during failed attempts. However, no significant difference in gape cycle duration was detected between successful and failed attempts to capture juvenile *A. guamensis* (P = 0.3311: Table 4.3).

Predators also exhibited faster jaw closing speeds during successful capture of juvenile *S. stimpsoni* than during failed attempts (by 42%; P = 0.0392: Table 4.3), but as in comparisons of overall cycle duration no significant difference was present between successful and failed attempts to capture juvenile *A. guamensis* (P = 0.2449: Table 4.3). Although maximum gape angle was significantly smaller in successful versus failed attempts to capture juvenile *S. stimpsoni*, the linear excursion of gape and the time to reach maximum gape did not differ between successful and failed attempts to capture either prey species (Table 4.3). *E. sandwicensis* did show a greater maximum gape area during successful strikes on juvenile *S. stimpsoni* compared to successful attempts on juvenile *A. guamensis* (by 5.6%; P = 0.0383: Table 4.4). However, maximum gape area did not differ significantly between successful and failed strikes on either prey species (P = 0.0634 for juvenile *S. stimpsoni*; P = 0.6364 for juvenile *A. guamensis*: Table 4.4).

	Prey Capture					
	Juvenile *S. stimpsoni*			Juvenile *A. guamensis*		
Kinematic Variable	Successful (N = 24)	Failed (N = 16)	P-value	Successful (N = 18)	Failed (N = 8)	P-value
Max gape angle (°)	86.96 ± 6.31	94.14 ± 9.89	0.0059*	71.02 ± 7.41	90.89 ± 15.13	0.2552
Max gape (BL)	0.084 ± 0.003	0.091 ± 0.006	0.1387	0.083 ± 0.003	0.077 ± 0.009	0.7847
	(11.68 ± 0.57 mm)	(13.08 ± 0.70 mm)		(12.04 ± 0.48 mm)	(11.08 ± 0.73 mm)	
Max mandibular depression angle (°)	69.94 ± 4.58	68.14 ± 5.78	0.607	58.91 ± 5.38	70.27 ± 8.85	0.1449
Max mandibular depression (BL)	0.087 ± 0.004	0.087 ± 0.009	0.5159	0.077 ± 0.004	0.077 ± 0.014	0.4639
	(12.25 ± 0.95 mm)	(12.68 ± 1.16 mm)		(11.18 ± 0.55 mm)	(11.19 ± 0.82 mm)	
Max premaxillary protrusion (BL)	0.030 ± 0.001	0.029 ± 0.002	0.6132	0.024 ± 0.002	0.028 ± 0.003	0.1026
	(4.20 ± 0.21 mm)	(4.23 ± 0.26 mm)		(3.53 ± 0.21 mm)	(4.07 ± 0.32 mm)	
Max cranial elevation angle (°)	14.84 ± 1.88	21.52 ± 2.49	0.0057*	12.35 ± 1.90	12.36 ± 3.30	0.9003
Max cranial elevation (BL)	0.036 ± 0.004	0.039 ± 0.004	0.3736	0.029 ± 0.004	0.027 ± 0.006	0.9010
	(5.06 ± 0.51 mm)	(5.62 ± 0.55 mm)		(4.17 ± 0.58 mm)	(3.85 ± 0.78 mm)	
Max hyoid depression angle (°)	11.47 ± 1.41	16.69 ± 1.62	0.0146*	11.80 ± 1.66	12.41 ± 2.48	0.8184
Max hyoid depression (BL)	0.056 ± 0.005	0.068 ± 0.007	0.0793	0.053 ± 0.006	0.054 ± 0.011	0.8022
	(7.91 ± 0.78 mm)	(10.06 ± 1.21 mm)		(7.69 ± 0.91 mm)	(7.82 ± 1.85 mm)	
Max hyoid retraction angle in excursion (°)	12.31 ± 1.11	17.30 ± 2.31	0.1493	11.93 ± 1.30	11.61 ± 3.53	0.5719
Max opercular expansion in excursion (BL)	0.077 ± 0.003	0.088 ± 0.003	0.0208*	0.076 ± 0.003	0.077 ± 0.004	0.8168
	(10.84 ± 0.47 mm)	(12.78 ± 0.58 mm)		(10.96 ± 0.42 mm)	(11.10 ± 0.63 mm)	
Max pectoral fin adduction angle (°)	20.61 ± 3.91	26.54 ± 6.14	0.4436	19.66 ± 4.59	22.21 ± 9.39	0.8664
Max pectoral fin abduction angle (°)	101.77 ± 2.70	107.58 ± 4.17	0.5437	104.74 ± 3.17	105.31 ± 6.38	0.4801
Gape cycle (ms)	64.17 ± 4.33	92.88 ± 11.33	0.0195*	73.44 ± 5.08	78.00 ± 17.33	0.3311
Time to max gape (ms)	28.04 ± 1.30	30.63 ± 2.52	0.1928	30.72 ± 1.52	27.13 ± 3.85	0.8928
Time to max mandibular depression (ms)	26.63 ± 1.07	29.88 ± 4.25	0.2104	30.00 ± 1.26	27.00 ± 6.50	0.8394
Time to max premaxillary protrusion (ms)	32.29 ± 3.14	35.13 ± 4.15	0.0262*	31.67 ± 2.05	33.38 ± 3.39	0.0773
Time to max cranial elevation (ms)	38.58 ± 3.62	35.38 ± 5.71	0.5779	53.89 ± 4.18	44.38 ± 8.08	0.0860
Time to max hyoid depression (ms)	31.67 ± 5.44	44.50 ± 6.71	0.2791	36.21 ± 4.63	42.13 ± 10.26	0.6468
Time to max hyoid retraction (ms)	40.25 ± 5.97	55.69 ± 7.91	0.0248*	52.06 ± 4.18	52.50 ± 12.80	0.5028
Time to max opercular expansion (ms)	50.17 ± 3.31	55.94 ± 4.38	0.1631	52.00 ± 2.74	51.50 ± 4.21	0.8353
Time to jaw closure from max page (ms)	36.13 ± 3.70	62.25 ± 10.77	0.0392*	42.72 ± 4.35	50.88 ± 16.47	0.2449
Time to max pectoral fin adduction (ms)	16.33 ± 2.84	20.34 ± 4.98	0.5208	18.72 ± 3.34	10.91 ± 7.62	0.2553
Time to max pectoral fin abduction (ms)	59.95 ± 4.58	88.17 ± 11.87	0.0512	72.80 ± 5.38	77.37±18.15	0.1537

Table 4.3: Angular and linear excursions, and timing variables associated with suction feeding kinematics in *Eleotris sandwicensis* for comparisons of successful versus failed prey capture and prey species (juvenile *Sicyopterus stimpsoni* vs. juvenile *Awaous guamensis*). Values are means ± SE. For variables standardized by body length (BL), raw non-standardized values are also provided in parentheses.

	Prey Capture					
	Juvenile *S. stimpsoni*			Juvenile *A. guamensis*		
Modeled Performance Variable	Successful (N = 24)	Failed (N = 16)	P-value	Successful (N = 18)	Failed (N = 8)	P-value
Max gape area (BL^2)	0.0057 ± 0.0004[a]	0.0068 ± 0.0007	0.0634	0.0054 ± 0.0005	0.0049 ± 0.0014	0.6364
	(117.06 ± 9.90 mm^2)	(98.95 ± 17.68 mm^2)		(111.73 ± 8.56 mm^2)	(142.24 ± 12.50 mm^2)	
Max buccal volume change (BL^3)	0.00096 ± 0.00007	0.00112 ± 0.00009	0.0520	0.00106 ± 0.00009	0.00098 ± 0.00018	0.8336
Maximum suction flow (BL/s)	59.11 ± 12.38	84.40 ± 13.21	0.0973	66.69 ± 14.51	36.49 ± 20.21	0.8049
	(8.34 ± 1.75 m/s)	(12.50 ± 2.07 m/s)		(9.46 ± 2.05 m/s)	(5.31 ± 3.16 m/s)	
Max pressure differential (kPa/BL^3)	385.86 ± 202.40	774.22 ± 284.29	0.1992	637.02 ± 292.83	105.44 ± 518.95	0.6307
	(55.75 ± 26.10 kPa)	(118.89 ± 39.53 kPa)		(89.18 ± 30.14 kPa)	(16.49 ± 55.91 kPa)	
Time to max buccal volume (ms)	41.80 ± 3.16	49.19 ± 5.52	0.1878	43.13 ± 4.20	44.73 ± 11.33	0.6526
Time to min buccal volume (ms)	2.27 ± 0.53	3.38 ± 0.57	0.5045	3.07 ± 0.71	1.99 ± 1.18	0.4447
Time to max buccal volume from min (ms)	39.53 ± 3.20	45.82 ± 5.51	0.2318	40.05 ± 4.25	42.75 ± 11.31	0.6267
Time to max suction flow (ms)	19.23 ± 5.55	21.61 ± 11.90	0.1115	14.03 ± 7.38	8.60 ± 10.18	0.3565

Table 4.4: Modeled suction feeding performance in *Eleotris sandwicensis* for comparisons of successful versus failed prey capture and prey species

(juvenile *Sicyopterus stimpsoni* vs. juvenile *Awaous guamensis*). [a]Values derived from empirical measurements, all other calculated from the model. Values are means ± SE. For variables standardized by body length (BL), raw non-standardized values are also provided in parentheses.

Maximum length of premaxillary protrusion did not differ between successful and failed attempts to capture either prey species (P = 0.6132 for juvenile *S. stimpsoni*; P = 0.1026 for *A. guamensis*: Table 4.3), and did not covary with predator-prey distance. However, predator-prey distance did covary with the time to reach maximum premaxillary protrusion. After ANCOVA was used to account for the effect of predator-prey distance, premaxillary protrusion reached its maximum significantly faster during successful captures of juvenile *S. stimpsoni* (by 8%; P = 0.0262: Table 4.3). Time to reach maximum premaxillary protrusion for successful capture of juvenile *A. guamensis* did not differ from that for successful capture of juvenile *S. stimpsoni* (P = 0.2524) or from that during failed attempts on *A. guamensis* (P = 0.0773: Table 4.3).

Accounting for the effect of predator-prey distance with ANCOVA, maximum cranial elevation angle was significantly smaller during successful attempts on juvenile *S. stimpsoni* than during failed attempts (by 31%; P = 0.0057: Table 4.3). Maximum cranial elevation angle for successfully capturing juvenile *S. stimpsoni* did not differ from the angle measured during successful (P = 0.3167) or unsuccessful (P = 0.9003) attempts to capture juvenile *A. guamensis* (Table 4.3). In other words, predators that failed to capture juvenile *S. stimpsoni* appear to have over-elevated the cranium during strikes.

Predator-prey distance covaried with the time to reach maximum cranial elevation only for feeding attempts on juvenile *A. guamensis*, although there was no difference in

this variable between successful and unsuccessful strikes (P = 0.0860: Table 4.3). Nonetheless, the time to reach maximum cranial elevation was significantly faster during successful capture of juvenile *S. stimpsoni* than during successful capture of juvenile *A. guamensis* (by 28.4%; P = 0.0308: Table 4.3), and during failed attempts on juvenile *S. stimpsoni* compared to failed attempts on juvenile *A. guamensis* (by 20.3%; P = 0.0211: Table 4.3).

Hyoid depression angle was significantly smaller during successful strikes on juvenile *S. stimpsoni* than during failed strikes (by 31.3%; P = 0.0146), but did not differ between successful and failed attempts to capture juvenile *A. guamensis* (P = 0.8184: Table 4.3). There were also no significant differences between successful and failed attempts across prey species (P = 0.8633 for successful capture; P = 0.2220 for failed). No significant difference was found between successful and failed attempts for the time to maximum hyoid depression (P = 0.2512 for juvenile *S. stimpsoni*; P = 0.6468 for juvenile *A. guamensis*: Table 4.3).

Within each prey species, no difference in the angular excursion of hyoid retraction was found between successful and failed capture attempts (P = 0.1493 for *S. stimpsoni*; P = 0.5725 for *A. guamensis*). There were also no differences in maximum hyoid retraction angle across prey species (P = 0.3928 for successful capture; P = 0.2963 for failed: Table 4.3). However, accounting for the effect of predator-prey distance on time to reach maximum angular excursion with ANCOVA, the time to reach maximum hyoid retraction was significantly faster during successful capture of juvenile *S. stimpsoni*

than during failed attempts (by 27.7%; P = 0.0248: Table 4.3). This difference was not found during feeding on juvenile *A. guamensis* (P = 0.5028: Table 4.3).

The linear excursion of opercular expansion was significantly smaller for successful versus unsuccessful attempts to capture juvenile *S. stimpsoni* (by 12%; P = 0.0208); however, this variable did not differ between successful and failed attempts on juvenile *A. guamensis* (P = 0.8168: Table 4.3). In addition, there was no difference in opercular expansion between prey species within each capture outcome (P = 0.1073 for successful capture; P = 0.0582 for failed). No difference was found in the time to reach maximum opercular expansion between successful and failed captures within each prey species (P = 0.1631 for *S. stimpsoni*; P = 0.8353 for *A. guamensis*), or during successful captures across prey species (P = 0.5037). However the time to reach maximum opercular expansion was significantly shorter during failed attempts to capture juvenile *S. stimpsoni* compared to failed attempts on juvenile *A. guamensis* (by 8%; P = 0.0416: Table 4.3).

No difference in suction flow was found between prey capture outcomes within each species (P = 0.1115 for *S. stimpsoni*; P = 0.3389 for *A. guamensis*: Table 4.4). Although there was no differences in suction flow across species during successful prey captures (P = 0.5282), during failed capture attempts *E. sandwicensis* was predicted to exert 56.8% greater suction flow on juvenile *S. stimpsoni* than on *A. guamensis* (P = 0.0418: Table 4.4). No difference in time to reach maximum suction flow was found between successful and failed capture attempts within each prey species (P = 0.0973 for *S. stimpsoni*; P = 0.8049 for *A. guamensis*: Table 4.4), or between prey species within

each outcome (P = 0.6564 for successful capture; P = 0.2283 for failed capture: Table 4.4).

No comparisons associated with the amount or timing of buccal volume change showed significant differences between successful and failed captureattempts within each prey species, or between prey species within each capture outcome (all P > 0.05). Predator-prey distance did not covary with these variables.

DISCUSSION

Evaluations of the functional abilities and constraints of predators can provide insight into the factors influencing predator-prey interactions, including the functional demands and selective pressures that predators impose on prey. Such insights could be of particular significance for systems with low taxonomic diversity such as oceanic island streams, where the variety of predators and competing pressures on prey might be limited, allowing assessment of major ecological and evolutionary impacts on prey species.

Structural and Kinematic Factors Underlying Suction Feeding Performance of *Eleotris sandwicensis*

Suction feeding requires the predator to establish a strong pressure differential between the interior of the buccal cavity and vicinity of the mouth, thereby generating a flow into the oral chamber, which overcomes the prey's escaping behavior. Although the large gape of *E. sandwicensis* (maximum of 8-9% BL, nearly twice other gobiids: Maie et

al., 2009b) could potentially reduce the hydrodynamic capacity to maximize pressure differentials (e.g., the Bernoulli equation), fast jaw movements at the right timing and position help alleviate this potential negative effect and induce strong suction flow (e.g., Day et al., 2005; Wainwright and Day, 2007). In fact, suction flow speed reaches its maximum only when gape is still small, and speed diminishes when gape, and then buccal volume, reach their maxima (Figure 4.5). However, the large head, and thus, buccal cavity of *E. sandwicensis* (18.5-2.15 times larger than other gobiids': Maie et al., 2009b) help maximize the capacity to take volumes of water (and potentially sizeable prey) into the mouth. The combination of these features contributes to the capacity of *E. sandwicensis* to produce levels of suction feeding performance that enable the capture of elusive free swimming prey such as amphidromous gobiid postlarvae.

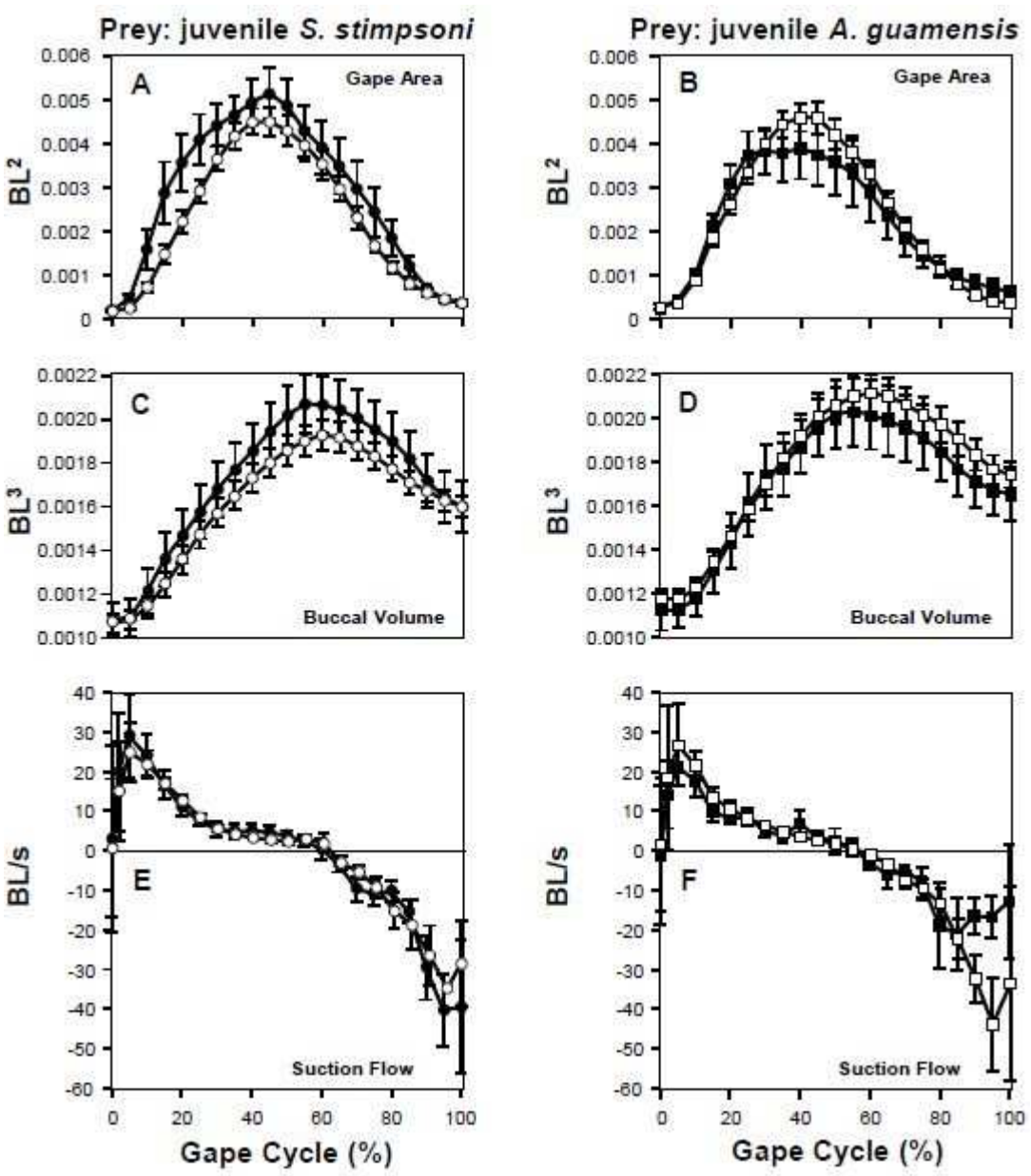

Figure 4.6: Estimated profiles of gape area (A, B), buccal volume (C, D), and flow speed (E, F) during suction feeding behaviors in *Eleotris sandwicensis* (open circle and square: successful prey capture; closed circle and square: failed prey capture) with two different prey fish species (circle: juvenile *Sicyopterus stimpsoni*; square: juvenile *Awaous guamensis*) based on high-speed video and geometrically modeled data. Profile construction followed procedures described for Figure 4.4.

Importance of Predator-prey Distance to Eleotrid Suction Feeding Performance

Comparisons of predator-prey distance between successful and unsuccessful feeding attempts across gobiid prey species indicate the significance of this factor on the effectiveness of the predation (e.g., suction feeding), and the different requirements for successful predation on each species. For example, juvenile *S. stimpsoni* can be captured from up to approximately 19% BL away from the mouth (2.2 times larger than maximum gape), but successful capture of *A. guamensis* requires attack from a closer distance of only 12% BL (1.5 times larger than maximum gape: Table 4.2). This difference in the distance required for effective predation might make the predator selective toward potential prey. For example, the ability to capture bigger fish from longer distances might make them easier prey, a factor that might make larger *S. stimpsoni* preferred targets compared to smaller *A. guamensis*, and might help to explain the tendency of *E. sandwicensis* to impose negative selection on body mass among *S. stimpsoni* juveniles (Blob et al., 2010). Future studies that examine locomotor performance (acceleration and velocity) during escape behaviors of prey fishes with different body size would provide further insight into the factors contributing to the different distances required for *E. sandwicensis* to successfully prey on different goby species (e.g., Webb, 1976; Domenici and Blake, 1993).

Modulation of Predatory Behavior Between Prey Species and the Factors Contributing to Successful Prey Capture

Based on kinematic and performance differences I observed, *E. sandwicensis* appeared capable of modulating its predatory behavior with respect to different prey species. For example, predators showed larger gape areas and faster cranial elevation during successfully captures of *S. stimpsoni* than during successful captures of *A. guamensis*. However, many kinematic variables showed no difference between successful and unsuccessful suction feeding attempts. For example, movements of the pectoral fins during feeding strikes, which showed no modulation, suggest that the sequence of acceleration and deceleration may be a stereotypical locomotor maneuver of the predator (Wainwright et al., 2008), perhaps playing an important role in improving its positioning and accuracy of prey capture (e.g., Lauder and Drucker, 2004; Higham et al., 2006a). In addition, during feeding attempts on juvenile *A. guamensis*, *E. sandwicensis* showed no differences in any kinematic variable between successful and unsuccessful strikes. Given that the volume change of the buccal cavity also did not differ across feeding outcomes (successful versus failed capture) or prey species, the factor that appears most important in determining the outcome of feeding on juvenile *A. guamensis* is simply predator-prey distance. It is possible that over the shorter suction distances employed against small *A. guamensis* compared to larger *S. stimsoni*, the opportunity for kinematic modulation by *E. sandwicensis* is constrained.

Although many kinematic variables showed no difference between successful and unsuccessful suction feeding attempts, variables that did differ significantly between outcomes could be of particular importance in determining feeding success by *E. sandwicensis*. For example, during strikes on juvenile *S. stimpsoni*, *E. sandwicensis*

showed faster gape cycles, jaw closing, premaxillary protrusion, and hyoid retraction in successful attempts, and exhibited smaller gape and cranial elevation angles, as well as smaller opercular expansion lengths (Table 4.3). The smaller values for cranial elevation and opercular expansion may help *E. sandwicensis* regulate water flow through the buccal cavity to achieve suction performance more efficiently.

In addition, the kinematic and performance data in my study would help predict which and how the cranial muscles could be activated by the cranial nerves, but future studies that empirically examine the electromyographical pattern of the muscles (e.g., Ralston and Wainwright, 1997; Matott et al., 2005) would provide more insightful understanding in the nature of modulation and perhaps trophic specialization in *E. sandwicensis*. Through this study, I only presented one side of predator-prey interaction, focusing on suction feeding of the predator, and future studies that evaluate the escape behavior and performance of juvenile gobiids up the predation by *E. sandwicensis* and how these prey fish detect and react to the pressure gradient generated by the predator would provide an opportunity to fully understand predator-prey interaction both the predator and the prey would experience in the streams.

Predatory Behavior and Performance of *Eleotris sandwicensis*: Functional Underpinnings of Evolutionary Impact

The sleeper gobies, eleotrids, are a speciose and geographically widely distributed group of gobioid fish (Nordlie, 1981; Miller, 1998; Winemiller and Ponwith, 1998; Keith et al., 2002; Pezold and Cage, 2002; Ziegler, 2002; Maeda et al., 2011). In Hawaiian

streams, *E. sandwicensis* is the primary or, commonly, exclusive predator on the postlarvae of goby species migrating through lower stream reaches on the way to adult habitats (Schoenfuss and Blob, 2007). The tendency of *E. sandwicensis* to be camouflaged and remain motionless until its prey swims close by has been documented previously (Tate, 1997; Corkum, 2002). Data from this study show that, like many other ambush predatory fishes (e.g., anglerfishes: Grobecker & Pietsch, 1979; stonefishes: Grobecker, 1983; Holzman & Wainwright, 2009), *E. sandwicensis* have an additional capacity for rapid predatory strikes, with total gape cycle durations averaging 64-73 ms and jaw opening lasting 28-30 ms during successful prey capture (Table 4.3). The potential evolutionary impact of *E. sandwicensis* predation on Hawaiian stream ichthyofauna has been indicated through laboratory selection experiments, which showed that eleotrid predation imposed significant selection on several aspects of the morphology of juvenile *S. stimpsoni* (Blob et al., 2010). Of the features affected, the strongest selection was imposed on body mass, which was significantly smaller in predation survivors (Blob et al., 2010). Data from this study indicate a potential biomechanical basis contributing to this selection against larger fish. It may be possible for *E. sandwicensis* to successfully capture larger juvenile gobies from longer predator-prey distances, increasing opportunities for encounters with larger individuals and opportunities to adjust predatory kinematics to enable capture success. Further tests across a size range of individuals within a prey species could help to evaluate this hypothesis and clarify biomechanical impacts on evolutionary selection.

LITERATURE CITED

Archer SD, Altringham JD, Johnston IA. 1990. Scaling effects on the neuromuscular system, twitch kinetics and morphometrics of the cod, *Gadus morhua*. Mar Behav Physiol 17:137-146.

Bacheler NM, Neal JW, Noble RL. 2004. Diet overlap between native bigmouth sleepers (*Gobiomorus dormitor*) and introduced predatory fishes in a Puerto Rico reservoir. Ecol Freshw Fish 13:111-118.

Blob RW, Bridges WC, Ptacek MB, Maie T, Cediel RA, Bertolas MM, Julius ML, Schoenfuss HL. 2008. Morphological selection in an extreme flow environment: body shape and waterfall-climbing success in the Hawaiian stream fish *Sicyopterus stimpsoni*. Integr Comp Biol 48:734-749.

Blob RW, Kawano SM, Moody KN, Bridges WC, Maie T, Ptacek MB, Julius ML, Schoenfuss HL. 2010. Morphological selection and the evaluation of potential tradeoffs between escape from predator and the climbing of waterfalls in the Hawaiian stream goby *Sicyopterus stimpsoni*. Integr Comp Biol 50:1185-1199.

Cabin RJ, Mitchell RJ. 2000. To Bonferroni or not to Bonferroni: When and how are the questions. Bull Ecol Soc Am 81:246-248.

Cediel RA, Blob RW, Schrank GD, Plourde RC, Schoenfuss HL. 2008. Muscle fiber type distribution in climbing Hawaiian gobioid fishes: ontogeny and correlations with locomotor performance. Zoology 111:114-122.

Corkum, LD. 2002. Discrimination among fish models by Hawaiian *Eleotris sandwicensis* (Eleotridae). Biotropica 34:584-588.

Coughlin DJ, Strickler RJ. 1990. Zooplankton capture by a coral reef fish: an adaptive response to evasive prey. Environ Biol Fishes 29:35-42.

Day SW, Higham TE, Cheer AY, Wainwright PC. 2005. Spatial and temporal flow patterns during suction feeding of bluegill sunfish (*Lepomis macrochirus*) by particle image velocimetry. J Exp Biol 208:2661-2671.

Domenici P, Blake RW. 1993. The effect of size on the kinematics and performance of angelfish (*Pterophyllum eimekei*) escape responses. Can J Zool 71:2319-2326.

Domenici P, Blake RW. 1997. The kinematics and performance of fish fast-start swimming. J Exp Biol 200:1165-1178.

Ferry-Graham LA, Wainwright PC, Lauder GV. 2003. Quantification of flow during suction feeding in bluegill sunfish. Zool 106:159-168.

Fitzsimons JM, Schoenfuss HL, Schoenfuss TC. 1997. Significance of unimpeded flows in limiting the transmission of parasites from exotics to Hawaiian stream fishes. Micronesica 30:117-125.

Grobecker DB. 1983. The 'lie-in-wait' feeding mode of a cryptic teleost, *Synanceia verrucosa*. Env Bio Fishes 8:191-202.

Grobecker DB, Pietsch TW. 1979. High-speed cinematographic evidence for ultrafast feeding in antennariid anglerfishes. Science 205:1161-1162.

Hedrick TL. 2008. Software techniques for two- and three-dimensional kinematic measurements of biological and biomimetic systems. Bioinspir Biomim 3:034001.

Herrel A, Van Wassenbergh S, Wouters S, Adriaens D, Aerts P. 2005. A functional morphological approach to the scaling of the feeding system in the African catfish, *Clarias gariepinus*. J Exp Biol 208: 2091-2102.

Higham TE. 2007. Feeding, fins and braking maneuvers: locomotion during prey capture in centrarchid fishes. J Exp Biol 210:107-117.

Higham TE, Day SW, Wainwright PC. 2006a. Multidimensional analysis of suction feeding performance in fishes: fluid speed, acceleration, strike accuracy and the ingested volume of water. J Exp Biol 209:2713-2725.

Higham TE, Day SW, Wainwright PC. 2006b. The pressures of suction feeding: the relation between buccal pressure and induced fluid speed in centrarchid fishes. J Exp Biol 209:3281-3287.

Higham TE, Malas B, Jayne BC, Lauder GV. 2005. Constraints on starting and stopping: behavior compensates for reduced pectoral fin area during braking of the bluegill sunfish *Lepomis macrochirus*. J Exp Biol 208:4735-4746.

Hill AV. 1950. The dimensions of animals and their muscular dynamics. Sci Prog 38: 209-230.

Holzman R, Wainwright PC. 2009. How to surprise a copepod: strike kinematics reduce hydrodynamic disturbance and increase stealth of suction-feeding fish. Limnol Oceanogr 54:2201-2212.

Holzman R, Day SW, Wainwright PC. 2007. Timing is everything: coordination of strike kinematics affects the force exerted by suction feeding fish on attached prey. J Exp Biol 210:3328-3336.

Keith P, Vigneux E, Marguet G. 2002. Atlas des poissons et des crustacés d'eau douce de Polynésie française. Paris: Patrimoines Naturels 55. pp.1-175.

Kido MH. 1996. Morphological variation in feeding traits of native Hawaiian stream fishes. Pac Sci 50:184-193.

Kido MH. 1997. Food relations between coexisting native Hawaiian stream fishes. Env Bio Fishes 49:481-494.

Kinzie RA III. 1988. Habitat utilization by Hawaiian stream fishes with reference to community structure in oceanic island streams. Env Bio Fishes 22:179-192.

Lauder GV, Drucker EG. 2004. Morphology and experimental hydrodynamics of fish control surfaces. IEEE J Oceanic Eng 29:556-571.

Lauder GV, Clark BD. 1984. Water flow patterns during prey capture by teleost fishes. J Exp Biol 104:1-13.

Maeda K, Mukai T, Tachihara K. 2011. Newly collected specimens of the sleeper *Eleotris acanthopoma* (Teleostei: Eleotridae) from French Polynesia indicate a wide and panmictic distribution in the West and South Pacific. Pac Sci 65:257-264.

Maie T, Schoenfuss HL, Blob RW. 2009a. Jaw lever analysis of Hawaiian gobioid stream fishes: a simulation study of morphological diversity and functional performance. J Morph 270:976-983.

Maie, T., Wilson, M.P., Schoenfuss, H.L., Blob, R.W. 2009b. Feeding kinematics and performance of Hawaiian stream gobies, *Awaous guamensis* and *Lentipes concolor*: linkage of functional morphology and ecology. J Morph 270: 344-356.

Maie T, Meister AB, Leonard GL, Schrank GD, Blob RW, Schoenfuss HL. 2011. Jaw muscle fiber type distribution in Hawaiian gobioid stream fishes: histochemical correlations with feeding ecology and behavior. Zoology 114:340-347.

Matott MP, Motta PJ, Hueter RE. 2005. Modulation in feeding kinematics and motor pattern of the nurse shark *Ginglymostoma cirratum*. Environ Biol Fish 74:163-174.

McHenry MJ, Lauder GV. 2005. The mechanical scaling of coasting in zebrafish (*Danio rerio*). J Exp Biol 208:2289-2301.

McHenry MJ, Lauder GV. 2006. Ontogeny of form and function: locomotor morphology and drag in zebrafish (*Danio rerio*). J Morph 267:1099-1109.

McKaye KR, Weiland DJ, Lim TM. 1979. The effect of luminance upon the distribution and behavior of the eleotrid fish *Gobiomorus dormitor*, and its prey. Rev Can Biol 38:27-36.

Miller PJ. 1998. The West African species of Eleotris and their systematic affinities (Teleostei: Gobioidei). J Nat Hist 32:273-296.

Moran MD. 2003. Arguments for rejecting the sequential Bonferroni in ecological studies. Oikos 100:403-405.

Müller UK, Stamhuis EJ, Videler JJ. 2000. Hydrodynamics of unsteady fish swimming and the effects of body size: comparing the flow fields of fish larvae and adults. J Exp Biol 203:193-206.

Nordlie FG. 1981. Feeding and reproductive biology of eleotrid fishes in a tropical estuary. J Fish Bio 18:97-110.

Norton SF. 1991. Capture success and diet of cottid fishes – the role of predator morphology and attack kinematics. Ecology 72:1807-1819.

Pezold F, Cage B. 2002. A review of the spinycheek sleepers, genus *Eleotris* (Teleostei: Eleotridae), of the Western Hemisphere, with comparison to the West African species. Tulane Stud Zool Bot 31:19-63.

Ralston KR, Wainwright PC. 1997. Functional consequences of trophic specialization in pufferfishes. Funct Ecol 11:43-52.

Schoenfuss HL, Blob W. 2003. Kinematics of waterfall climbing in Hawaiian freshwater fishes (Gobiidae): vertical propulsion at the aquatic-terrestrial interface. J Zool Lond 261:191-205.

Schoenfuss HL, Blob RW. 2007. The importance of functional morphology for fishery conservation and management: applications to Hawaiian amphidromous fishes. Bishop Mus Bull Cult Environ Stud 3:125-141.

Schoenfuss HL, Blanchard TA, Kuamo'o DGG. 1997. Metamorphosis in the cranium of postlarval *Sicyopterus stimpsoni*, an endemic Hawaiian stream goby. Micronesica 30:93-104.

Tate DC. 1997. The role of behavioral interactions of immature Hawaiian stream fishes (Pisces: Gobioidei) in population dispersal and distribution. Micronesica 30:51-70.

Tate DC, Fitzsimons JM, Cody RP. 1992. Hawaiian freshwater fishes (Osteichthyes, Gobioidei): A field key to the species of larvae and postlarvae during recruitment in fresh waters. Occasional Papers of the Museum of Natural Science, Louisiana State University 65:1-10.

Thacker CE. 2003. Molecular phylogeny of the gobioid fishes (Teleostei: Perciformes: Gobioidei). Molecular Phylogenetics and Evolution 26:354-368.

Van Wassenbergh S, Aerts P, Herrel A. 2006. Scaling of suction feeding performance in the catfish *Clarias gariepinus*. Physiological and Biochemical Zoology 79: 43-56.

Wainwright PC, Day SW. 2007. The forces exerted by aquatic suction feeders on their prey. J R Soc Interface 4:553-560.

Wainwright PC, Ferry-Graham LA, Waltzek TB, Carroll AM, Hulsey CD, Grubich JR. 2001. Evaluating the use of ram and suction during prey capture by cichlid fishes. J Exp Biol 204:3039-3051.

Wainwright PC, Mehta RS, Higham TE. 2008. Stereotypy, flexibility and coordination: key concepts in behavioral functional morphology. J Exp Biol 211:3523-3528.

Webb PW. 1976. The effect of size on the fast-start performance of rainbow trout *Salmo gairdneri*, and a consideration of piscivorous predator-prey interactions. J Exp Biol 65:157-177.

Webb PW, Kosteck PT, Stevens ED. 1984. The effect of size and swimming speed on locomotor kinematics of rainbow trout. J Exp Biol 109:77-95.

Weihs D. 1980. Energetic significance of changes in swimming modes during growth of larval anchovy, *Engraulis mordax*. Fish Bull 77:597-604.

Winemiller KO, Ponwith BJ. 1998. Comparative ecology of eleotrid fishes in Central American coastal streams. Env Bio Fishes 53:373-384.

Yamamoto MN, Tagawa AW. 2000. Hawai'i's Native and Exotic Freshwater Animals. Honolulu: Mutual Publishing. pp. 5-200.

Ziegler AC. 2002. Hawaiian Natural History, Ecology, and Evolution. Honolulu: University of Hawai'i Press. pp.144-156.

CHAPTER FIVE

ONTOGENETIC SCALING OF JAW MORPHOLOGY AND PERFORMANCE IN HAWAIIAN GOBIOID STREAM FISHES, *ELEOTRIS SANDWICENSIS* AND *SICYOPTERUS STIMPSONI*: FUNCTIONAL DEMANDS AND FEEDING SPECIALIZATION

SUMMARY

Many fishes exhibit patterns of allometric growth in their feeding apparatus that help to accommodate size related changes in functional demands and to maintain performance through ontogeny. In this study, I compared the ontogenetic allometry of structure and performance for the jaw closing adductor mandibulae muscle complex between two Hawaiian gobioid stream fishes that consume food of unchanged relative size throughout postmetamorphic life, but which acquire food through different strategies: *Eleotris sandwicensis*, an ambush predator on primarily juvenile fishes, and *Sicyopterus stimpsoni*, an herbivore that grazes diatoms by scraping rock surfaces. I predicted that *E. sandwicensis* might show positive allometry of jaw closing force that could help maintain its ability to capture small evasive prey by conveying greater acceleration of the jaws to peak closing force, whereas herbivorous *S. stimpsoni* would not show such patterns. To evaluate jaw closing performance of these species through ontogeny, I dissected and measured the A2 and A3 bundles of the adductor mandibulae across a wide size range of specimens in each species, and used these data, in combination with newly reported data on muscle fiber type proportions and jaw closing duration, as input parameters in a previously published anatomical model to simulate jaw function in fishes. In addition, I simulated jaw performance in two possible functional

scenarios that might occur during a jaw closing event: (1) all muscle fibers were recruited, and thus both white and additional red fibers contributed to the shortening speed of the adductor mandibulae; (2) only white fibers were recruited, and red fibers did not contribute to the overall muscle contraction. My predictions for patterns of jaw closing performance were met, with isometric change in jaw closing performance in *S. stimpsoni*, and positively allometric increases in jaw closing force relative to body size in *E. sandwicensis* that were achieved through positively allometric growth of A2 and A3 cross sectional area, rather than ontogenetic changes in the mechanical advantage of these muscles. Even with these differences between the species, some similarities in functional ontogeny of jaw closing were also identified that might relate to ecological specialization, or to the consumption of consistently sized food throughout their lives. For example, in both species A2 and A3 showed less functional differentiation in force vs. velocity performance than has been identified in many other fishes, potentially reflecting a reduction in feeding modulation capacity for species with specialized diets. Also, neither angular velocity nor power output showed significant relationships with body size in either species, potentially reflecting the maintenance of consistent absolute feeding performance in species capturing a consistent size of food throughout their lives. Ontogenetic analyses on jaw morphology and performance provide insights into the musculoskeletal capacity of the feeding apparatus of trophically specialized Hawaiian gobioids, which reflects into their feeding ecology and behavior exhibited in streams.

INTRODUCTION

As animals grow, the functional demands that they experience often change as a consequence of their increasing body size. Such changes can be correlated with size-related changes in a wide range of parameters, including physical forces imposed by the environment, energetic requirements, and intrinsic physiological properties of body tissues like muscle (Hill, 1950; McMahon, 1975; Calder, 1984; Schmidt-Nielsen, 1984; Koehl, 2000; Biewener, 2005). To accommodate size-related changes in functional demands, many species exhibit compensatory allometry in the growth of anatomical structures or their performance (McGuire, 2003; Toro et al., 2003; McHenry and Lauder, 2006), with the requirements of size-related changes in demands providing a basis for predicting the pattern of growth necessary to maintain performance during ontogeny (Carrier, 1996; Herrel and Gibb, 2006; Maie et al., 2012).

The feeding systems of fishes have provided a rich source for studies of the scaling of structures and performance in relation to functional demand. Alternative bases for predictions of scaling patterns have included differences in ecological characteristics of populations, such as prey size and availability (e.g., Magnhagen and Heibo, 2001), and the limitations of muscular performance characteristics, such as power demands (e.g., Van Wassenbergh et al., 2006; Van Wassenbergh et al., 2007). In this context, data on the scaling of feeding morphology and performance of Hawaiian stream fishes would provide interesting examples for comparison for understanding functional demands which these fishes may face in the streams. Only five species of fishes, four gobies and one eleotrid, are native to Hawaiian streams (Yamamoto and Tagawa, 2000; Schoenfuss and Blob, 2007). All five species share an amphidromous life cycle, in which juveniles

hatched in freshwater are swept by stream currents to the ocean, where they grow for three to six months before returning to streams to metamorphose into juveniles (Radtke et al., 1988; Blob et al., 2008). After metamorphosis, the eleotrid *Eleotris sandwicensis* (Vaillant and Sauvage 1875) remains in lower stream reaches or estuaries for the rest of its life as an ambush predator (Fitzsimons et al., 1997; Nishimoto and Kuamo'o, 1997), where a primary component of its diet is the incoming larvae (and immediately postmetamorphic juveniles) of the other four native fish species (Kido, 1996a; Tate, 1997; Yamamoto and Tagawa, 2000). For three of these four species, time spent in lower stream reaches is quite short, lasting as little as a few days before juveniles begin climbing waterfalls toward upper stream reaches out of the range of piscivorous eleotrids (Fitzsimons and Nishimoto, 1995; Schoenfuss and Blob, 2003; Blob et al., 2008). Thus, as eleotrids grow (from < 2 cm to > 16 cm total length: Table 5.1; Schoenfuss and Blob, 2007), their main prey item changes little in size, ranging between 1 and 2 cm (Schoenfuss and Blob, 2003; Schoenfuss and Blob, 2007). A similar relation between food size and body size is present for one of the climbing species, *Sicyopterus stimpsoni*, although its feeding behavior is quite different from that of *E. sandwicensis*. *S. stimpsoni* is an obligate herbivore, specialized to feed on algal diatoms by cyclically protruding its premaxilla and scraping with tricuspid teeth on the premaxilla along rock surfaces in streams (Kido, 1996b; Fitzsimons et al., 2003; Julius et al., 2005; Cullen et al., 2013). Thus, as *S. stimpsoni* grows, it also continues to consume food items of the same size (though it is able to scrape more of them per cycle). Given such relationships between

food size and body size, how might scaling patterns for feeding differ between these closely related (Thacker, 2003) carnivorous and herbivorous species?

Species	*N*	Body Length (cm)	Stream Locality	Year
Eleotris sandwicensis	23	5.4 - 16.2	Hakalau, Nanue, & Wailoa Pond (Hawai'i)	2003-2007, 2011
Sicyopterus stimpsoni	30	5.5 - 13.3	Hakalau & Nanue (Hawai'i); Hanakapi'ai & Limahuli (Kaua'i)	2004, 2011

Table 5.1: List of specimens of Hawaiian gobioid stream fishes with body size, locality, and year of collection.

Although feeding kinematics have been measured for both *E. sandwicensis* (Chapter 4) and *S. stimpsoni* (Cullen et al., 2013), data were only collected from individuals with a limited range of sizes in each case. However, with appropriate morphometric data, modeling approaches can be used to evaluate several aspects of musculoskeletal performance from individuals spanning a wide range of body sizes (e.g., Westneat, 2003; Van Wassenbergh et al., 2005). In a previous study (Maie et al., 2009a), I used morphometric data from adults of each species to simulate their jaw closing performance, using a published anatomical model (Westneat, 2003). This model also requires an input value for jaw closing duration; these were not available for *E. sandwicensis* and *S. stimpsoni* at the time of the study, and were estimated from values of other gobiid species (Maie et al., 2009b). In addition, the model used values for physiological properties of jaw muscles that assumed the muscles were composed entirely of fast twitching white muscle fibers (Westneat, 2003). However, since the time of that study, new data on jaw closing durations have become available for both *E. sandwicensis* (Chapter 4) and *S. stimpsoni* (Cullen et al., 2013), as well as data on the

proportions of red and white muscle fibers in the jaw muscles of both species (Maie et al., 2011).

In this study, I modeled a new jaw closing performance of *E. sandwicensis* and *S. stimpsoni*, incorporating refined evaluations of jaw closing duration and jaw muscle fiber type proportions, and including a broad size range of individuals from each species. Even for a suction feeder like *E. sandwicensis*, jaw closing performance is critical to feeding success because rapid closure of the jaws prevents flow reversal and the escape of prey (Van Wassenbergh et al., 2005; Chapter 4). Similarly, for an herbivore in high velocity Hawaiian streams, fast jaw closing performance will secure small diatoms dislodged from rocks that would otherwise be subject to rapid downstream displacement. These new analyses allow us to test for differences in the scaling of jaw closing performance between a piscivorous predator and herbivore that each exploits food of a nearly uniform size throughout their growth. In particular, because small animals tend to move relatively more quickly than larger animals (Hill, 1950; Herrel et al., 2005; Van Wassenbergh et al., 2006), and the evasive prey of *E. sandwicensis* remains small as this predator grows larger, it is possible that the jaw muscles of *E. sandwicensis* might exhibit positive allometry of jaw closing force that might help compensate by conveying greater acceleration of the jaws to peak closing velocity (Van Wassenbergh et al., 2005). Such scaling patterns might not be expected in herbivorous *S. stimpsoni* which are not feeding on evasive food.

MATERIALS AND METHODS

Morphological Measurements of the Adductor Mandibulae Muscles and Feeding Apparatus

The two species of gobioid fishes (*Sicyopterus stimpsoni* (Gill 1860) and *Eleotris sandwicensis* were collected (Clemson AUP# 40061, 50056, 2011-057) from their native habitat on the Islands of Hawai'i and Kaua'i (Table 5.1). Fish were collected by net while snorkeling or, for fish from Waiakea Pond, while standing on shore. Captured specimens were preserved in 70% ethanol, subsequent to jaw muscle and skeletal dissection under a dissecting scope (Nikon SMZ 1000). Dissected specimens were photographed using a digital camera (Nikon CoolPix 4300 or 5100), and ImageJ (Abramoff et al., 2004) was used to collect measurements of morphological input variables for the Westneat (2003) model of jaw closing performance.

The adductor mandibulae muscles are the major force-generating muscle complex powering jaw closing in teleosts during feeding behaviors. This muscle complex pulls the mandible around a point of rotation at the quadrato-mandibular joint in a third-order lever mechanism (Westneat, 2003). This adductor muscle complex is situated on the superficial aspect of the cranium of teleosts (Winterbottom, 1974; Gosline, 1986). Although a few variations in the muscle complex (e.g., size and point of insertion) can be found among Hawaiian stream gobies (Maie et al., 2009a), basic external configurations in *S. stimpsoni* and *E. sandwicensis* are comparable (Figures 5.1A, 5.1B).

The Westneat (2003) model focuses on the A2 and A3 divisions of this complex as the primary jaw closing muscles, and uses twelve linear measurements of the feeding apparatus to simulate jaw movement and performance (Figure 5.1C): (1) in-lever arm for

A2, distance between the quadrato-mandibular joint and the superior tip of the coronoid process of the dentary, where A2 inserts; (2) in-lever arm for A3, distance between the quadrato-mandibular joint and the medial surface of the articular, where A3 inserts; (3) in-lever arm for jaw opening, distance between the quadrato-mandibular joint and the postero-ventral aspect of the articular, where the interoperculo-mandibular ligament inserts; (4) out-lever arm of the mandible, distance between the quadrato-mandibular joint and the anterior tip of the dentary; (5) A2 muscle length; (6) A3 muscle length; (7) tendon length for A3; (8) distance between A2 origin and the quadrato-mandibular joint; (9) distance between A3 origin and the quadrato-mandibular joint; (10) distance between A2 and A3 insertions; (11) dorsal length of the mandible, distance between the superior tip of the coronoid process of the dentary and the anterior tip of the dentary; (12) ventral length of the mandible, distance between the postero-ventral aspect of the articular to the anterior tip of the dentary. The superficial aspect of the A2 division, where the muscle has the greatest long axis, was used for measurement of A2 length. After measuring its length including its tendon, it was removed and its mass was measured to the nearest 0.0001g with a digital balance (Denver Instrument). After the removal of A2, the length and mass of A3 were measured in a similar manner. Points of origin for both A2 and A3 were determined by locating areas of origin on the cranium, where their muscle fibers run parallel to their respective tendons. In addition to these measurements, body length (from the tip of snout to the tip of caudal fin) of each specimen was also measured, and the mass and length of each A2 and A3 were used to calculate the physiological cross-sectional area (CSA) as CSA = (Muscle Mass/Fiber Length)(cosβ/Muscle density), where

β is the pennation angle of muscle fiber. In my study, the angle β was 0^{o} for all individuals because pennation of these muscles appears negligible in these species (Maie et al., 2009a). A value of 1.05 g/cm for muscle density was applied in simulations (Lowndes, 1955).

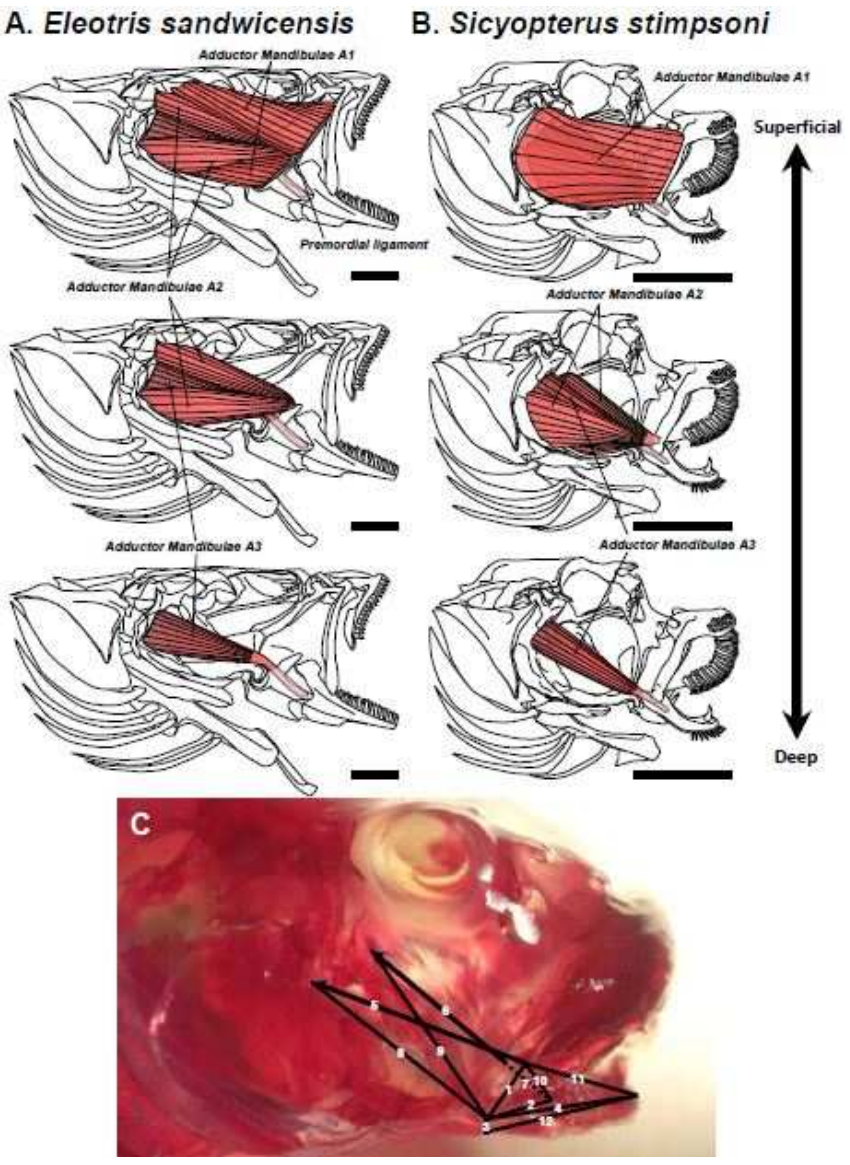

Figure 5.1: Morphological design of the feeding apparatus of (A) *Eleotris sandwicensis* (scale bars indicate 5 mm) and (B)*Sicyopterus stimpsoni* , and (C) linear

measurements in the feeding apparatus of *S. stimpsoni* used in the mandibular lever model. Note: (1) in-lever arm for A2; (2) in-lever arm for A3; (3) in-lever arm for jaw opening; (4) out-lever arm of the mandible; (5) A2 muscle length; (6) A3 muscle length; (7) tendon length for A3; (8) distance between A2 origin and the quadrato-mandibular joint; (9) distance between A3 origin and the quadrato-mandibular joint; (10) distance between A2 and A3 insertions; (11) dorsal length of the mandible; (12) ventral length of the mandible.

Simulation of Mandibular Movement

To evaluate jaw closing performance of *E. sandwicensis* and *S. stimpsoni*, I used measurements from the feeding apparatus of each species (see above) as input variables into a simulation of a jaw closing event using MandibLever 3.0, software developed by M. Westneat (2003) and available at (http://www.fieldmuseum.org/). Based on these measurements and non-linear contractile properties of muscle fibers (e.g., Westneat, 2003), this simulation can calculate estimates of the transmission of speed and force, as well as other functional parameters associated with the jaws. To refine my previous analysis of jaw closing performance in these species (Maie et al., 2009a), I accounted for several recently measured differences in their feeding kinematics and jaw muscle physiology. First, these two species exhibit different jaw closing durations: 33.9 msec by *E. sandwicensis* (N = 5: Chapter 4) and 91.9 msec by *S. stimpsoni* (e.g., Cullen et al., 2013). These species specific values were used accordingly in my simulations, rather than the value of 50 msec used in my previous analysis (Maie et al., 2009a). Second, whereas my previous study (Maie et al., 2009a) made a simplifying assumption (Westneat, 2003) that the jaw closing muscles were comprised entirely of fast-twitch white fibers, recent data on adductor mandibulae fiber types for these species showed

significant red (slow-twitch) components that differed between the species (Maie et al., 2011). To account for these data in my simulation, I converted the reported scores of different fiber types into a fiber ratio (fast-twitch white fiber/slow-twitch red fiber), from which I estimated maximum muscle shortening speed (V_{max}) following two possible functional scenarios that might occur (e.g., Akster and Osse, 1978; Herrel et al., 2008) during a jaw closing event: (1) all muscle fibers were recruited, and thus both white and additional red fibers contributed to the shortening speed of the adductor mandibulae; (2) only white fibers were recruited, and red fibers did not contribute to the overall muscle contraction. To simplify modeling (and following Westneat, 2003), a single value of V_{max} was employed for both adductor bundles. From my conversion of fiber type scores (white fiber % = (5 - red fiber type score)/4 X 100: Maie et al., 2011), I determined that, *E. sandwicensis* averaged 72.0% fast twitch white fibers between A2 and A3 and *S. stimpsoni* averaged 86.4% fast twitch white fibers between A2 and A3. With V_{max} ranging between 10 length/sec for white fibers and V_{max} = 5 length/sec for red fibers in fish jaw musculature, and with a maximum isometric stress (P_c) ranging between 200 kPa for white fibers and P_c = 100 kPa for red fibers (e.g., Westneat, 2003), I determined that in the first scenario, where both white and red muscle fibers were recruited, V_{max} is calculated as: V_{max} = white fiber % X 0.1 + (1 - white fiber %) X 0.05). With this formula, *E. sandwicensis* reaches V_{max} = 8.60 length/sec and Pc = 172.0 kPa, and *S. stimpsoni* reaches V_{max} = 9.32 length/sec and P_c = 186.4 kPa. In the second scenario with only white fibers being recruited, I determined that *S. stimpsoni* reaches V_{max} = 8.64 length/sec and P_c = 172.8 kPa, and *E. sandwicensis* reaches V_{max} = 7.20 length/sec and P_c

= 144 kPa. These values appear to be consistent with data for fishes available elsewhere (e.g., Johnston and Salamonski, 1984; Hammond et al., 1998; Rome et al., 1999; Coughlin, 2000).

Four performance variables were computed from the simulation for each of the A2 and A3 divisions, using measurements from one side of the head (unilateral performance variables): (1) bite force output (F_{OUT}), normalized to body size (i.e., divided by BL^3); (2) angular velocity; (3) effective mechanical advantage (EMA), which is calculated for each muscle as the product of the skeletal lever ratio for jaw closing and the sine of the angle of muscle insertion on the mandible; (4) jaw power output, also normalized to body size. Calculations were performed starting with an initial opening of the mandible at 30º and progressed as the jaw angle closed toward 0º. Values of performance variables from each species were plotted over fractional increments of time through each of their jaw closing cycles, with consistent increments in time obtained via mathematical transformations followed by curvilinear regressions. From values of performance variables predicted from V/V_{max}, the inverse functions of the obtained regressions were plotted against each jaw-closing variable to determine actual variable values for consistent time intervals for both species. Maximum performance values along with CSA of both A2 and A3 were compared using one-way ANOVA and Fisher's LSD post hoc tests at $\alpha = 0.05$ level to evaluate the significance of differences in performance between species.

Scaling Analysis

For each muscle division in each species, I evaluated scaling relationships between body-length and: (1) CSA *in situ*, (2) maximum F_{OUT}, (3) maximum angular velocity, (4) maximum EMA, and (5) maximum jaw power output. For these analyses, all data were $\log_{10}$-transformed and used to generate model II reduced major axis (RMA) regressions, which account for structural relationships between variables when both are subject to error (Rayner, 1985; McArdle, 1988; LaBarbera, 1989). A scaling relationship was considered allometric if the 95% confidence interval (e.g., Jolicoeur and Mosimann, 1968) for its RMA slope failed to overlap the slope predicted for isometry. In addition, I used Tsutakawa's non-parametric quick test (Tsutakawa and Hewett, 1977) to evaluate differences in each variable between species while accounting for differences in body mass across the species (Swartz, 1997; Blob, 2000). In these comparisons, a pooled RMA regression line was calculated for the two groups compared, and the numbers of points above and below the line were counted for each group, producing a 2x2 contingency table to which I applied Fisher's Exact test (Tsutakawa and Hewett, 1977; Swartz, 1997; Blob, 2000; Maie et al., 2007).

Under isometric growth, CSA, F_{OUT}, and jaw power output of muscles would be expected to increase as body length $(L)^3$, whereas body length would be expected to increase as L^1, producing an expected slope of 3. In contrast, as angular and unitless variables, respectively, angular velocity and EMA could be predicted to show independence relative to body size (i.e., increase in proportion to L^0 with respect to increase of body length in proportion to L^1, producing an expected isometric slope of 0, or no significant relationship).

RESULTS

Analysis of Mandibular Movements

As the mandible closes, output bite forces of both A2 and A3 increase linearly for both simulated scenarios of differential muscle fiber recruitment in each species (Figures 5.2A, 5.2B). ANOVAs indicated no significant differences between *E. sandwicensis* and *S. stimpsoni* for maximum output force (reached at the end of the jaw closure) in either A2 or A3 bundles if all muscle fibers were recruited (P=0.4411 for A2; P=0.2236 for A3: Table 5.2). However, in the scenario where only white fibers were recruited, *S. stimpsoni* produced greater maximum output force than *E. sandwicensis* for both muscle bundles (by 39.8% in A2 , P=0.0228; by 31.2% in A3, P=0.0304: Table 5.2). This pattern was not predicted in my previous mandibular simulation (e.g., Maie et al., 2009a). In comparisons within species, ANOVA did not indicate significant differences between the fiber recruitment scenarios for maximum output force of either A2 or A3 in *S. stimpsoni* (P=0.1093 for A2; P=0.3737 for A3: Table 5.3). In contrast, for both A2 and A3, *E. sandwicensis* produced significantly greater output force when all muscle fibers recruited than when only white fibers were recruited (by 27.7% in A2; by 27.0% in A3: Table 5.3). Comparing A2 and A3, in *S. stimpsoni*, output forces for these muscles did not differ under corresponding recruitment scenarios (P=0.1908 for all fibers being recruited; P=0.1632 for only white fiber being recruited: Table 5.4). However, in *E. sandwicensis*, A2 produced ~1.3 times greater output force than A3 under both recruitment scenarios, (P=0.0478 for all fibers; P=0.0483 for only white fibers: Table 5.4).

Performance Variables	Only white muscle fibers			All muscle fibers (white + red)		
	E. sandwicensis	*S. stimpsoni*	*P*-value	*E. sandwicensis*	*S. stimpsoni*	*P*-value
max output force A2 (*10^{-5} N/cm^3)	5.59 ± 0.57	7.30 ± 0.46	0.0228*	7.73 ± 0.80	8.46 ± 0.54	0.4411
max output force A3 (*10^{-5} N/cm^3)	4.21 ± 0.37	6.12 ± 0.69	0.0304*	5.77 ± 0.54	7.11 ± 0.86	0.2236
max angular velocity A2 (°/ms)	2.01 ± 0.12	2.59 ± 0.14	0.0044*	2.84 ± 0.38	2.81 ± 0.15	0.9495
max angular velocity A3 (°/ms)	2.37 ± 0.44	6.02 ± 0.46	<0.0001*	2.82 ± 0.53	6.42 ± 0.51	<0.0001*
max effective mechanical advantage A2	0.286 ± 0.011	0.346 ± 0.010	0.0003*	0.290 ± 0.012	0.346 ± 0.010	0.0007*
max effective mechanical advantage A3	0.285 ± 0.022	0.224 ± 0.010	0.0086*	0.289 ± 0.022	0.224 ± 0.010	0.0056*
max jaw power A2 (W/kg/cm^3)	0.208 ± 0.042	0.268 ± 0.033	0.2613	0.296 ± 0.061	0.311 ± 0.038	0.8198
max jaw power A3 (W/kg/cm^3)	0.236 ± 0.052	0.263 ± 0.033	0.6429	0.345 ± 0.078	0.305 ± 0.039	0.6214

Table 5.2: Maximum performance values during jaw closing comparing species within possible functional scenarios (only white fibers recruited and all fibers recruited in the adductor mandibulae muscles A2 and A3) between two Hawaiian stream gobioids, *Eleotris sandwicensis* and *Sicyopterus stimpsoni*. For E. sandwicensis, maximum contraction speed (Vmax) was 8.60 L/s with maximum isometric stress (Pc) = 172.0 kPa (all fibers), and 7.20 L/s with P_c = 144 kPa (only white fibers). For S. stimpsoni, Vmax of the adductor mandibulae muscles was 9.32 L/s with Pc = 186.4 kPa (all fibers recruited) and 8.64 L/s with Pc = 172.8 kPa (only white fibers recruited). P-values are based on one-way ANOVA and Fisher's LSD post hoc tests (*P<0.05) comparing performance variables with the differential contribution of muscle fibers in the adductor mandibulae. Values are means ± SEM.

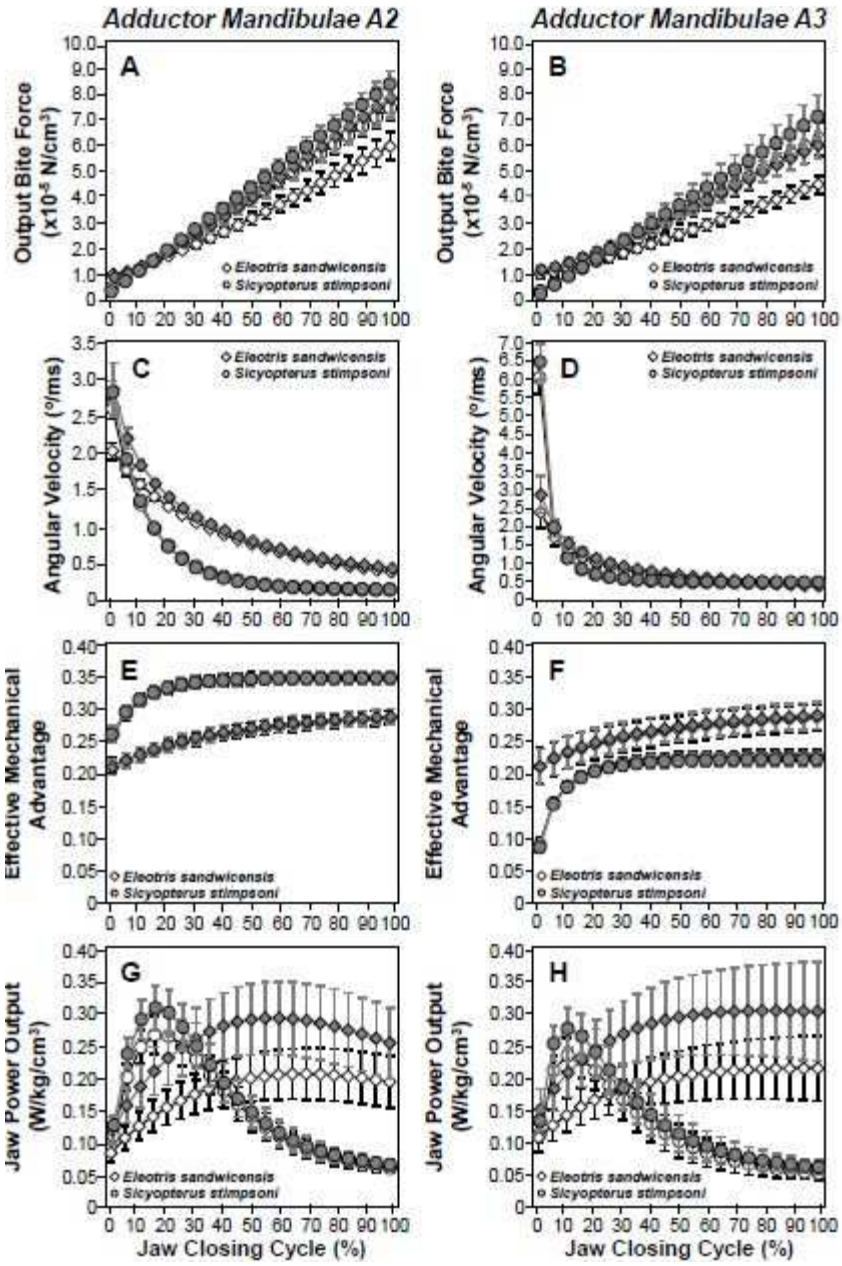

Figure 5.2: Profiles of performance variables (body size-normalized output force: A and B; angular velocity: C and D; effective mechanical advantage: E and F; body size-normalized jaw power output: G and H) produced by the adductor mandibulae muscles A2 and A3 in jaw closing cycles (%) for the Hawaiian stream gobioids, *Eleotris sandwicensis* (diamond) and *Sicyopterus stimpsoni* (circle), with calculations distinguished under different scenarios of muscle fiber contribution in each muscle. For *E. sandwicensis*, maximum contraction speed (V_{max}) was 8.60 L/s with

maximum isometric stress of the adductor mandibulae muscles (P_c) = 172.0 kPa (all fibers: filled diamonds) and 7.20 L/s with P_c = 144.0 kPa (only white fibers: empty diamonds). For *S. stimpsoni*, V_{max} was 9.32 L/s with P_c = 186.4 kPa (all fibers recruited: filled circles) and 8.64 L/s with P_c = 172.8 kPa (only white fibers recruited: empty circles).

Angular velocity decreases exponentially as the mandible closes, with maximum values at the beginning of mandibular closure (Figures 5.2C, 5.2D). ANOVA indicated no significant difference between species in maximum angular velocity by A2 with all muscle fibers recruited (P=0.9495: Table 5.2). However, *S. stimpsoni* produced greater angular velocities than *E. sandwicensis* for A2 with only white fibers recruited (by 22.4%, P=0.0044: Table 5.2) and for A3 under both fiber recruitment scenarios (by 56.1% for all muscle fibers being recruited; by 60.6% for only white fiber being recruited; P<0.0001 for both scenarios: Table 5.2). For intraspecific comparisons of each muscle, *S. stimpsoni* showed no significant differences between the two fiber recruitment scenarios, and *E. sandwicensis* showed no difference for A3; however, A2 of *E. sandwicensis* with all fibers recruited produced a greater angular velocity than with only white fibers recruited (by 16%, P=0.0419: Table 5.3). ANOVA further indicated that A3 produced ~2.3 times greater maximum angular velocity than A2 with both fiber recruitment scenarios in *S. stimpsoni* (i.e., 56.2% for all muscle fibers recruited; 57.0% for only white muscle fiber recruited; P<0.0001 for both scenarios: Table 5.4). However, *E. sandwicensis* showed no difference between A2 and A3 in either recruitment scenario (P=0.9776 for all fibers being recruited; P=0.4401 for only white fiber being recruited: Table 5.4).

Performance Variables	*Eleotris sandwicensis* (N=23)			*Sicyopterus stimpsoni* (N=30)		
	Only white muscle fibers	All muscle fibers	*P*-value	Only white muscle fibers	All muscle fibers	*P*-value
max output force A2 (*10^{-5} N/cm^3)	5.59 ± 0.57	7.73 ± 0.80	0.0346*	7.30 ± 0.46	8.46 ± 0.54	0.1093
max output force A3 (*10^{-5} N/cm^3)	4.21 ± 0.37	5.77 ± 0.54	0.0223*	6.12 ± 0.69	7.11 ± 0.86	0.3737
max angular velocity A2 (°/ms)	2.01 ± 0.12	2.84 ± 0.38	0.0419*	2.59 ± 0.14	2.81 ± 0.15	0.2837
max angular velocity A3 (°/ms)	2.37 ± 0.44	2.82 ± 0.53	0.5148	6.02 ± 0.46	6.42 ± 0.51	0.5592
max effective mechanical advantage A2	0.286 ± 0.011	0.290 ± 0.012	0.8294	0.346 ± 0.010	0.346 ± 0.010	0.9978
max effective mechanical advantage A3	0.285 ± 0.022	0.289 ± 0.022	0.9041	0.224 ± 0.010	0.224 ± 0.010	0.9959
max jaw power A2 (W/kg/cm^3)	0.208 ± 0.042	0.296 ± 0.061	0.2445	0.268 ± 0.033	0.311 ± 0.038	0.3943
max jaw power A3 (W/kg/cm^3)	0.236 ± 0.052	0.345 ± 0.078	0.2467	0.263 ± 0.033	0.305 ± 0.039	0.4158

Table 5.3: Maximum performance values during jaw closing based on two possible functional scenarios (only white fibers recruited vs. all fibers recruited in the adductor mandibulae muscles A2 and A3) for two Hawaiian stream gobioids, *Eleotris sandwicensis* and *Sicyopterus stimpsoni*. For *E. sandwicensis*, maximum contraction speed (Vmax) was 8.60 L/s with maximum isometric stress (Pc) = 172.0 kPa (all fibers), and 7.20 L/s with Pc = 144.0 kPa (only white fibers). For *S. stimpsoni*, Vmax of the adductor mandibulae muscles was 9.32 L/s with Pc = 186.4 kPa (all fibers recruited) and 8.64 L/s with Pc = 172.8 kPa (only white fibers recruited). P-values are based on one-way ANOVA and Fisher's LSD post hoc tests (*P<0.05) comparing performance variables with the differential contribution of muscle fibers in the adductor mandibulae. Values are means ± SEM.

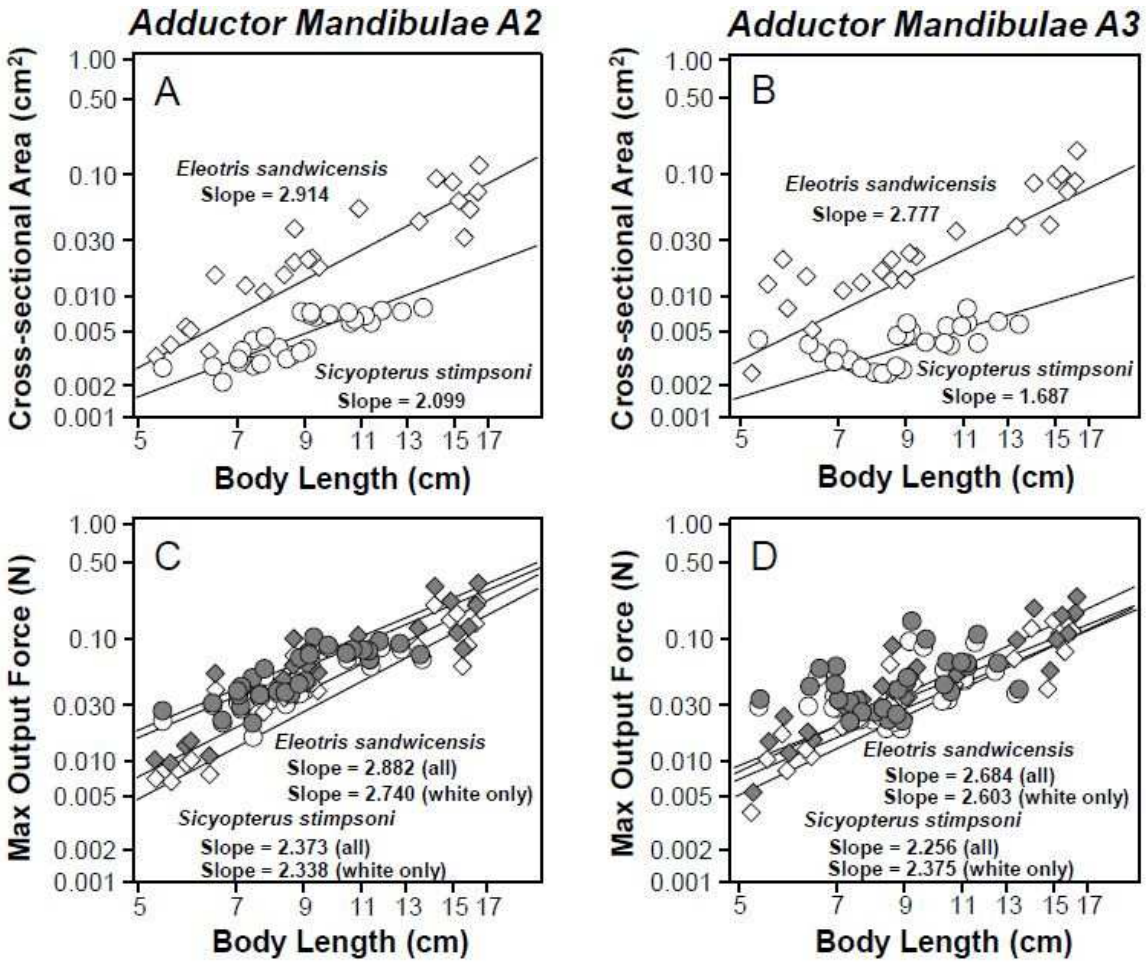

Figure 5.3: Log-log Plots of RMA regression for cross-sectional area of the adductor mandibulae muscles A2 (A) and A3 (B), and maximum output force for jaw closing for A2 (C) and A3 (D) for Hawaiian stream gobioids, *Eleotris sandwicensis* (diamond) and *Sicyopterus stimpsoni* (circle). See Figure 2 for V_{max} and P_c values under different fiber recruitment scenarios for each species. Scaling coefficients for each plot are indicated. See Table 5 for parameters of scaling equations.

EMA of both A2 and A3 increase as the mandible closes and reach a plateau at 20-30% of the jaw closing cycle (Figures 5.2E, 5.2F). ANOVA indicated that A2 in *S. stimpsoni* had 1.2 times greater maximum EMA than *E. sandwicensis* under both of the two fiber recruitment scenarios (P=0.0007 for all fibers being recruited; P=0.0003 for

only white fiber being recruited: Table 5.2). On the contrary, A3 in *E. sandwicensis* showed 1.3 times greater maximum EMA than *S. stimpsoni* (P=0.0056 for all fibers being recruited; P=0.0086 for only white fiber being recruited: Table 5.2). In both species, the two fiber recruitment scenarios produced no difference from each other in mechanical advantage (Table 5.3). For intraspecific comparisons, *S. stimpsoni* showed ~1.5 times greater EMA for A2 than for A3 (P<0.0001 for both scenarios: Table 5.4), but *E. sandwicensis* did not show any difference in EMA between A2 and A3 (P=0.9671 for all fibers being recruited; P=0.9605 for only white fiber being recruited: Table 5.4).

Power output of both A2 and A3 reach maxima before the end of the jaw closing cycle in both species (Figures 5.2G, 5.2H). Power output in *S. stimpsoni* reached its maximum at 16.3-17.2% and 13.2-14.0% of the cycle for A2 and A3, respectively, much earlier than in *E. sandwicensis* (56.5-66.1% for A2 and 71.1-73.6% for A3). Although the time to reach the peak power was different between species (*E. sandwicensis* would take ~3.5 times longer to reach the peak for A2 and ~5.3 times longer for A3 than *S. stimpsoni*), ANOVA indicated no significant differences in the maximum power output for all comparisons (e.g., P>0.05: Table 5.2) consistent with previously predicted patterns (Maie et al., 2009a).

Performance Variables	Species	Recruited Muscle Fiber	A2	A3	P-value
max output force (*10^{-5} N/cm^3)	*E. sandwicensis*	Only white muscle fibers	5.59 ± 0.57	4.21 ± 0.37	0.0483*
		All muscle fibers (white + red)	7.73 ± 0.80	5.77 ± 0.54	0.0478*
	S. stimpsoni	Only white muscle fibers	7.30 ± 0.46	6.12 ± 0.69	0.1632
		All muscle fibers (white + red)	8.46 ± 0.54	7.11 ± 0.86	0.1908
max angular velocity (^{o}/ms)	*E. sandwicensis*	Only white muscle fibers	2.01 ± 0.12	2.37 ± 0.44	0.4401
		All muscle fibers (white + red)	2.84 ± 0.38	2.82 ± 0.53	0.9776
	S. stimpsoni	Only white muscle fibers	2.59 ± 0.14	6.02 ± 0.46	<0.0001*
		All muscle fibers (white + red)	2.81 ± 0.15	6.42 ± 0.51	<0.0001*
max effective mechanical advantage	*E. sandwicensis*	Only white muscle fibers	0.286 ± 0.011	0.285 ± 0.022	0.9605
		All muscle fibers (white + red)	0.290 ± 0.012	0.289 ± 0.022	0.9671
	S. stimpsoni	Only white muscle fibers	0.346 ± 0.010	0.224 ± 0.010	<0.0001*
		All muscle fibers (white + red)	0.346 ± 0.010	0.224 ± 0.010	<0.0001*
max jaw power (W/kg/cm^3)	*E. sandwicensis*	Only white muscle fibers	0.208 ± 0.042	0.236 ± 0.052	0.6835
		All muscle fibers (white + red)	0.296 ± 0.061	0.345 ± 0.078	0.6182
	S. stimpsoni	Only white muscle fibers	0.268 ± 0.033	0.263 ± 0.033	0.9147
		All muscle fibers (white + red)	0.311 ± 0.038	0.305 ± 0.039	0.9055

Table 5.4: Maximum performance values during jaw closing comparing A2 and A3 of the adductor mandibulae muscle within possible functional scenarios (only white fibers recruited and all fibers recruited) in two Hawaiian stream gobioids, *Eleotris sandwicensis* and Sicyopterus stimpsoni. P-values are based on one-way ANOVA and Fisher's LSD post hoc tests (*P<0.05) comparing performance variables with the differential contribution of muscle fibers in the adductor mandibulae. Values are means ± SEM.

Ontogenetic Scaling Patterns

Both species showed strong positive correlations between CSA of the adductor mandibulae muscles A2 and A3 and body length (Table 5.5, Figures 5.3A, 5.3B). Scaling exponents for CSA of both A2 and A3 with respect to body length indicated isometry for *S. stimpsoni* (i.e., 95% CI of regression slope overlaps predicted slope of 2 for isometry: Table 5.5, Figures 5.3A, 5.3B) and positive allometry for *E. sandwicensis* (i.e., 95% CI > 2: Table 5.5, Figures 5.3A, 5.3B). Tsutakawa's quick test indicated that *E. sandwicensis* had larger CSA than *S. stimpsoni* at any given body length (P=0.0003 for A2; P<0.0001 for A3). Neither species showed a significant difference in CSA between A2 and A3 at any given body length (P=0.1205 for *S. stimpsoni*; P>0.9999 for *E. sandwicensis*: Fisher's Exact test).

Species	x	y	Recruited Muscle Fiber	N	r^2	RMA intercept ± 95% CL	RMA slope (95% CI)	Expected RMA by isometry	Allometry
Eleotris sandwicensis	BL	Muscle CSA A2	n/a	23	0.857	-4.734 ± 5.501	2.914 (2.456 - 3.456)	2.000	+
	BL	Muscle CSA A3	n/a	23	0.827	-4.612 ± 5.774	2.777 (2.301 - 3.351)	2.000	+
	BL	Max Output Force A2	White fiber only	23	0.246	-4.482 ± 0.531	2.882 (2.397 - 3.465)	2.000	+
	BL	Max Output Force A2	All fibers	23	0.179	-4.137 ± 0.530	2.740 (2.293 - 3.275)	2.000	+
	BL	Max Output Force A3	White fiber only	23	0.858	-4.309 ± 0.457	2.684 (2.264 - 3.182)	2.000	+
	BL	Max Output Force A3	All fibers	23	0.847	-4.065 ± 0.460	2.603 (2.182 - 3.106)	2.000	+
	BL	Max Angular Velocity A2	White fiber only	23	--	n.s	n.s	0.000	0
	BL	Max Angular Velocity A2	All fibers	23	--	n.s	n.s	0.000	0
	BL	Max Angular Velocity A3	White fiber only	23	--	n.s	n.s	0.000	0
	BL	Max Angular Velocity A3	All fibers	23	--	n.s	n.s	0.000	0
	BL	Max EMA A2	White fiber only	23	0.392	-1.055 ± 0.173	-0.492 (-0.696 to -0.348)	0.000	-
	BL	Max EMA A2	All fibers	23	0.383	-1.044 ± 0.175	-0.493 (-0.699 to -0.347)	0.000	-
	BL	Max EMA A3	White fiber only	23	--	n.s	n.s	0.000	0
	BL	Max EMA A3	All fibers	23	--	n.s	n.s	0.000	0
	BL	Max Jaw Power Output A2	White fiber only	23	--	n.s	n.s	3.000	0
	BL	Max Jaw Power Output A2	All fibers	23	--	n.s	n.s	3.000	0
	BL	Max Jaw Power Output A3	White fiber only	23	--	n.s	n.s	3.000	0
	BL	Max Jaw Power Output A3	All fibers	23	--	n.s	n.s	3.000	0
Sicyopterus stimpsoni	BL	Muscle CSA A2	n/a	30	0.711	-4.315 ± 6.064	2.099 (1.767 - 2.494)	2.000	0
	BL	Muscle CSA A3	n/a	30	0.331	-4.017 ± 7.409	1.687 (1.301 - 2.188)	2.000	0
	BL	Max Output Force A2	White fiber only	30	0.661	-3.593 ± 0.421	2.373 (1.970 - 2.858)	2.000	0
	BL	Max Output Force A2	All fibers	30	0.682	-3.493 ± 0.402	2.338 (1.952 - 2.800)	2.000	0
	BL	Max Output Force A3	White fiber only	30	0.833	-3.775 ± 0.596	2.256 (1.713 - 2.972)	2.000	0
	BL	Max Output Force A3	All fibers	30	0.844	-3.977 ± 0.655	2.375 (1.782 - 3.165)	2.000	0
	BL	Max Angular Velocity A2	White fiber only	30	--	n.s	n.s	0.000	0
	BL	Max Angular Velocity A2	All fibers	30	--	n.s	n.s	0.000	0
	BL	Max Angular Velocity A3	White fiber only	30	--	n.s	n.s	0.000	0
	BL	Max Angular Velocity A3	All fibers	30	--	n.s	n.s	0.000	0
	BL	Max EMA A2	White fiber only	30	--	n.s	n.s	0.000	0
	BL	Max EMA A2	All fibers	30	--	n.s	n.s	0.000	0
	BL	Max EMA A3	White fiber only	30	--	n.s	n.s	0.000	0
	BL	Max EMA A3	All fibers	30	--	n.s	n.s	0.000	0
	BL	Max Jaw Power Output A2	White fiber only	30	--	n.s	n.s	3.000	0
	BL	Max Jaw Power Output A2	All fibers	30	--	n.s	n.s	3.000	0
	BL	Max Jaw Power Output A3	White fiber only	30	--	n.s	n.s	3.000	0
	BL	Max Jaw Power Output A3	All fibers	30	--	n.s	n.s	3.000	0

Table 5.5: Scaling coefficients (RMA Intercept ± 95% Confidence Limits, CL) and exponents (RMA slope, with asymmetric 95% Confidence Interval, CI) for maximum performance variables with respect to body length (BL), angular velocity, effective mechanical advantage (EMA), and jaw power output from the adductor mandibulae A2 and A3 muscles of Hawaiian stream gobiid species, *Eleotris sandwicensis* and *Sicyopterus stimpsoni* with simulated contributions of muscle fibers. Calculations were obtained from reduced major axis (RMA) regressions of log10-transformed measurements: x, regression abscissa; y, regression ordinate; n, sample size. Scaling pattern is indicated as isometric (0), positively allometric (+) or negatively allometric (–).

Both species also showed strong positive correlations between maximum output force and body length (Table 5.5, Figures 5.3C, 5.3D). Scaling exponents for both A2 and A3 with respect to body length indicated similar patterns to those found in CSAs (e.g., isometry for *S. stimpsoni*; positive allometry for *E. sandwicensis*: Table 5.5, Figures 5.3C, 5.3D). Tsutakawa's quick test did not show any significant differences between species for each of the fiber recruitment scenarios in both A2 and A3 (e.g., $P>0.05$: Fisher's Exact test). In each species, the quick test did not indicate significant differences between maximum output force under the two fiber recruitment scenarios for either A2 or

A3, except for A3 in *E. sandwicensis* with the scenario where all fibers were recruited generating greater force than when only white fibers were recruited (P=0.0377: Fisher's Exact test) at any given body length. Comparing A2 and A3 bundles, Tsutakawa's quick test indicated that, in *S. stimpsoni*, A2 produced a greater output force than A3 at any given body length under both scenarios (P=0.0092 for all fibers being recruited; P=0.0041 for only white fiber being recruited: Fisher's Exact test). However, in *E. sandwicensis*, A2 and A3 generated comparable output forces under both fiber recruitment scenarios (P=0.1392 for all fibers; P=0.0758 for only white fiber: Fisher's Exact test) suggesting a diminished functional differentiation between these muscles in this species (e.g., Maie et al., 2009a).

Maximum EMA of A2 and A3 did not produce any correlations with body length in *S. stimpsoni*; thus, this species would maintain the same lever ratio for jaw closing (e.g., 0.346 for A2; 0.224 for A3: Table 5.3) throughout its ontogeny. However, *E. sandwicensis* exhibited a different pattern. Although maximum EMA of A3 did not correlate with body length, indicating the ontogenetic maintenance of the jaw closing lever ratio in A3 (e.g., 0.285-0.289: Table 5.2), maximum EMA of A2 correlated with body length in each fiber recruitment scenario, with scaling exponents indicating negative allometry (Table 5.5). In addition, Tsutakawa's quick test indicated that the two fiber recruitment scenarios did not differ significantly from each other (P=0.7683: Fisher's Exact test).

Maximum angular velocity and power output showed no correlations with body length for either A2 or A3 in either species (Table 5.5). Thus, the velocity of jaw closing

and maximum power output stayed unchanged through ontogeny in both fishes (see Table 5.2 for specific values of maximum angular velocity).

DISCUSSION

My new simulations of jaw closing in *E. sandwicensis* and *S. stimpsoni*, in which revised input parameters for jaw closing speed and jaw muscle fiber composition reflect more realistic design of the feeding apparatus than in my previous study (Maie et al., 2009a), have helped to refine understanding of the feeding performance of these fishes. In addition, my results provide insight into how feeding performance changes ontogenetically in relation to functional demands of food capture in two distinct types of feeding specialists (ambush predator vs. herbivore) in which the size of ingested items remains consistent as animals grow.

Effects of Muscle Fiber Type and Recruitment on Simulations of Jaw Closing Performance

Despite the significantly larger size of the adductor mandibulae muscle complex in *E. sandwicensis* compared to *S. stimpsoni* (Figures 5.3A, 5.3B), *S. stimpsoni* showed jaw closing forces as great as (or greater than) those of *E. sandwicensis*. This pattern is substantially influenced by the differing muscle fiber type proportions of these species, with the herbivore *S. stimpsoni* having a nearly 15% greater proportion of fast-twitch white fibers in the adductor mandibulae complex than the ambush predator *E. sandwicensis* (Maie et al., 2011). This difference in fiber proportions is surprising given

the measured differences in jaw closing speed for these species, with *S. stimpsoni* taking almost triple the time as *E. sandwicensis* (Cullen et al., 2013; Chapter 4). However, with differences in V_{max} and maximum isometric stress between white and red fibers (Westneat, 2003), the magnitude of fiber type proportion differences found between my focus species appears to contribute substantial compensation for differences in muscle performance related to muscle size. It is possible that successful dislodging of diatoms from rock surfaces requires the application of high jaw forces by *S. stimpsoni*, although this assessment is complicated by the coordination of jaw closing with premaxillary raking movements in this species (Cullen et al., 2013).

Based on my simulation results, the additional recruitment of slow-twitch red muscle fibers has the capacity to improve jaw closing performance (e.g., comparing values for all muscle fibers vs. only white muscle fibers: Table 5.3). Such performance elevation by additive slow-twitch fiber recruitment was especially significant for jaw closing force and angular velocity in the predator *E. sandwicensis* (see Table 5.3), a result that reflects the greater proportion of red fibers in the adductor mandibulae complex of this species compared to *S. stimpsoni* (Maie et al., 2011). Experimental methods such as electromyography would be useful to verify how the different muscle fiber types in the adductor mandibulae complex are activated and modulated during feeding (e.g., Liem, 1980), although the small body size of Hawaiian stream gobioids complicates such direct *in vivo* approaches.

Functional Differentiation Between A2 and A3 Bundles

Results from my new simulations show patterns of functional differentiation between A2 and A3 that maintain some consistency with previous findings in teleosts, in which A2 has been found to emphasize force and A3 speed (Westneat, 2003; Grubich et al., 2008; Maie et al., 2009a), but also show some variations from this general trend. For example, although A2 showed higher output forces than A3 under both fiber recruitment scenarios in *S. stimpsoni* (Table 5.5), these differences were not significant (see Results). In addition, differentiation in angular velocity between A2 and A3 was not indicated for *E. sandwicensis*, primarily because its mechanical advantages for A2 and A3 were similar, resulting in a similar velocity advantage for both muscle bundles in this species. It is possible that diminished functional differentiations between A2 and A3 in these species might be correlated with each of their different specializations in diet, perhaps enhancing performance of the feeding apparatus differently in each species at the potential expense of a capacity to modulate performance in response to different types of food that might be expected in more generalist gobies (e.g. *A. guamensis* and *L. concolor*: Maie et al., 2009a, b).

Feeding Performance and Ecology

The jaw closing performance exhibited by these specialists on two different primary food types may also reflect differing energetic demands for these food capturing strategies. For example, although jaw movement in herbivorous *S. stimpsoni* is nearly three times slower than in predatory *E. sandwicensis*, both are modeled as showing similar power output for the jaw closing muscles (i.e., both species show similar rates of

performing mechanical work: Table 5.2). This suggests that algal grazing in *S. stimpsoni* may be an energetically more expensive mode of feeding, as work is performed at a similar rate as in *E. sandwicensis*, but over a longer duration of time. The nearly continuous feeding behavior of *S. stimpsoni* (Julius et al., 2005; Cullen et al., 2013) may further reflect such energetic demands. Although diatoms contain lipids, an individual feeding event on diatoms likely captures fewer calories than an individual feeding event on a small fish performed by *E. sandwicensis*; moreover, feeding by *S. stimpsoni* is performed against a nearly constant rush of flowing water, in contrast to the slower flowing lower stream reaches where *E. sandwicensis* 'sits-and-waits' and ambushes when its prey is close-by (Schoenfuss and Blob, 2007). Future studies that examine the efficiency of caloric gain (e.g., caloric intake per food capture) in these species would provide further insights into differences found in feeding strategy and behavior in the streams.

Intraspecific Comparisons of Ontogenetic Scaling Patterns

The different feeding behaviors of *E. sandwicensis* (ambush predation) and *S. stimpsoni* (algal scraping) led us to predict a potential difference in the ontogenetic scaling of feeding performance between these species. Because *E. sandwicensis* continues to prey on small, rapidly moving evasive prey as it grows larger, I predicted it might exhibit positive allometry of jaw closing force that could help compensate for expected size-related decreases in speed (e.g., Richard and Wainwright, 1995; Herrel et al., 2005; Van Wassenbergh et al., 2006; Carroll and Wainwright, 2009) by conveying

greater acceleration of the jaws to peak closing velocity (Van Wassenbergh et al., 2005). In contrast, I did not predict such scaling patterns for herbivorous *S. stimpsoni*, which is not consuming evasive food. These predictions were, in fact, borne out, as *E. sandwicensis* showed positive allometry of jaw closing force for both A2 and A3 under either fiber recruitment scenario, but *S. stimpsoni* showed isometric increases in the jaw closing force of both muscles under either recruitment scenario (Table 5.5; Figures 5.3C, 5.3D). Differences in the growth of the A2 and A3 bundles are a major contributor to these patterns, as cross-sectional areas of both A2 and A3 grow with positive allometry with respect to body length in *E. sandwicensis*, but both bundles grow isometrically in *S. stimpsoni*. Positively allometric growth of A2 and A3 EMAs would also have the potential to contribute to positive output force allometry for these muscles, but such EMA allometry is not observed in either species. *S. stimpsoni* shows no significant relationship between EMA and body size for either muscle, and *E. sandwicensis* actually shows negative allometry of EMA for A2 with respect for body size (Table 5.5). This scaling pattern suggests that the lever ratio in A2 for jaw closing becomes more advantageous for speed as the fish grows larger in size (e.g., Richard and Wainwright, 1995). Consequently, its velocity advantage would contribute to the maintenance of the maximum angular velocity throughout the ontogeny of *E. sandwicensis*, however, this indicates that positive allometry of force output is achieved in spite of countervailing patterns of growth in EMA. Changes in EMA might be viewed as a less energetically demanding mechanism for achieving positive allometry of force output, as they rely on changes in the insertion point and orientation of muscle fibers, rather than increases in the

mass metabolically active muscle tissue itself. The fact that *E. sandwicensis* exhibits solely allometric changes in muscular cross sectional area raises a question of possible constraints on EMA growth for these species (e.g., Richard and Wainwright, 1995).

Angular velocity and power output also failed to show significant relationships with body size in either species. This indicates that similar absolute values of these performance variables are maintained throughout growth in both species. From a different perspective, these patterns could also be viewed as lack of performance decline with growth in these variables (Carroll et al., 2009). For animals in which the size of food items remains consistent as animals grow, such patterns may successfully suit both predatory and herbivorous species.

Future Perspectives

Fishes use jaw closing movement to capture their prey, as major part of biting/scraping machinery or at least as a part of suction feeding, which mediated by kinetic musculoskeletal architecture of the feeding apparatus. My new modeling approach, comparing two gobioid trophic specialists, integrates morphologically, physiologically, and kinematically realistic and possible scenarios in their feeding apparatus to formulate the fish's true capacity in feeding, and thereby, demonstrates a strong potential for improving our understanding of relationships between biomechanics, behavior, and ecology of fishes.

LITERATURE CITED

Abramoff MD, Magelhaes PJ, Ram SJ. 2004. Image Processing with ImageJ. Biophotonics Int 11:36-42.

Akster HA, Osse JWM. 1978. Muscle fibre types in head muscles of the perch *Perca fluviatilis* (L), Teleostei. A histochemical and electromyographical study. Neth J Zool 28:94-110.

Biewener AA. 2005. Biomechanical consequences of scaling. J Exp Biol 208:1665-1676.

Blob RW. 2000. Interspecific scaling of the hindlimb skeleton in lizard, crocodilians, felids and canids: does limb bone shape correlate with limb posture? J Zool Lond 250:507-531.

Blob RW, Bridges WC, Ptacek MB, Maie T, Cediel RA, Bertolas MM, Julius ML, Schoenfuss HL. 2008. Morphological selection in an extreme flow environment: body shape and waterfall-climbing success in the Hawaiian stream fish *Sicyopterus stimpsoni*. Int Comp Biol 48:734-49.

Boddeke R, Slijper EJ, van der Stelt A. 1959. Histological characteristics of the body musculature of fishes in connection with their mode of life. Proc K Ned Akad Wet C 62:577-588.

Burke RE, Levine DN, Zajack III RE, Tasiris P, Engle WK. 1971. Mammalian motor units: physiological-histochemical correlation in three types in cat gastrocnemius. Science 174:709-712.

Calder WA. 1984. Size, Function, and Life History. Cambridge: Harvard University Press.

Carrier DR. 1996. Ontogenetic limits on locomotor performance. Physiol Zool 69: 467-488.

Carroll AM, Wainwright PC. 2009. Energetic limitations on suction feeding performance in centrarchid fishes. J Exp Biol 212:3241-3251.

Carroll AM, Ambrose AM, Anderson TA, Coughlin DJ. 2009. Feeding muscles scale differently from swimming muscles in sunfish (Centrarchidae). Biol Lett 5:274-277.

Coughlin DJ. 2000. Power production during steady swimming in largemouth bass and rainbow trout. J Exp Biol 203:617-629.

Cullen JA, Maie T, Schoenfuss HL, Blob RW. 2013. Evolutionary novelty versus exaptation: Oral kinematics in feeding versus climbing in the waterfall-climbing

Hawaiian goby *Sicyopterus stimpsoni*. PLoS ONE 8(1):e53274. DOI:10.1371/journal.pone.0053274.

Fitzsimons JM, Nishimoto RT. 1995. Use of fish behaviour in assessing the effects of Hurricane Iniki on the Hawaiian island of Kaua'i. Environ Biol Fish 43:39–50.

Fitzsimons JM, Schoenfuss HL, Schoenfuss TC. 1997. Significance of unimpeded flows in limiting the transmission of parasites from exotics to Hawaiian stream fishes. Micronesica 30:117–25.

Fitzsimons JM, McRae MG, Schoenfuss HL, Nishimoto RT. 2003. Gardening behavior in the amphidromous Hawaiian fish *Sicyopterus stimpsoni* (Osteichthyes: Gobiidae). Ichthyol Explor Freshwaters 14:185-191.

Gosline WA. 1986. Jaw muscle configuration in some higher teleostean fishes. Copeia 1986:705-713.

Granzier HLM, Wiersma J, Akster HA, Osse JWM. 1983. Contractile properties of a white- and a red-fibre type of the m. hyohyoideus of the carp (*Cyprinus carpio* L.) J Comp Physiol 149:441-449.

Grubich JR, Rice AN, Westneat MW. 2008. Functional morphology of bite mechanics in the great barracuda (*Sphyraena barracuda*). Zoology 111:16-29.

Hammond L, Altringham JD, Wardle CS. 1998. Myotomal slow muscle function of rainbow trout *Onchrhynchus mykiss* during steady swimming. J Exp Biol 201:1659-1671.

Helfman G, Colette BB, Facey DE. 1997. The Diversity of Fishes: Biology, Evolution, and Ecology. Malden, Massachusettes: Blackwell Science, Inc.

Herrel A, Gibb AC. 2006. Ontogeny of performance in vertebrates. Phys Biochem Zool 79:1-6.

Herrel A, Van Wassenbergh S, Wouters S, Adriaens D, Aerts P. 2005. A functional morphological approach to the scaling of the feeding system in the African catfish, *Clarias gariepinus*. J Exp Biol 208: 2091-2102.

Herrel A, Schaerlaeken V, Ross C, Meyers J, Nishikawa K, Abdala V, Manzano A, Aerts P. 2008. Electromyography and the evolution of motor control: limitations and insights. Integ Comp Biol 48:261-271.

Hill AV. 1950. The dimensions of animals and their muscular dynamics. Sci Prog 38: 209-230.

Hoh JFY. 2002. ‘Superfast’ or masticatory myosin and the evolution of jaw-closing muscles of vertebrates. J Exp Biol 205:2203–2210.

Johnston IA, Moon TW. 1980. Endurance exercise training in the fast and slow muscles of a teleost fish (*Pollachus virens*). J Comp Physiol 13:147-156.

Johnston IA, Salamonski J. 1984. Power output and force-velocity relationship of red and white muscle fibers from the pacific blue marlin (*Makaira nigricans*). J Exp Biol 111:171-177.

Jolicoeur R, Mosimann JE. 1968. Intervalles de confiance pour la pente de l’axe majeur d’une distribution normale bidimensionelle. Biometrie-Praximetrie 9:121-140.

Julius ML. 2007. Why sweat the small stuff: the importance of microalgae in Hawaiian stream ecosystems. Bishop Mus Bull Cult Environ Stud 3:183-193.

Julius ML, Blob RW, Schoenfuss HL. 2005. The survival of *Sicyopterus stimpsoni*, an endemic amphidromous Hawaiian gobiid fish, relies on the hydrological cycles of streams: evidence from changes in algal composition of diet through growth stages. Aquatic Ecology 39: 473-484.

Kammerer CF, Grande L, Westneat MW. 2006. Comparative and developmental functional morphology of the jaws of living and fossil gars (Actinopterygii: Lepisosteidae). J Morph.

Kido MH. 1996a. Diet and food selection in the endemic Hawaiian amphidromous goby, *Sicyopterus stimpsoni* (Pisces: Gobiidae). Environ Biol Fishes 45:199-209.

Kido MH. 1996b. Morphological variation in feeding traits of native Hawaiian stream fishes. Pac Sci 50: 184-193.

Koehl MAR. 2000. Consequences of size change during ontogeny and evolution. In *Scaling in Biology* (eds JH Brown and GB West). Oxford: Oxford University Press.

LaBarbera M. 1989. Analyzing body size as a factor in ecology and evolution. Ann Rev Ecol Syst 20:97-117.

Liem KF. 1980. Acquisition of energy by teleosts: adaptive mechanisms and evolutionary patterns. In Environmental Physiology of Fishes (ed. MA Ali). New York: Plenum Press.

Lowndes AG. 1955. Density of fishes. Some notes on the swimming of fish to be correlated with density, sinking factor and the load carried. Ann Mag Nat Hist 8:241-256.

Magnhagen C, Heibo E. 2001. Gape size allometry in pike reflects variation between likes in prey availability and relative body depth. Funct Ecol 15:754-762.

Maie T, Schoenfuss HL, Blob RW. 2009a. Jaw lever analysis of Hawaiian gobioid stream fishes: a simulation study of morphological diversity and functional performance. J Morph 270: 976-983.

Maie T, Wilson MP, Schoenfuss HL, Blob RW. 2009b. Feeding kinematics and performance of Hawaiian stream gobies, *Awaous guamensis* and *Lentipes concolor*: linkage of functional morphology and ecology. J Morphol 270:344-356.

Maie T, Schoenfuss HL, Blob RW. 2012. Performance and scaling of a novel locomotor structure: adhesive capacity of climbing gobiid fishes. J Exp Biol 215: 3925–3936.

Maie T, Meister AB, Leonard GL, Schrank GD, Blob RW, Schoenfuss HL. 2011. Jaw muscle fiber type distribution in Hawaiian gobioid stream fishes: histochemical correlations with feeding ecology and behavior. Zool 114: 340-347.

McArdle BH. 1988. The structural relationship: regression in biology. Can J Zool 66:2329-2339.

McGuire JA. 2003. Allometric prediction of locomotor performance: an example from Southeast Asian flying lizards Am Nat 161:337-349.

McHenry MJ, Lauder GV. 2006. Ontogeny of form and function: locomotor morphology and drag in zebrafish (*Danio rerio*). J Morphol 267:1099-1109.

McMahon TA. 1975. Using body size to understand the structural design of animals: quadrupedal locomotion. J Appl Physiol 39:619-627.

Nishimoto RT, Kuamo'o DGK. 1997. Recruitment of goby postlarvae into Hakalau Stream, Hawai'i Island. Micronesica 30:41–9.

Radtke RL, Kinzie RW III, Folsom SD. 1988. Age at recruitment of Hawaiian freshwater gobies. Environ Biol Fishes 23:205-213.

Rayner JMV. 1985. Linear relations in biomechanics: the statistics of scaling functions. J Zool Lond 206:415-439.

Richard BA, Wainwright PC. 1995. Scaling the feeding mechanism of largemouth bass (*Micropterus salmoides*): kinematics of prey capture. J Exp Biol 198:419-433.

Rome LC, Swank DM, Coughlin DJ. 1999. The influence of temperature on power production during swimming. II. Mechanics of red muscle fibres *in vivo*. J Exp Biol 203:333-345.

Rome LC, Funke RP, Alexander RM, Lutz G, Aldrigde H, Scott F, Freadman M. 1988. Why animals have different muscle fibre types. Nature 335:824–827.

Schmidt-Nielsen K. 1984. Scaling: Why is Animal Size Important? Cambridge: Cambridge University Press.

Schoenfuss HL, Blanchard TA, Kuamo'o DG. 1997. Metamorphosis in the cranium of postlarval *Sicyopterus stimpsoni*, an endemic Hawaiian stream goby. Micronesica 30:93-104.

Schoenfuss HL, Blob RW. 2003. Kinematics of waterfall climbing in Hawaiian freshwater fishes (Gobiidae): vertical propulsion at the aquatic-terrestrial interface. J Zool Lond 261:191-205.

Schoenfuss HL, Blob RW. 2007. The importance of functional morphology for fishery conservation and management: application to Hawaiian amphidromous fishes. Bishop Mus Bull Cult Environ Stud 3:125-141.

Schoenfuss HL, Julius ML, Blob RW. 2004. Colonization of a recent, volcanically formed freshwater habitat: an example of primary succession. Ichthyol Explor Freshwaters 15:83-90.

Swartz SM. 1997. Allometric patterning in the limb skeleton of bats: implications for the mechanics and energetics of powered flight. J Morphol 234:277-294.

Tate DC. 1997. The role of behavioral interactions of immature Hawaiian stream fishes (Pisces: Gobiodei) in population dispersal and distribution. Micronesica 30:51–70.

Thacker CE. 2003. Molecular phylogeny of the gobioid fishes (Teleostei: Perciformes: Gobioidei). Molecular Phylogenetics and Evolution 26: 354-368.

Toro E, Herrel A, Vanhooydonck B, Irschick DJ. 2003. A biomechanical analysis of intra- and interspecific scaling of jumping and morphology in Caribbean *Anolis* lizards. J Exp Biol 206:2641-2652.

Tsutakawa RK, Hewett JE. 1977. Quick test for comparing two populations with bivariate data. Biometrics 33:215-219.

Van Wassenbergh S, Aerts P, Herrel A. 2006. Scaling of suction feeding performance in the catfish *Clarias gariepinus*. Physiological and Biochemical Zoology 79: 43-56.

Van Wassenbergh S, Herrel A, James RS, Aerts P. 2007. Scaling of contractile properties of catfish feeding muscles. J Exp Biol 210:1183-1193.

Van Wassenbergh S, Aerts P, Adriaens D, Herrel A. 2005. A dynamic model of mouth closing movements in clariid catfishes: the role of enlarged jaw adductors. J Theor Biol 234:49-65.

van Wessel T, Langenbach GEJ, Korfage JAM, Brugman P, Kawai N, Tanaka E, van Eijden TMGJ. 2005. Fibre-type composition of rabbit jaw muscles is related to their daily activity. Eur J Neurosci 22:2783–2791.

Westneat MW. 2003. A biomechanical model for analysis of muscle force, power output and lower jaw motion in fishes. J Theor Biol 223: 269-281.

Winterbottom R. 1974. A descriptive synonymy of the striated muscles of the teleostei. Proc Acad Nat Sci Phil 125:225-317.

Yamamoto MN, Tagawa AW. 2000. Hawai'i's native and exotic freshwater animals. Honolulu: Mutual Publishing.